ISSN: 1863-5598

ZKZ 64717
11-18

Bodo´s Power Systems®

Electronics in Motion and Conversion

November 2018

WELCOME TO THE HOUSE OF COMPETENCE

ENGINEERING | PRODUCTION | GvA SOLUTIONS | DISTRIBUTION

POWER
IS IN OUR NATURE!

Power is in our nature. Everyday we deliver full power for your success.

- **ENGINEERING:** Quick design-to-product using state-of-the-art technologies
- **PRODUCTION:** Extensive production experience with maximum flexibility
- **GvA SOLUTIONS:** Short time-to-market with innovative plug&play system solutions
- **DISTRIBUTION:** Vast product knowledge and consulting expertise

GvA Leistungselektronik GmbH
Boehringer Straße 10 - 12
D-68307 Mannheim
Phone +49 (0) 621/7 89 92-0
info@gva-leistungselektronik.de
www.gva-leistungselektronik.de

GvA Power Electronics

The Gallery

crystal clear
frequencies.

WÜRTH ELEKTRONIK

© eiSos

TEAM WORLD CHAMPION
FIA FORMULA E 2017/2018

#CRYSTALCLEAR

WE speed up the future

electronica Hall B6 Booth 404

The WE-CMBNC is a VDE certified series of common mode chokes with a highly permeable **nanocrystalline core material.** Despite the small size, it delivers outstanding broadband attenuation performance, high rated currents and low DC resistance values. Low profile and high voltage ratings can also be realized by the common mode chokes of the WE-CMB family.

For further information, please visit:
www.we-online.com/we-cmb

- High permeability nanocrystalline core material
- High I_R & low R_{DC} in a small size
- Broadband suppression
- Stable inductance values at high temperatures
- Improved isolation through plastic case and patented winding spacer

Nanocrystalline WE-CMBNC | MnZn WE-CMB | NiZn WE-CMB NiZn | MnZn/NiZn WE-ExB | Horizontal WE-CMBH | High Voltage WE-CMB HV

Bodo's Power Systems®

A Media
Katzbek 17a
D-24235 Laboe, Germany
Phone: +49 4343 42 17 90
Fax: +49 4343 42 17 89
info@bodospower.com
www.bodospower.com

Publishing Editor
Bodo Arlt, Dipl.-Ing.
editor@bodospower.com

Junior Editor
Holger Moscheik
Phone + 49 4343 428 5017
holger@bodospower.com

Editor China
Min Xu
Phone: +86 156 18860853
xumin@i2imedia.net

UK Support
June Hulme
Phone: +44 1270 872315
junehulme@geminimarketing.co.uk

US Support
Cody Miller
Phone +1 208 429 6533
cody@eetech.com

Creative Direction & Production
Repro Studio Peschke
Repro.Peschke@t-online.de

Free Subscription to qualified readers
Bodo´s Power Systems
is available for the following
subscription charges:
Annual charge (12 issues)
is 150 € world wide
Single issue is 18 €
subscription@bodospower.com

circulation print run 24 000

Printing by:
Brühlsche Universitätsdruckerei GmbH
& Co KG; 35396 Gießen, Germany

www.bodospower.com

Show Time is On

Having just survived "Oktoberfest", the next big thing for Munich is electronica. electronica is a big party for the electronics industry to display their technology and future dreams. Every second year all of us come to Munich to celebrate a week of communication, between semiconductor manufacturing and system level users.

When I was a young engineer I landed by plane in Riem Airport, which has now become the fairground. The old location for the Fair was in the center of Munich, at the "Theresienwiese", 40 years ago - the "great old days". It seems soon after that I was crossing the Atlantic in a 747, all the way to Chicago. Bipolar transistors were widely used. The world was mostly analog in communication, it was before cell phones. Silicon had replaced germanium in bipolar transistor technology, and MOS gated devices then took over from bipolar in power transistors. The IGBT was invented and became a workhorse for power applications at line voltage level. Those indeed were good years for me - introducing to industry MOSFETs and IGBTs for RCA, then GE-Solid State and finally for Harris Semiconductor.

Compared to bipolar, MOSFET's and IGBT's improved efficiency in all kinds of applications. We are again in a similar position, with wide band gap devices emerging with even higher switching frequencies, and a step forward in efficiency. We see SiC and GaN as the materials advancing the performance of power electronic switches - SiC capable of several kilovolts, while GaN has just reached one kilovolt ratings.

As I pioneered in getting IGBTs introduced to users in the 80's, it is now my pleasure to have experts in Wide Band Gap devices present their technology.

Mark your calendar for the Wide Band Gap Conference in Munich on December 4th at the Hilton Airport Hotel. Building on last year's success, the program this year will continue and be strengthened with the cooperation of ICC Media / AspenCore. Visit www.Power-Conference.com for further information. The speakers program is finalized, and we look forward to interesting presentations and good networking!

Bodo's magazine is delivered by postal service to all places in the world. It is the only magazine that spreads technical information on power electronics globally. We have EETech as a partner to serve North America efficiently. If you are using any kind of tablet or smart phone, you will find all of our content on the website www.eepower.com. If you speak the language, or just want to have a look, don't miss our Chinese version: www.bodospowerchina.com

My Green Power Tip for the Month:
Cut your grass with a battery powered mower. Fuel powered mowers contribute a high amount of pollution to the environment.

Best Regards

Events

ESARS-ITEC 2018
Nottingham, United Kingdom, November 7-9
www.esars-itec.org

electronica 2018
Munich, Germany, November 13-16
https://electronica.de/

SEMICON Europa 2018
Munich, Germany, November 13-16
www.semiconeuropa.org

SPS/IPC/DRIVES 2018
Nuremberg, Germany, November 27-29
www.mesago.de/de/SPS

SemIsrael 2018
Tel Aviv, Israel, November 27
www.semisrael-expo.com

Power Electronics Conference 2018
Munich, Germany, December 4
www.power-conference.com

BEVA Europe 2018
London, UK, December 4-6
www.beva-europe.com

IEEE IEDM
San Francisco CA, USA, December 1-5
https://ieee-iedm.org/

SEMICON Japan 2018
Tokyo, Japan, December 13-15
www.semiconjapan.org/en

SPS/IPC/
Drives
Hall 3A.400

State of the ART & ATO

ATO Series

Split-core Current Transformers

- Compact, self-powered
- 10 & 16mm diameter aperture
- Accuracy class 1 & 3
- Operating frequency: 50 / 60 Hz

PERFECT LOOP TECHNOLOGY
Patent
ref. WO 2009
/001185 A1

ART Series

Unique, IP57, flexible and thin 1 kV Rogowski coil

- Rated insulation voltage 1 kV CATIII
- Accuracy class 0.5 without calibration
- 2mm hole to pass security seal
- Electrostatic shield

www.lemcity.com

At the heart of Smart Cities.

LEMcity™

electronica Medical Electronics Conference (eMEC)—the Debut

In 2018, the spotlight will be shining on medical electronics for the very first time when the field has its own dedicated conference (November 15, ICM—Internationales Congress Center München). The event will see doctors and electronics engineers entering into discussions about the future of the medical sector. The issues covered will include smart medical devices, cloud computing, data security and sovereignty, blockchain technology, collaborative robots, smart contracts, usability, artificial intelligence, telemedicine, and Medicine 4.0.

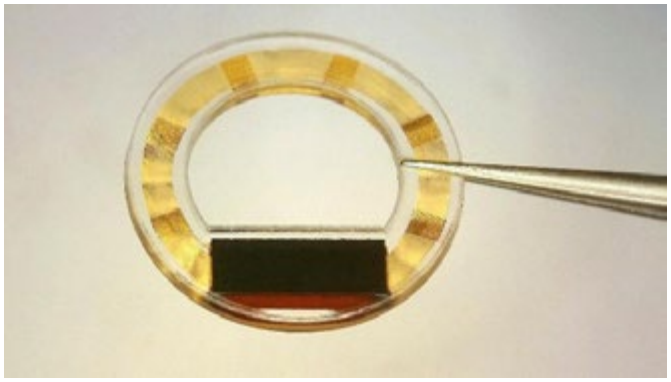

Medical Electronics Forum—all things wearables

The focus of the Medical Electronics Forum (Hall C3, Stand 534 in the morning on November 16) is on wearables. After all, they are set to have a major impact on the health care sector and medical treatment. Once they are connected to the Internet, they enable doctors to monitor their patients' health remotely and give constant care to chronically sick people. Older people will also be able to live independent lives in familiar surroundings for longer thanks to wearables. Plus, smart analysis of the data will allow for the health care system to be optimized even further.

Medical electronics—the exhibitors

Medical products and services can mainly be found in the exhibition areas covering embedded systems, sensors, printed circuit boards and other bare circuit carriers, wireless technology, power supplies, and micro and nano systems.

https://electronica.de/index.html

Tool for GaN-on-Silicon Monolithic microLEDs Display Innovation

Plessey announces it has placed an order for its next reactor from AIXTRON SE. The AIX G5+ C metal organic chemical vapour deposition (MOCVD) reactor will boost Plessey's manufacturing capability of gallium nitride on silicon (GaN-on-Si) wafers targeting next-generation microLED applications. With an automatic cassette-to-cassette (C2C) wafer transfer module, the new AIXTRON reactor will be installed and operational during Q1 of 2019 at Plessey's 270,000 sq ft fabrication facility located in Plymouth, UK. The AIX G5+ C MOCVD system has two separate chamber set-up options, which enables configurations of 8 x 6in or 5 x 8in GaN-on-Si wafers to be automatically loaded and removed from the system in an enclosed cassette environment. The system will be an addition to the company's existing metal organic chemical vapour deposition (MOCVD) reactors, also supplied by AIXTRON, which provide configurations of 7 x 6in or 3 x 8in with manual loading. Productivity is further enhanced by the new reactor's automated self-cleaning technology, which helps to deliver a very low level of wafer defects by ensuring the reactor is clean on every run, significantly reducing downtime for maintenance. The new equipment also provides faster ramp and cool down along with a high susceptor unload temperature to reduce the recipe time.

www.plesseysemiconductors.com

www.aixtron.com/en

Analysing Technical Cleanliness According to VDA/ISO

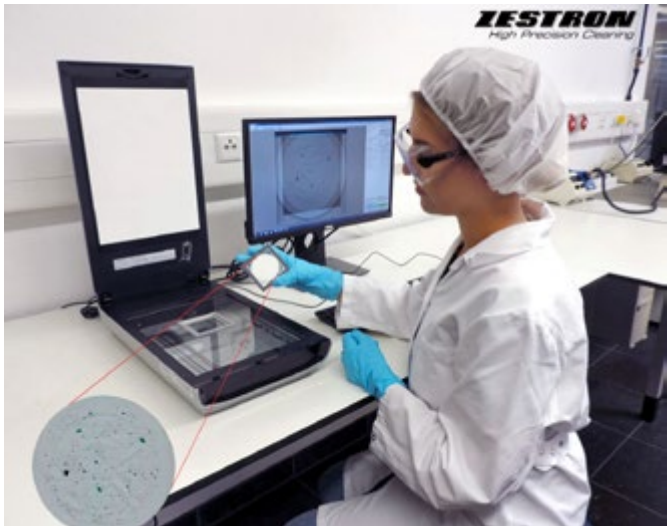

ZESTRON has expanded its analytical services available at the Analytical Center in Ingolstadt, Germany, by integrating a particle extraction and analysis unit. Electronic manufacturers can now have their electronic boards analysed for particle residues according to VDA 19 and ISO 16232 at ZESTRON. Especially in the automotive industry, particle impurity has increasingly become the focus since it can affect the production process or the service life of the electronic assemblies. Particle contamination of electronic assemblies can be reliably analysed through particle extraction and analysis. This qualitative and quantitative measurement tool can define the particles by type and size distribution, and be applied to assess the risk of failure on electronic boards. Furthermore, this method can be used to evaluate particulate contamination with regard to its influence on the cause of damage of the assembly.

www.zestron.com

SMALLER STRONGER FASTER

ROHM SEMICONDUCTOR

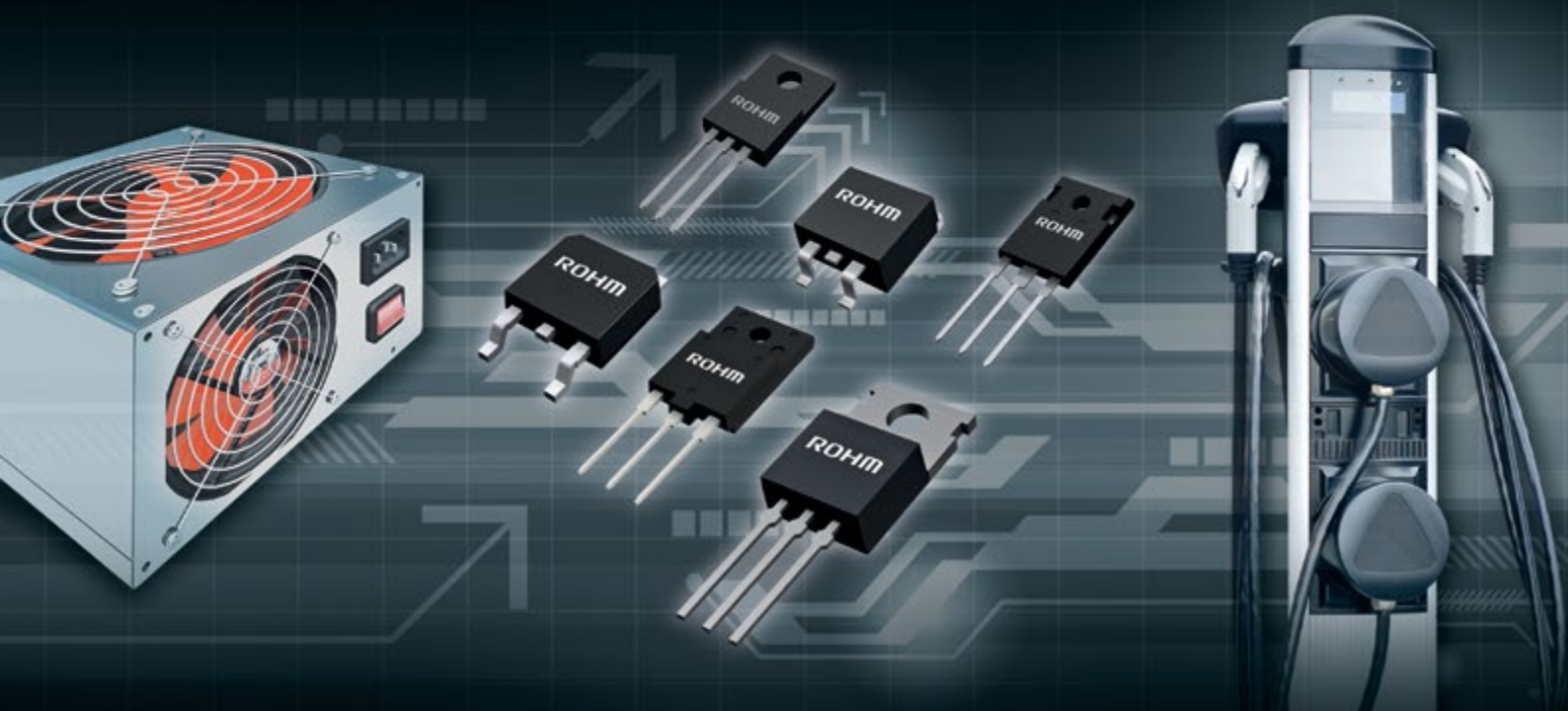

HIGH VOLTAGE SUPERJUNCTION MOSFETS FOR EFFECTIVE PERFORMANCE

PrestoMOS™ JN series 600V

- Part number R60xxJNx
- FRD is implemented in body diode of MOSFET
- Best-in-class fast & soft recovery body diode
- Suitable for inverter application
- Max. current up to 70A
- Packages: TO-220FN, TO-247, TO-3PF, D2PAK, DPAK

Super Junction-MOS EN series 600V / 650V

- Part number R60xxENx (600V) & R65xxENx (650V)
- Low switching noise and easy to use
- Usable for SMPS
- Max. current up to 76A
- Packages: TO-220FM, TO-247, TO-3PF, D2PAK, DPAK

Super Junction-MOS KN series 600V / 650V / 800V

- Part number R60xxKNx (600V), R65xxKNx (650V) & R80xxKNx (800V)
- Fast switching and low switching loss
- Usable for high efficiency SMPS
- Max. current up to 76A (600V, 650V) and 52A (800V)
- Packages: TO-220FM/AB, TO-247, TO-3PF, D2PAK, DPAK

Body diode recovery wave form of PrestoMOS™

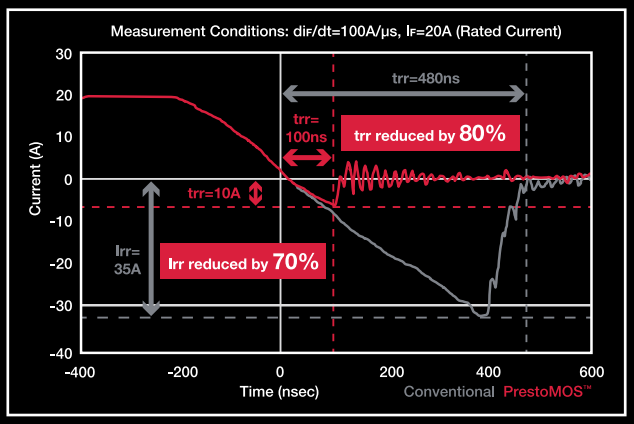

SIGN UP

ROHM e-Newsletter

www.rohm.com

More International Exhibitors than Ever, New Conference Schedule as of 2019

The complete short-form analysis of the SENSOR+TEST 2018 with all key figures and the results of the visitor and exhibitor poll is now available for download at www.sensor-test.com. Remarkable: The 40% share of international exhibitors sets a new record. As of 2019 the conferences parallel to the leading fair for sensor, measuring, and testing technology will alternate in a new schedule and structure: New International Conference in 2020 and New Schedule as of 2019 As of 2020, the previous AMA Conferences SENSOR and IRS2 will be joined by the new international symposium SMSI 2020 – Sensor and Measurement Science International (www.smsi-conference.com). For this reason, the SENSOR+TEST will be accompanied next year by the 20th GMA/ITG conference on Sensors and Measuring Systems 2019. This new structure for the conferences is explained by Holger Bödeker, the AMA Service's executive manager, stating, "Thanks to the intensive support of the scientific community, we're now able to offer an annually alternating platform for the presentation of the latest research results with the Sensors and Measuring Systems and the SMSI – Sensor and Measurement Science International. The SMSI ideally complements the topics of the AMA Conferences SENSOR and IRS2 in the area of scientific measuring technology and meteorology. Both conferences thus cover the technological spectrum of the trade fair and ensure suppliers and users well-informed insights into the research results relevant to the future."

The next SENSOR+TEST will be held from 25 to 27 June 2019 as always at the Nuremberg Exhibition Center, this time with the special topic Sensors and Measurement for Process Automation.

www.sensor-test.com

Included in Dow Jones Sustainability Index for the 9th time

Infineon has been listed in the Dow Jones Sustainability™ Europe Index (DJSI) for the 9th consecutive year. This was announced by the Sustainability Investing (SI) specialist RobecoSAM. In addition to its incorporation in the European Index, Infineon is also part of the Dow Jones Sustainability™ World Index for the fourth time in a row. Infineon can therefore be ranked in the top ten percent of the world's most sustainable companies. "Business success and responsible behavior are indivisible for us", says Dominik Asam, CFO of Infineon Technologies AG and responsible for sustainability issues. "Environmental sustainability alone counts for little in the long run, if a company isn't commercially successful as well." Companies considered for inclusion in the DJSI are assessed with regard to economic stability as well as environmental and social performance. The longest-running index of its kind, the Dow Jones Sustainability Index contains the most sustainable companies in a particular geographic region. This makes it the key reference point for companies and investors who place a high value on sustainability criteria when making investment decisions. The DJSI is created and managed cooperatively by S&P Dow Jones Indices and RobecoSAM (Source: CSR News).

www.infineon.com

Project to Improve Reliability and Speed of Low-Cost Electronic Devices for Autos

Leti, a research institute of CEA Tech, and EFI Automotive announced a project to dramatically improve reliability and response time of low-cost automotive components by equipping the devices with sophisticated model predictive control techniques. Model predictive control (MPC) is an advanced method of process control that makes use of a model of the system to predict its behavior. The control law is based on an optimization technique that computes the system inputs, taking into account the reference that the system output has to follow, together with the effort (energy) that is applied on the system inputs and some constraints that may exist within the system, typically saturation of the system inputs. MPC also allows electronics equipment to perform at levels that are not possible with standard control laws, e.g. proportional-integral-derivative (PID) controllers. But this sophisticated technique is rarely used on low-cost, low-capability computing units, because it requires solving optimization problems under constraints, which is a complex computational task.

Leti and EFI Automotive are evaluating the implementation of MPC on low-cost, low-computational-capability computing platforms, such as microcontrollers or low-cost digital signal processors (DSPs). The goal is to improve the dynamics of the systems considered, because automotive certification is easier when the control law is implemented on a DSP or a microcontroller. An example of EFI Automotive product, which will benefit from the MPC implementation, is the Air Loop Actuator.

www.leti-cea.com

www.efiautomotive.com

HITACHI
Inspire the Next

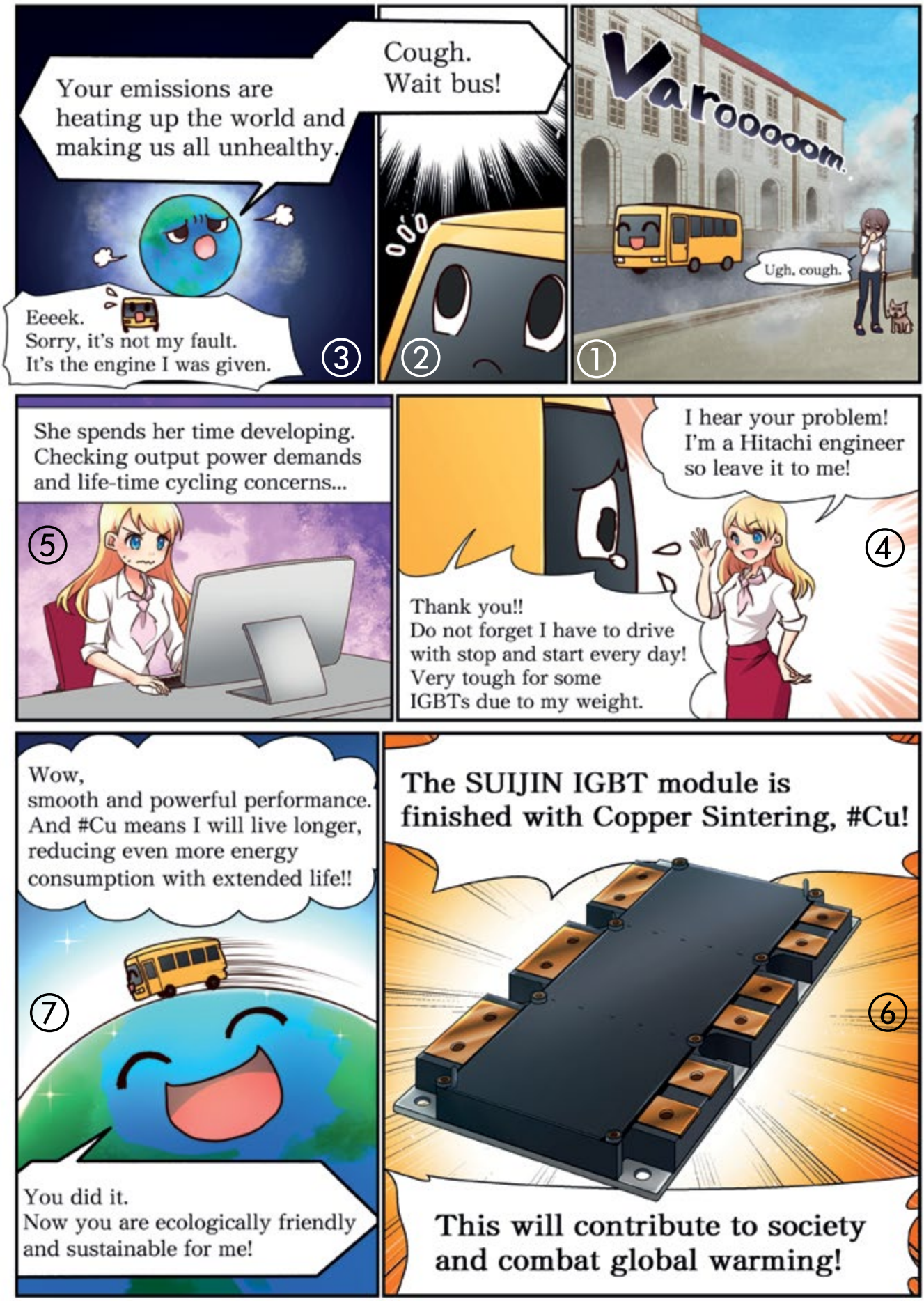

Please read right-to-left, in respect to Akira Toriyama and Manga artists around the world. Just follow the numbers.

650V – 1200V SUIJIN AUTOMOTIVE IGBT MODULES

www: pdd.hitachi.eu/ev tel: +44 (0)1628 585151 email: pdd@hitachi-eu.com

Scan me

EPCOS AG Changes its Name to TDK Electronics AG

TDK Corporation announces that it has changed the name of its subsidiary EPCOS AG to TDK Electronics AG. The name change of EPCOS AG, the parent company of the EPCOS Group, goes into effect October 1, 2018, and will thus further strengthen the uniform market presence of the TDK Group. In parallel with EPCOS AG, all other EPCOS entities worldwide will also be renamed. Because the country-specific legal requirements vary, the renaming process will likely take 9 to 12 months. These requirements will also have an impact on the individual company names, which in all cases will include TDK as an integral part of the names. The new company names will have no effect on the EPCOS product portfolio, the organizational and business structure of the company, or the scope of its services.

https://en.tdk-electronics.tdk.com

Upcoming ECPE Events

- ECPE Workshop 'The Future of Modelling and Simulation in PE Packaging for Thermal and Stress Management'
  20 - 21 November 2018, Nuremberg, Germany
  Chairmen: Prof. U. Scheuermann (Semikron), Prof. B. Wunderle (TU Chemnitz)
- ECPE Workshop 'New Technologies for Medium-Frequency Solid-State Transformers'
  14 - 15 February 2019, Lausanne, Switzerland
  Chairmen: Prof. D. Dujic (EPFL), Prof. J.W. Kolar (ETH Zurich)
- ECPE SiC & GaN User Forum
  26 - 27 March 2019, Erding / Munich, Germany
  Chairmen: Prof. A. Lindemann (Univ. of Magdeburg), Prof. L. Lorenz (ECPE), Dr. P. Friedrichs (Infineon)
  in conjunction with the ECPE Annual Event

www.ecpe.org/events

Over 100,000 New Models on SnapEDA

Samtec is releasing digital models for over 100,000 of its products on SnapEDA, the industry-leading circuit board design library. Traditionally, designers have spent days creating digital models - such as symbols and footprints - for each component in their designs. Connectors are especially time-consuming to create models for, due to their non-standard shapes, pitches, pads, and cutouts.
With this new collaboration, designers can now easily discover, download, and design with over 100,000 ready-to-use Samtec connector models, helping accelerate the design process. The new models include USB, card edge, board-to-board, headers, and RF coaxial connectors.
Created by Samtec's Signal Integrity Team, these detailed, high-quality models include accurate assembly, silkscreen and 3D features to support high density applications. The footprints employ courtyards, built-in dimensioning, and applicable metadata. "We pride ourselves on being the service leader, which means investing the time and energy into providing models that expedite the design process for SnapEDA users," said Greg Horlick, ECAD Systems Architect, at Samtec. Downloading the printed circuit board (PCB) models is simple: designers create a free account on the SnapEDA website, and then can download for free. Samtec has made the files available for OrCad, Allegro, Eagle and PADS, and using SnapEDA's translation technology, the files can also be downloaded for Altium, KiCad, PCB123, Proteus 8.8, and Pulsonix.

www.snapeda.com

Graphene-Based Ultracapacitors Boost Double Deck Buses

Skeleton Technologies and Wrights Group Ltd have signed a high-volume, multi-million-euro contract over the next 5 years. Skeleton Technologies supplies graphene-based ultracapacitors to the latest KERS enabled hybrid-electric double and single deck buses produced by the Wrights Group. The demand to reduce CO2 emissions in city centers is one of the key drivers for Wrightbus to implement new technology which cuts down CO_2 emissions by saving fuel.
The integration of graphene-based ultracapacitors into test WrightBus double deck buses enables a 36% fuel saving compared to a UK based EuroVI diesel bus baseline. It also adds at least another 3 passengers to the capacity of these buses compared to a lithium battery-based hybrid equivalent. Skeleton Technologies has taken Graphene from the lab to the real world:
Graphene as part of the ultracapacitor technology significantly increases power and energy density extractable from ultracapacitors whilst keeping their internal resistance low and prolonging their lifetime.
With Skeleton Technologies' cells, Wrightbus operators are also cutting down on maintenance costs. Whilst the lithium battery may last around 4 to 5 years, during their 1 million cycles, the ultracapacitors will quietly sit undisturbed for at least 7.5 years, with an estimated life of 12 to 15 years.

www.skeletontech.com

www.wrightsgroup.com

Covering Analog Needs From Simple to Complex

High-Performance Devices to Handle Every Design Challenge

www.microchip.com/AnalogProducts

microchip DIRECT
www.microchipdirect.com

MICROCHIP

APEC 2019 Sponsors Continue Student Travel Support Program

The joint sponsors of the Applied Power Electronics Conference (APEC) have announced the continuation of the popular Student Attendance Travel Support Program. Awarding up to $1,000 per student to cover a portion of their travel and conference expenses, the program disperses up to $60,000 to as many as 60 students who are participating in APEC 2019, to be held in Anaheim, CA, March 17-21, 2019. Interested students must apply by Oct. 26h, 2018.

www.psma.com/technical-forums/education/news

Achieving IATF 16949: 2016 Certification

Rogers Corporation announced that its Advanced Connectivity Solutions (ACS) business has achieved IATF 16949: 2016 certification, the highest international quality standard for the automotive industry. The certification covers the company's Chandler, Arizona, Rogers, Connecticut, Suzhou China and Belgium manufacturing and R&D facilities. "This certification is a major accomplishment for the ACS team and demonstrates our commitment to manufacturing high-quality, innovative, best-in-class products for our automotive customers," said Jeff Grudzien, Senior Vice President and General Manager of ACS. ACS supplies copper clad RF laminate materials into automotive applications such as 24 GHz and 77 GHz radar sensors, which are used for the fast-growing Advanced Driver Assistance Systems (ADAS) market. "With the expected growth in ADAS and autonomous driving applications, IATF 16949:2016 certification is a critical piece of our automotive customer support strategy, along with development of innovative new products, long-term investments in global manufacturing capacity, and world-class technical support," Mr. Grudzien added.

www.rogerscorp.com

International Platform Enables a Unique Market Overview

The outlook for the 29th SPS IPC Drives event is again very positive and testifies to the importance of the exhibition for smart and digital automation. Some 1,700 automation providers from all over the world are expected in Nuremberg on 27 - 29 November 2018. Products and solutions, as well as trend-setting technologies of the future, will be on show. As in the previous year, Industry 4.0 and digital change are topics of focus at SPS IPC Drives 2018. Exhibitors will present not only their solutions, but also various products and example applications for digital transformation. This will be accompanied by topic-related showcases and presentations at the exhibition forums. The firm commitment that IT companies such as SAP bring to exploring industrial communication topics (such as OPC UA and TSN) shows how the IT and automation industries are increasingly merging. This process is also reflected in the hall occupation at SPS IPC Drives: in 2018, the topic of software and IT in manufacturing will be on display in Halls 5 and 6. Industrial web services, virtual product development and design, digital business platforms, IT/OT technologies, fog/edge and cloud computing, and many other topics will be covered here. Cybersecurity is also being addressed by numerous vendors, who will offer explanatory demonstrations at their booths of how companies can protect themselves against online attacks.

www.mesago.de/en/SPS/home

Reorganization in Record-Breaking Quarter

pSemi Corporation (formerly known as Peregrine Semiconductor) announces several organizational changes, including the promotion of two directors to vice presidents, a simplified organizational structure and a change in role for CEO Stefan Wolff. These changes come in the midst of a record-breaking quarter as pSemi prepares for additional rapid growth. pSemi is projected to end this quarter in September with revenue 15 percent higher than the prior record. Stefan Wolff stepped down as CEO on Oct. 1. The former CEO and current CTO, Jim Cable, will serve as pro term CEO. To support the transition, Stefan will remain as strategic advisor until December, when he will return to Germany to be closer to his family. "It is with a heavy heart that I announce I must return to Germany in December to be with my family," says Stefan Wolff, CEO of pSemi. "pSemi is only beginning to harness and deliver its innovative products on a large scale. We have a fantastic team to deliver what the market needs next, a full design-win pipeline, an award-winning patent portfolio and outstanding support from our parent company, Murata. In my time at pSemi, we've made tremendous progress, and our team, our business and our product portfolio have grown substantially. With our simplified organizational structure and the addition of further industry expertise to our leadership team, I am confident pSemi can effectively scale the business to the next level and become Murata's center of excellence for RF, mixed signal, power, optical and ASIC semiconductors."

www.psemi.com

I-PACE eTROPHY Announces Official Charging Partner

Jaguar I-PACE eTROPHY has announced an agreement with ABB to serve as the Official Charging Partner for the new Jaguar I-PACE eTROPHY series. As part of this partnership, ABB will provide

custom-made, compact fast chargers for each of the participating teams in this new electric racing series. The Terra DC fast chargers were specially designed for the series and are capable of quickly charging the Jaguar I-PACE eTROPHY racecars in the short breaks between practice, qualifying and the races. The compact design also allows for the chargers to be easily transported to the series' 10 rounds, keeping freight to a minimum. The partnership builds on ABB's role as title sponsor of the ABB FIA Formula E Championship and extends the company's commitment to support and expand the future of e-mobility. The Jaguar I-PACE eTROPHY is the world's first all-electric, production-based racing series. It will take place on the same weekends and on the same city street circuits as the ABB FIA Formula E Championship. The series, which will exclusively feature up to 20 Jaguar I-PACE eTROPHY racecars, will give participating teams the chance to showcase racing talent and performance, while competing on the world stage in zero-emissions motorsport.

www.abb.com

GaN-on-Silicon Technology for Power Conversion Applications

STMicroelectronics and Leti announced their cooperation to industrialize GaN (Gallium Nitride)-on-Silicon technologies for power switching devices. This power GaN-on-Si technology will enable ST to address high-efficiency, high-power applications, including automotive on-board chargers for hybrid and electric vehicles, wireless charging, and servers. The collaboration focuses on developing and qualifying advanced power GaN-on-Silicon diode and transistor architectures on 200mm wafers, a market that the research firm IHS Markit estimates to grow at a CAGR of more than 20 percent from 2019 to 2024 IHS Markit, April 2018. Together, in the framework of IRT Nanoelec, ST and Leti are developing the process technology on Leti's 200mm R&D line and expect to have validated engineering samples in 2019. In parallel, ST will set up a fully qualified manufacturing line, including GaN/Si hetero-epitaxy, for initial production running in ST's front-end wafer fab in Tours, France, by 2020. In addition, given the attractiveness of GaN-on-Si technology for power applications, Leti and ST are assessing advanced techniques to improve device packaging for the assembly of high power-density power modules.

www.st.com

www.leti-cea.com

www.leti.fr/en

3D Power Packaging Report Focuses on Passives and Substrates

The Power Sources Manufacturers Association (PSMA) Packaging Committee announces the publication of its latest report titled, "3D Power Packaging with Focus on Embedded Passive Component and Substrate Technologies." This is the third in a series of reports focused on using embedded substrate technology for building power sources. It is the first extensive study of embeddable passive components both available and in development for use in the power path of power sources. The report contains extensive research and product illustrations geared to an audience of technology executives and design engineers. Miniaturization of passive components without compromising their power handling and efficiency and their integration with actives has always been a key focus for power packaging. There is also an increasing trend to vertical or 3D package integration to address the performance issues by eliminating parasitics from interconnections. Embedding gives lowest package inductance and enables co-integration of power systems and drivers in a single package with direct interconnection between gate driver circuits and switches with shortest interconnection length. This has become even more important with the rapid emergence of wide bandgap power switching devices. This, however, leads to several process integration and reliability challenges that need to be systematically addressed.

www.psma.com

Global Automotive Business Development Vice President

Vicor Corporation announced the appointment of Patrick Wadden as Vice President, Global Automotive Business Development, effective October 1, 2018. In his role, Mr. Wadden will be responsible for developing and coordinating Vicor's business in the global automotive market.

Prior to joining Vicor, Mr. Wadden was leading North American sales in the automotive segment for Integrated Device Technology. His prior experience includes leadership roles in sales, marketing, and product line management for Analog Devices, Altera, and Intersil. Mr. Wadden holds a BSBA from Northeastern University. Commenting on the appointment, Vicor's CEO, Dr. Patrizio Vinciarelli, stated, "I am delighted to have Patrick join Vicor as 48V based power systems gain traction in hybrid, pure electric, and autonomous driving vehicles. Patrick will lead our initiative to expand the use of Vicor's IP in automotive 48V power systems with a mix of product sales and technology licensing agreements."

www.vicorpower.com

AC-Power Series Suitable for "Harsh Environment" Applications

Following the increasing demand for components suitable for critical environmental operating conditions, after long development and test, ICEL S.r.l. added a brand-new AC-Power series to the existing range.
The THZ series is a solution for power applications at operating conditions with high temperature and high humidity levels ("Harsh environments").

Main project targets:
- excellent performances in AC-Power applications up to high voltage and current ratings
- additional very good performances under high temperature and humidity
- slight sizes increase compared to standard AC power series
- competitive price
- radial boxed execution

Related development guidelines:
- special finishing-protection materials
- special film metallization design
- innovative production processes
- dedicated machines
- proper testing equipment

High operation temperature and high humidity levels combined, even more with AC voltage operation, are particularly dangerous: a critical condition for metallized film capacitors.
Upon humidity reaching the units inside, electrochemical corrosion phenomena may occur, driven by the applied voltage.
This may cause a fast capacitors ageing, with related parameters variation, potential body distortion, decrease of the expected life-time and rise of the failure probability.
The higher is the energy density of the component, the higher is the detrimental effect, making difficult to combine critical environmental stresses withstanding with reasonable sizes.
It is necessary to minimize the humidity penetration in the capacitor, so that the related ageing effects remain negligible for a long time, compared to the component expected life-time and reliability.

Biased high temperature and high humidity tests are not yet mandatory proofs in plastic film capacitors normative, but are in use for other categories of components (among them the "85/85/1000" test). Nevertheless they are, often unproperly, required also by capacitors users, since critical environmental stress usage together with high power stress is rapidly increasing and wide-spreading.

The main biased humidity tests taken as a reference for THZ design are:
- AEC Q-200 cockpit test, 40°C 93% RH 1000h at rated voltage
- 70/70/1000, 70°C 70% RH 1000h at rated voltage
- IEC60068-2-67 humidity load test (Test Cy), 85°C 85% RH 504h at rated voltage
- AEC Q-200 85/85/1000 (Level 1), 85°C 85% RH 1000h at derated voltage

The new THZ series passes the above special tests with a moderate impact on the electrical parameters, where std. power series may rapidly show suffering signs up to possible important damages.
The new materials and technologies developed by ICEL S.r.l. do additionally improve the performances, the reliability and the global capacitors behavior under "normal" operating conditions: this acquired know-how will be fundamental for the design of new capacitors series.

Further information available at

www.icel.it

PrimePACK™ 7G IGBT Modules

Upgrading to 1200 A in PP2 and 1800 A in PP3

Power dissipation at 6 kHz
6 Gen vs 7 Gen
Modul rating: 1700 V/1400 A

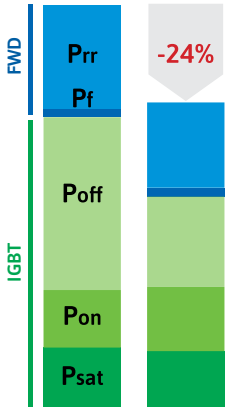

FEATURES

- IGBT & FWD
- High reliability solder material
- Higher lifetime at same ΔTj
- Increased output power at same lifetime
- Higher power cycling capability
- Lower losses at same conditions
- 2nd label with $V_{CE(sat)}$ and V_F classification for easier paralleling

Win a SAM L11 Xplained Pro Evaluation Kit

Win a Microchip SAM L11 Xplained Pro Evaluation Kit (DM320205) from Bodo's Power.

The Microchip SAM L11 Xplained Pro Evaluation Kit is ideal for evaluating and prototyping with the ultra-low power SAM L11 ARM® Cortex®-M23 based microcontrollers. The new SAM L11 MCU features Arm TrustZone® for Armv8-M, a programmable environment that provides hardware isolation between certified libraries, IP and application code. Microchip enables robust security by including chip-level tamper resistance, secure boot and secure key storage which, when combined with TrustZone technology, protects customer applications from both remote and physical attacks.

The SAM L11 Xplained Pro Evaluation kit features a microBUS socket and Xplained pro extension headers to expand the development with Mikroelektronika click boards and Xplained pro extension kits.

The kit also includes an on-board Embedded Debugger and a Xplained Pro Analog Module(XAM) that can be used with the Data Visualizer tool to monitor and analyze power consumption in real time.

The Pro Evaluation Kit supports all SAM L10/11 MCUs by the Atmel Studio 7 Integrated Development Environment (IDE), IAR Embedded Workbench, Arm Keil® MDK as well as the Atmel START. Microchip's QTouch® Modular Library, 2D Touch Surface Library and QTouch Configurator are also available to simplify touch development.

For your chance to win a Microchip SAM L11 Xplained Pro Evaluation Kit, visit http://page.microchip.com/bodo-saml11.html and enter your details in the online entry form.

www.microchip.com

Test&Measurement

YOKOGAWA

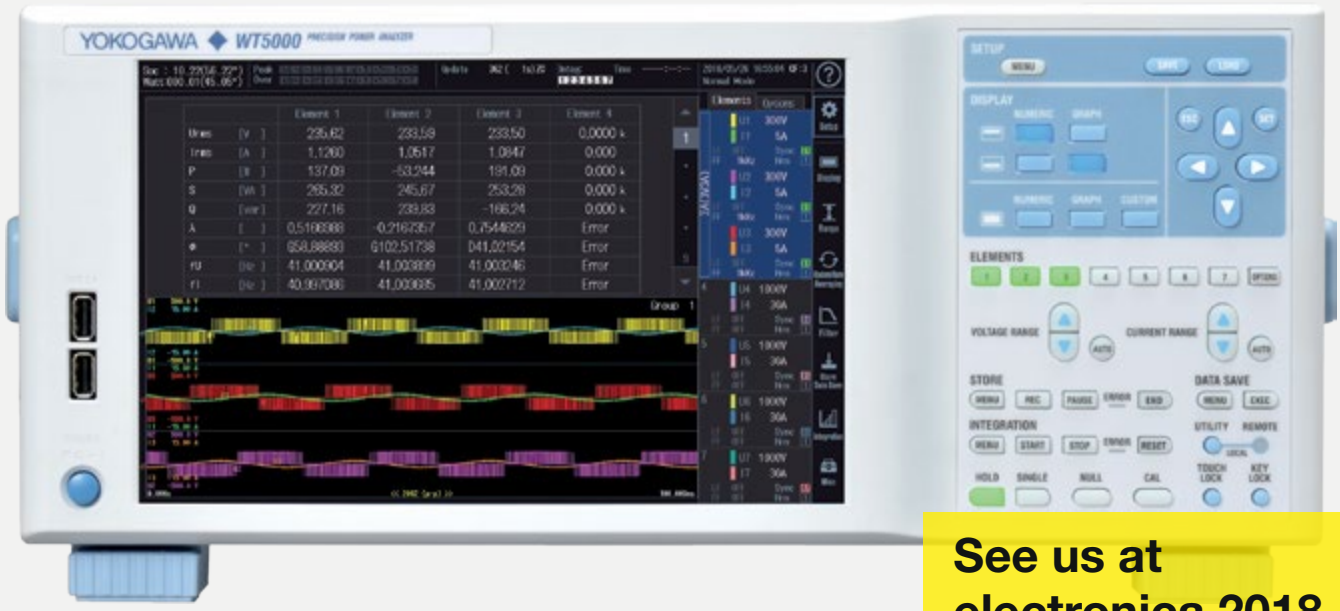

See us at electronica 2018 Hall A3 stand 117

Next Generation in Precision

WT5000 Precision Power Analyser

Meet the new WT5000 Precision Power Analyser, the extensible measurement platform that unlocks precision power analysis for electromechanical systems in electric vehicles, renewable energy, home and office appliances and industrial equipment.

- World's greatest accuracy - 0.01 % reading, 0.02% range at 50/60 Hz
- Insights from up to 7 swappable input elements
- Evaluate up to 4 motors simultaneously
- Analyse harmonics up to the 500th order for fundamentals up to 300 kHz

To unlock your precision, learn more at:
tmi.yokogawa.com:
Next Generation in Power Measurements

Precision Making

www.tmi.yokogawa.com

The Difference Between Accurate and Precise

VIP-Interview with Kelvin Hagebeuk, Marketing Manager – Test & Measurement, Yokogawa Europe

By Roland R. Ackermann, Correspondent Editor Bodo's Power Systems

Please give us a short overview about Yokogawa Test & Measurement and its position in the market.
In 1915 Yokogawa Electric Corporation was established to manufacture the first electric meters in Japan and as the foundation of its business, measurement remains an important and valuable division.

Today, Yokogawa's test & measurement business provides high quality, reliable measurement solutions across the globe. It offers a wide product portfolio from compact, entry-level power meters to the world's most accurate precision power analyzers.

Yokogawa's test & measurement business is positioned in the market as a strong, reputable organization that understands the needs of scientists and engineers. Yokogawa takes pride in its reputation for quality and level of service it provides to clients.

Key industries include automotive, telecommunications, energy generation, sustainable energy and transportation. These industries demand high-accuracy and precision measurements, along with stability and reproducibility.

What is your company philosophy?
Based on our founding principles 'Quality first, pioneering spirit and contribution to society' this philosophy conveys Yokogawa's social mission and sets out the values that guide the actions of its people.

Governing its corporate activities, these principles aim to ensure Yokogawa continues to live up to the ideals of its founders. As a company, its goal is to contribute to society through broad-ranging activities in the areas of measurement, control and information.

Why do you think – as you claim – Yokogawa Test & Measurement is the world's most trusted measurement partner?
Yokogawa's test & measurement business is the world's most trusted measurement partner because it has pioneered new technologies and kept abreast of evolving standards used in the measurement industry.

Our team of highly experienced and dedicated engineers have positioned Yokogawa's test and measurement business as the leading and unmatched measurement partner. We believe that precise and effective measurement lies at the heart of successful innovation and we have focused our R&D on providing the tools that researchers and engineers need to address challenges great and small.

You make a difference between accurate and precise – what do you mean by that?
A measurement system can have multiple scenarios: - Accurate but not precise, or, precise but not accurate, or accurate and precise or inaccurate and not precise.

It is only when a measurement system is considered both accurate and precise is it valid and fit for purpose. If you measure once and are very close to the known standard you are accurate. If you can do it repeatedly to the same closeness over a period of time your instrument is precise.

We are known for being 'precision makers' and by that we mean we are committed to making the most reliable instruments that operate with the highest level of certainty in the readings taken over their lifetime.

How is your product and service portfolio composed and what are your top priorities, at present and in the future?
Our product and service portfolio is composed of precision power analyzers, data acquisition systems (including ScopeCorder), oscilloscopes, data loggers, handheld measurement devices, and optical test equipment.

Our top priorities include the recent groundbreaking next-generation WT5000 Precision Power Analyzer. The WT5000 is the world's most accurate precision power analyzer and the first of a new generation of precision power analyzer that offers exceptional measurement accuracy of ± 0.03% combined with stability, noise immunity and plug-in modular flexibility. This product has been developed to meet the measurement needs of today's developers of energy-efficient systems.

WT5000 has a flexible, modular design which has been developed as a long-term solution. This versatile and adaptable platform adapts to changing markets and specific application requirements.
Yokogawa continuously keeps ahead of market requirements which include increased switch frequencies of power conversion devices and the requirement to build efficient and effective products.

a) How is the measuring instrument market developing overall?
b) Where within this market do you see your position and your particular strengths now and in the future?
(a) There are a number of factors that are driving the development of the measuring instrument market. These include governmental and social pressures, which are increasingly demanding new solutions that are more efficient at using energy.

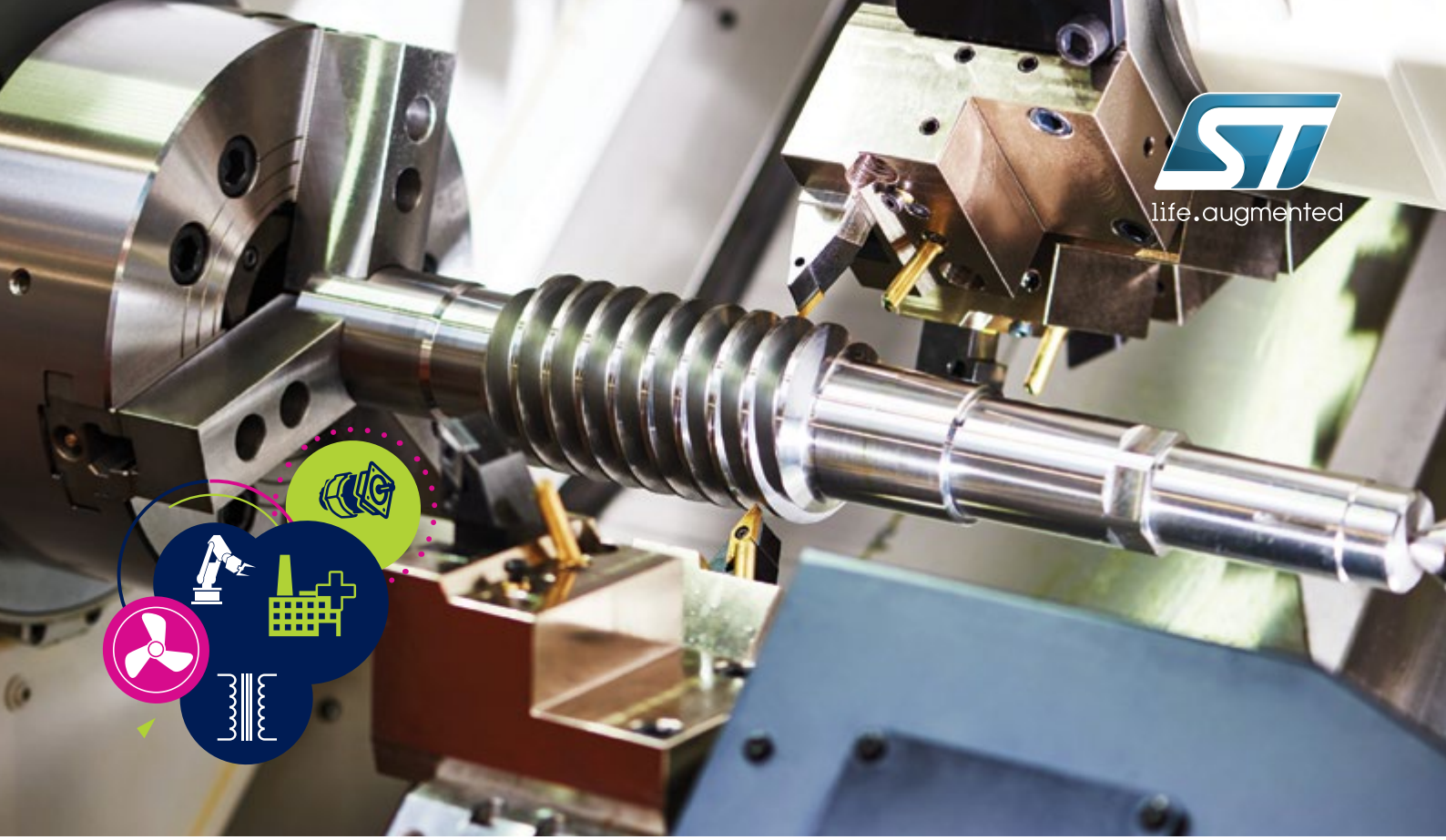

STGAP Protects Your System in Challenging Industrial Applications

ST galvanic isolated gate drivers for MOSFETs, SiC FETs & IGBTs deliver outstanding robustness, noise immunity & design flexibility

- Able to withstand up to 1.7 kV, while maintaining good noise immunity and low switching losses
- Ideal for high-power applications, thanks to rail-to-rail outputs and sink/source current capability up to 4 A
- Fully protected by UVLO circuit and thermal shutdown, along with interlocking function
- Flexible options with Miller clamp or separated outputs to optimize the tradeoff between turn-off speed and induced turn-on phenomenon

STGAP isolated gate drivers are the perfect solution for industrial drives and fans, welding equipment, DC-DC converters and battery chargers

Part number	Option	Voltage max (V)	Output current max (A)	Common-mode transient immunity (V/ns)	Supply voltage max (V)	TTL/ CMOS logic inputs (V)	Propagation delay (ns)	Additional features	Package
STGAP2SCM	Single channel, Miller clamp	1700	4	± 100	26	3.3, 5	80	UVLO, thermal shutdown and interlocking function	SO-8
STGAP2SM	Single channel, separated outputs								
STGAP2DM	Dual channel, separated outputs								SO-16

For further information and full design support, visit us at **www.st.com/stgap**

Both the automotive and energy industry are key markets looking to address these environmental issues with effective measurement instrumentation solutions. In the pursuit of improvements, engineers require more precision and certainty. They are also looking for solutions that can replicate laboratory conditions in the field.
New technologies such as 5G are also demanding more and more accurate measurement data.

(b) Yokogawa T&M is positioned as the world's leading and most trusted provider of quality measurement solutions. Its instruments are renowned for maintaining high levels of precision and for continuing to deliver value far longer than the typical shelf-life of such equipment.

We believe precise and effective measurement lies at the heart of successful innovation - and have a research and development program headed by a team of researchers and engineers who are addressing these challenges. Our particular strengths are in quality, both in terms of the products delivered, and the level of service and advice provided to clients.

In addition, Yokogawa has its own European standards laboratory which is the only industrial (i.e. non-government or national) organization in the world to offer accredited power calibration, at frequencies up to 100 kHz. Yokogawa has achieved ISO17025 accreditation which further demonstrates the competency and capability of its laboratory.

Which market segments are the most demanding drivers for measuring instruments? (e.g. Automotive? Automation? Autonomous vehicles? Medical?)
All market segments require ongoing and continual improvement in efficiencies as quality and performance are a prerequisite in these sectors.

The measured value must be reliable. It is not acceptable for a measuring instrument to measure only on given days. It must obtain the same value over intervals of time, regardless of the environmental conditions it must endure.

In respect to automotive, a big drive for manufacturers who are developing E-drives is reducing the effective powertrain loss, currently at approximately 10-20%, which will increase the efficiency and therefore the range of the vehicle.

Yokogawa helps engineers to develop individual components that are more efficient, and which collectively create a complete system that has high performance and achieves the highest possible efficiency. Understanding these efficiencies and performance requires access to accurate, stable and precise measurement data.

To achieve some of the goals, instruments will need to take measurements across many different vectors. As an example, in the case of an electric vehicle, being able to characterize the performance of each propulsion motor at the same time is key to understanding the performance of the overall systems and not just the individual motor.

What is driving the development of measuring instruments:
- **Technological complexity, efficiency, automated test runs, measuring speed?**
- **Or is it smaller and higher integrated electronic components and sensors, big data, increasing accuracy demand, bandwidth to transfer ever more data over the air, higher frequency ranges?**
- **Or user-friendliness?**

Looking at the development goals for the WT5000 there were three key areas:

Reliability:
Reliability is a key requirement, in particular, the ability to produce accurate and stable measurement data over a prolonged period of time. Trust in this data must be achieved.

Versatility:
Market requirements continuously evolve. The flexible architecture of the WT5000 enables us to be versatile and flexible within ever-changing market requirements.

Simplicity:
The WT5000 provides ease of operation with features such as a touchscreen display. So whether a user has worked with power analyzers for years, or they are a new engineer, we provide ease of use and excellent functionality.

The latest semiconductor developments are enabling faster switching speeds. This generates higher frequency content which requires wider bandwidth for power measurement. In our European standards laboratory, we provide ISO17025 accredited calibrations for power analyzers up to 100kHz.

Is the functionality more than before defined by software?
a) Must the customer buy software options, or will SaaS become increasingly important?
b) Are you striving to minimize hardware, especially the mechanical overhead, e.g. by eliminating connectors and backplane?

(a) There is an expression that 'software is eating the world'.
At the instrument level, we see a trend for future instruments whereby new analysis features will also be made available as software modules. At the same time, instrument hardware will become more flexible and modular allowing for one instrument to be quickly configured for different tasks extending its operational envelope. Together they provide not only flexibility, but a more cost-effective way of configuring an instrument with the exact requirements.

In respect to SaaS, we do see a need to collect data from multiple instruments so we can carry detailed analysis on the conditions detected. This may be a complex system, large facility or even globally.

(b) Precision hardware will continue to be important in ensuring our customers have reliable data. We continually review what is required and make sure our products deliver, whilst being aware of the need to minimize hardware. Yokogawa continuously reviews its product portfolio to ensure products deliver accuracy with maximum stability. If this requires certain hardware to achieve this, we will utilize it.

Do cloud-based solutions, and in the near future 5G, play an important role in this context?
As 5G transitions from standard development to implementation, networks need to make sure they deliver the potential we are all expecting for the next generation of fast mobile communications. This will not only be in the main infrastructure, but any pieces of equipment connected to it will need to be certified.

In respect to measurement, the compliance measurement setups will need to be taken into the field which requires new high precision and accurate portable instruments.

Not only do we provide the instruments to accurately measure the network hardware (power analyzers and oscilloscopes) we also offer a range of Optical Time Domain Reflectometers (ODTR) for checking the fiber connections that form the backbone of the network. Yokogawa also provides high-end optical measurement equipment, such as Optical Spectrum Analyzers (OSA), which has enabled the development of next-generation optical communication network components used by telecommunications suppliers.

What will the price development be like?
Yokogawa provides customers with state-of-the-art products and solutions which enable them to develop efficient, high-quality systems. These systems can be used today, tomorrow and into the future. As a result, customers receive value for money and a competitive lead in increasingly competitive markets.

www.tmi.yokogawa.com/eu

Getting Innovative Designs to Market Faster and Easier

VIP-Interview with Graham Maggs, VP Marketing Europe, at Mouser Electronics, about the company's position in a worldwide distribution environment with a focus on power electronics.

By Henning Wriedt, US-Correspondent Bodo's Power Systems

Henning Wriedt: Mouser was founded in the early 1970s. Very brief: Which were the major milestones in the company's history until today?

Graham Maggs: What began as a small high school electronics program by Physics teacher Jerry Mouser in 1964 in El Cajon, California has grown to become what Mouser Electronics is today. This start-up, originally called Western Components, laid the groundwork from which Mouser Electronics was formed in 1973, the same year Glenn Smith joined the company and began his career with Mouser.

Ten years later, in 1983, Mouser Electronics moved its headquarters and distribution centre to Mansfield, Texas. The move placed Mouser in the middle of a growing high-tech industry in the Dallas/Fort Worth Metroplex. Being only 30 minutes from the DFW International Airport gave Mouser an important distribution advantage for serving North America and extending its reach worldwide.

In January 2000, Mouser's success caught the attention of TTI, Inc., the world's leading authorized distributor specialist offering passive, connector, electromechanical and discrete components. Mouser became a TTI subsidiary and together, the two offer the ideal distribution solution for design engineers and production buyers in the electronics manufacturing industry. With Mouser's focus on new designs combined with TTI's expertise in volume distribution, the two companies provide the complete answer from the design chain to the supply chain.

The success of the Mouser/TTI partnership caused Warren Buffett, Berkshire Hathaway's Chairman of the Board, to take notice of the two companies. In March 2007, the acquisition by Berkshire Hathaway Inc was finalized, positioning TTI and Mouser for the long-term. Both companies gained the added recognition and financial strength from one of the most successful companies in the world. Today, Mouser continues to grow globally focusing on providing the widest selection of the newest products that gets innovative designs to market faster and easier.

Henning Wriedt: Why is Mouser headquartered in Mansfield/Texas and not in the Silicon Valley?

Graham Maggs: As detailed above, Mouser started in California then moved to Texas to be in the middle of a growing high-tech industry in the Dallas/Fort Worth Metroplex. Being so close to a major airport complex enables Mouser to service the world from one global warehouse, and there is a ready pool of talent which is always required as Mouser is continually adding to its headcount.

Of course, Texas Instruments - one of Mouser's key lines is close by, as is Mouser's parent company, TTI. Silicon Valley is a fantastic and vibrant centre, but most distributors are headquartered in more 'economically reasonable' places. It is rare to find a large warehouse facility – for example – in Silicon Valley purely because the value of real estate is so high. Our facility in Texas provides a same day shipping and next day delivery service in the US; and 2-3 day delivery service in EMEA.

Henning Wriedt: TTI and Mouser "provide the complete answer from design chain to supply chain". What do you mean by that?

Graham Maggs: According to a press statement given by my colleagues, Mark Burr-Lonnon, Senior VP Global Service, EMEA & Asia Mouser Electronics and Geoff Breed, TTI's VP European Marketing at Electronica a couple of years back, the two companies are complementary. Breed: "Under one umbrella we have two organisations that cover the customer's total needs with complementary structures and solutions. From the supplier's perspective it's similar: combined we provide a proven vehicle for new product introductions, a complete go-to-market solution - reliable partners who understand the needs of the supplier and can deliver that to the customer."

Burr-Lonnon explains the different approaches: "Mouser is the Global NPI specialist with great on-line tools, search engines, e-commerce, broad inventory, high semiconductor and engineering-based web content. We offer small volumes on a quick turn-around to support design activities. But when the project moves into volume production, it's more difficult for the high service model to flourish due to the greater depth of inventory needed, sophisticated logistics programs, inside and and outside sales support."

Vincotech

MORE POWER LESS SPACE

SOLAR UPS SMPS

Upgrade your three-phase solar inverters to the next class.

Engineered for high power density, Vincotech's latest three-phase NPC modules will put your next solar inverter on the fast track to the highest performance class for size, efficiency and weight.
Our new *flow*3xNPC 1 modules combine the latest IGBT technology and enhanced thermal packaging to deliver the best performance across a wide range of loads.

The new 1200 V 30 A and 50 A modules are housed in a 12 mm, low-inductance *flow* 1 package.

Main benefits

- Optimized for three-phase solar applications
- Compact solution increases power density and reduces system weight
- Highly efficient three-level NPC topology maximizes ROI
- Lower system cost with reduced filtering and enhanced thermal performance
- Entire range from 7 kW to 20 kW available now

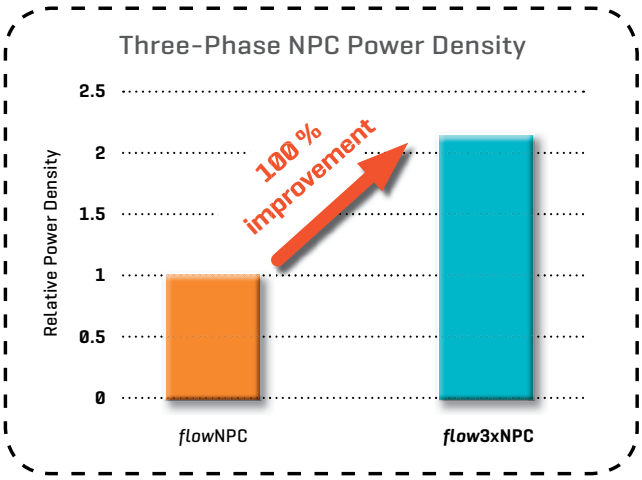

www.vincotech.com/3xNPC-1

EMPOWERING **YOUR IDEAS**

Breed picks up the narrative: “TTI offers engineering support but in a different and again, complementary way. In many cases, the design cycle starts with the Mouser model and then, as the customer project develops, TTI steps in at an engineering level to offer the face-to-face support where an engineer can discuss solutions, or meet with a supplier. This is why we keep TTI and Mouser as separate entities, while some competitors continually try to merge two very complex and different models.”

Suppliers, apparently, react very well to the synergistic relationship between TTI and Mouser. Breed: “Because the combination offers them the right path to market - whether its small volume, NPI, engineering support, pro-active marketing, breadth and depth of inventory or local sales team support - they really like it. They can work one product program through our two models and achieve their goals.” Adds Burr-Lonnon: “We provide customers with a seamless ‘design chain to supply chain’ service, and our suppliers see very real benefits. Our model is unique and that’s what customers and suppliers love. Together, our joint approach ensures that customers get what they want - which is, after all what suppliers want too. ”

Henning Wriedt: What kind of impact had the takeover by Berkshire Hathaway in 2007 for your company?

Graham Maggs: Berkshire Hathaway has a small board and a very flat hierarchy. It has a policy of buying successful businesses that share a common philosophy, but leaving the existing management in place, allowing them to follow the same approach that made them successful in the first place. So, Paul Andrews is still the head of TTI, and Glen Smith is CEO at Mouser. All other key staff stayed after the ‘07 acquisition too.

From Mouser’s point of view, being part of Berkshire Hathaway has enabled us to continue to invest in large, freely-available stocks, which mean that designers can access new technology and components faster than through other distributors. Berkshire Hathaway has enormous resources so we are able to fund significant warehouse expansions as the market demands.

Henning Wriedt: You are a distributor for more than 700 manufacturers. How can you and your customers stay current with products and technologies, without overloading the various information channels? Is AI going to help?

Graham Maggs: We are very anxious to ensure that we only provide information to our customers that is useful to them in their current role. Therefore we try to understand the profile of our customers so that we can better serve them. Our role is to be the ‘New Product Introduction’ (NPI) distributor, offering all the latest technology, therefore we need all the major names as well as the interesting start-ups. Our website is very important in the respect and we spend a great deal of time ensuring that it is easy to use and full of good design-in information.

AI is impacting our lives in so many ways already, and information dissemination is one of the most obvious – eg Siri, Alexis, Google Home and others. It would be possible to envisage an AI system where engineers could ask specific questions relating to technology, applications or products. The AI system would search the company database and provide answers. But Mouser is not introducing such a system yet.

Henning Wriedt: You are a worldwide distributor. How do you manage different countries, different languages, and different locations for same day shipments?

Graham Maggs: My colleague, Mark Burr-Lonnon, Senior VP Global Service, EMEA & Asia Mouser Electronics, has described Mouser as a ‘marketing company that happens to deal in Electronics’. Our aim is to get parts to our customers in two to three days from one central warehouse, so we have to be very good at logistics. Have a look at the video “Mouser by the numbers”, which provides a lot more stats!

Yet although we only have one warehouse, we have many other branches worldwide whose task is to be close culturally, linguistically and physically to customers. Currently we have offices in 23 locations so customers can talk to someone in their own language on the same time zone and deal in the local currency.

Henning Wriedt: Over time: How important are power electronics components for you and your customers?

Graham Maggs: As one famous commentator once said: “Everything needs power.” We have separate technology sections on power – low power, power management and power supply – which provide design notes, articles and other resources. As you note in your next question, we have a significant number of power products from all the world’s key manufacturers – including the recent addition of Linear Technology (through Analog Devices), so we consider power to be a very important topic, an opinion that I am sure you share!

Henning Wriedt: You are listing more than 56000 power management ICs. How do electronic designers, with just specific interests in power electronics, get through this huge amount of information?

Graham Maggs: Of course it is a challenge, but our mission is to provide immediate access to as many components as we can, so having all the information clearly presented in one place must be an advantage for engineers. The web site has sophisticated search algorithms which help users to find the best part(s) for their application, and we can cross-reference alternatives too.

Henning Wriedt: Which market segments and which regions are right now high in demand of power electronics, and which power products are benefiting from this trend?

Graham Maggs: As we have said before “everything needs power” so there is high demand across the board. However, the emergence of electric and hybrid vehicles is sucking up huge quantities of every type of power component. Asia is a huge user in this field and others too, especially smartphones. Another significant market for power components of all types is the IoT – (Smart Factory/Industry 4.0, Smart Home, Smart Office, Wearables, Connected Auto, Remote Diagnostics etc. etc.).

Henning Wriedt: According to market experts, “power modules are anticipated to exhibit the highest growth”. Do you agree?

Graham Maggs: We do not have figures for the growth of all types of components, but certainly our website traffic would indicate that power modules are very interesting for our customers. GaN and other wide bandgap devices also attract a lot of interest.

Electronic Concepts

Film Capacitor Innovation Without Limits

A SWEET SOLUTION

for Resonant Power Supply Capacitors.

5PT SERIES "SUGARCUBE"

Polypropylene Film Capacitor.

Specifically designed to meet higher current carrying requirements of resonant power circuits.

5PT SERIES FEATURES

- ☑ Minimum inductance, lower impedance and ESR
- ☑ Compact configuration
- ☑ Direct plug-in spade lugs

Visit us online at **www.ecicaps.com**

North America: sales@ecicaps.com **Europe:** sales@ecicaps.ie

Henning Wriedt: How does your new BOM Tool operate, and how is the acceptance of these tools like browser and MS-Office add-ons in the worldwide market?

Graham Maggs: FORTE is a comprehensive, intelligent BOM tool that quickly evaluates millions of parts to improve order accuracy, save time and increase confidence in specifying and purchasing semiconductors and electronic components. It is free to anyone with a 'My Mouser account', and was created to provide a better experience and help speed up part research and purchasing. Key Features are:

- New look featuring an easy-to-understand interface with clear steps for processing ease
- Time-saving, one-step BOM spreadsheet importer that maintains your original format
- Access millions of orderable part numbers on online
- Easily add and delete parts, plus see multiple quantities and prices without exporting
- Analyzes partial part numbers and descriptions to intelligently suggest parts
- Part match confidence and design risk indicators help you match and choose the best parts for design
- Recommends alternative products to reduce design and product lifecycle risks

Henning Wriedt: How do you keep the quality of your components high and fake ones out of the delivery system?

Graham Maggs: That is a very simple question to answer. We NEVER buy from anywhere else apart from our franchise manufacturing partners, who have all the component quality approvals in place.

Henning Wriedt: Can electronic designers study on your website about new technologies and trends, like SiC, GaN, IEGT and Wide Bandgap? How about tutorials and white papers?

Graham Maggs: Yes, you can search under products for all those categories and for more detailed information, go to the 'Applications and Technologies' part of our website and click on 'Wide Bandgap' where you'll find articles white papers, and other resources from leading manufacturers.

Henning Wriedt: How do you stay on top of environmental issues?

Graham Maggs: At Mouser our environmental policy encompasses lead-free and RoHS, WEEE, packaging waste, and proper disposal of batteries and chemicals. We also work closely with our manufacturers and customers to support their recycling and disposal efforts and encourage all of our customers to recycle old catalogues.

Mouser Electronics is committed to diligently addressing all environmental issues that face the electronics industry and our customers - both domestically and globally. Our environmental project encompasses not only Lead-Free and RoHS, but also WEEE, Packaging Waste, Batteries and Chemicals and any other directives or legislation that appears in the future.

As a distributor of electronic components, equipment and supplies, Mouser intends to properly identify all environmental aspects of the products we carry. We are committed to include accurate and traceable identification to part numbers via certified documentation from our producers (a.k.a. manufacturers). In addition, we will prevent the mixing of products with different environmental aspects through strict inventory control and conservative return policies.

Additionally, we want you to know that Mouser and its manufacturers are working together to assure our customers that all products are in compliance with existing directives and legislation.

Henning Wriedt: One of your European competitors complains about very thin margins, because he sees his company in an unpleasant sandwich position between vendor and end customer. What is your take on this?

Graham Maggs: That's an interesting view, and I would love to know which distributor said that (although I have my suspicions). Mouser's position is that if you provide a valuable service you will be able to charge for it. Let me continue: you say 'one of our competitors', but Mouser has very few direct competitors, because we only operate in the design fulfillment space.

We do not (by and large) supply high volumes of parts for production orders - I know that for companies that focus in this area are continually under price pressure. We focus on supplying the latest parts to design engineers in small quantities very quickly so they can begin a new project using the latest technology. Our customers and manufacturing partners understand our niche and our business is growing at an extremely fast rate, so we must be doing something right!

Henning Wriedt: The World Economic Forum is expecting these technologies in the near future: 2-D electronics, organic electronics, memristors, spintronics, molecular electronics. If this is going to happen, are you prepared for these challenges?

Graham Maggs: Mouser spends a lot of time researching new companies that are offering real solutions. As soon as a company has an innovative part it can sell, we are interested in stocking it. But more than just stocking it, we will promote, support and bring it to the market supported by technical and application information.

Visitors and customers coming to our site can access a huge wealth of information, application and technology news ... just sign up to receive Mouser's Newsletters, including our NPI and Electronics Industry Update magazines.

Maggs, an industry veteran with over 28 years of experience in European and global roles, joined the Mouser team in April 2010 and has been instrumental in building Mouser's EMEA marketing team that spans supplier marketing, web marketing, advertising, public relations, media and events.

Graham Maggs,
VP Marketing Europe, Mouser Electronics

Maggs has directed, built and elevated the Mouser brand across EMEA into a key industry position, overseeing significant growth since 2010. The global distributor has excelled under his leadership, with highly successful EMEA exhibitions at Embedded World and Electronica in Germany, and more recently the Maker Faire events in Italy and Germany. Maggs is a key industry face of Mouser in EMEA and is invited to speak at many industry events on Mouser's behalf.

www.mouser.com

Automotive | Home Appliances | Industrial | Power Transmission | Renewables | Railway

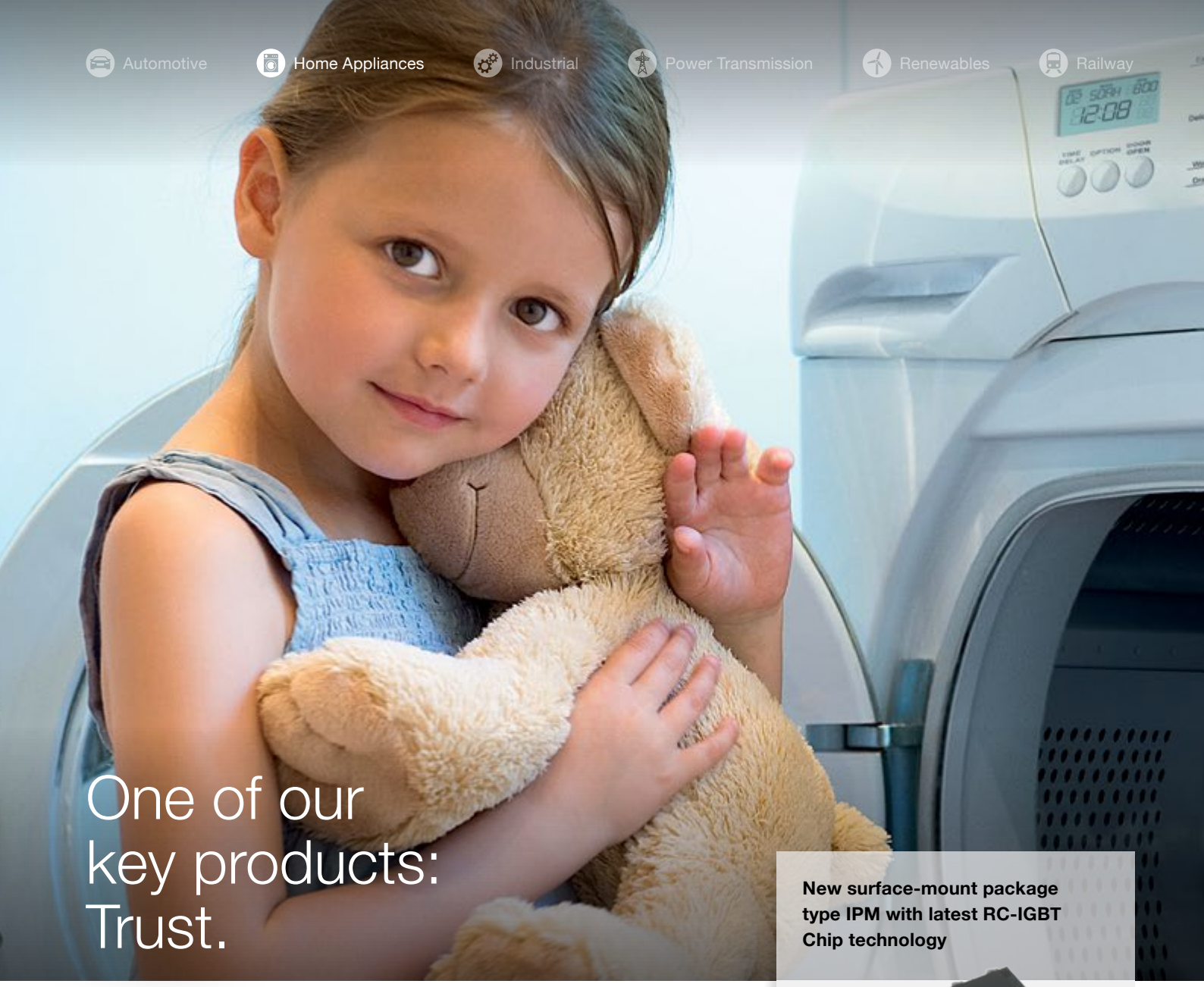

One of our key products: Trust.

Power Devices from Mitsubishi Electric.

Home appliances are becoming more and more demanding regarding functionality, reliability and efficiency. In the field of Power Semiconductors Mitsubishi Electric had created the necessary basis already 20 years ago as the pioneer of the DIPIPM™ Transfer molded package intelligent power modules, followed by the continuous development and expansion of this series. Consequently, with the new MISOP™ a surface-mount package Intelligent Power Module has been added to the line-up to realise compactness and easy assembling in small power inverters for pumps and fans. Also low power servos in industrial applications can be covered. The versatile integrated features are designed to give the benefit of reduced development time for the complete inverter system.

New surface-mount package type IPM with latest RC-IGBT Chip technology

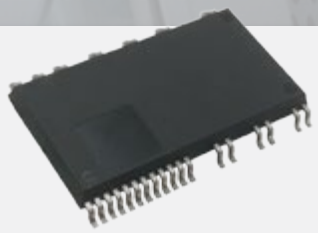

The MISOP™ Surface-mount Package IPM

- Optimized terminal layout enabling simple and compact PCB design
- Integrated driver ICs (HVIC and LVIC)
- Integrated bootstrap diodes and capacitors
- Short circuit protection through external shunt resistor
- Power supply under-voltage protection: Fo output on N-side
- Over temperature protection
- Analog temperature voltage signal output
- Interlock function

eco Changes **for a greener tomorrow**

More Information:
semis.info@meg.mee.com
www.mitsubishichips.eu

Scan and learn more about our Power Semiconductors on YouTube.

MITSUBISHI ELECTRIC
Changes for the Better

nHPD^2 Power Modules - Where Innovation Meets Requirements

Our next generation High Power Dual Modules provides a standardized, scalable and high-performance solution providing reliability and power density

More than two decades ago the first high voltage IGBT based power module was introduced and is today an industry standard used for traction, motor drives and renewable energy applications. With increased requirements regarding temperatures, switching frequencies and higher power density combined with reduced system costs and enhanced reliability arises a new solution. The new industrial standard package introduced by Hitachi, named nHPD^2. The nHPD^2 package implies an evolution for medium voltage power converter design.

By Michael Sleven, Hitachi Europe Limited

Lowest stray inductances enable optimized performance for both SiC and Hitachi's Side Wall Gate IGBTs, allowing the market to choose the best solution for their particular design challenge and set up in the range of 1700V up to 6.5kV.

The nHPD^2 Package

The nHPD^2 Series provides high function half bridge power modules, incorporating temperature sensors and current sense terminals for optimum design performance.

The series offers a dual package outline for the full range of voltage and current ratings with same foot print but different heights to align with the transition from the established heights set by the former IHM standard, allowing for a common mechanical design and high level of design re-use for converters with different ratings. The compact form factor, high power density facilitates and robust construction enables the designer to realize industry leading converter designs.

Figure 1: nHPD^2 Series Low (left) and High Voltage Package

Product Line up

The nHPD^2 Series product line up covers from 1700V up to 6500V rated modules with current ratings up to 1200A. All products in LV package are available now as samples or in mass production.

1700V, 900A SiC – MBM900FS17AL
1700V, 1000A Si – MBM1000FS17G
1700V, 1200A Si – MBM1200GS17G2
3300V, 450A Si – MBM450FS33F
3300V, 600A SiC – MSM600FS33AL
3300V, 800A SiC – MSM800FS33AL

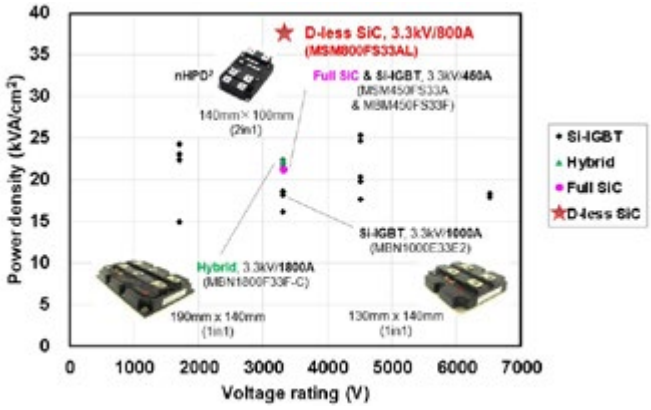

Figure 2: World's highest power density with nHPD^2 3.3kV/800A without SBR diode

The target portfolio for the HV package which will begin roll out from first half of 2019, shown in table 1.

Voltage	Current	Chip
3300V	600A	Si
3300V	600A	SiC
3300V	800A	SiC
4500V	450A	Si
4500V	600A	SiC
6500V	300A	Si
6500V	450A	SIC

Table 1: HV Target Portfolio

plexim
electrical engineering software

plecs

THE SIMULATION SOFTWARE PREFERRED
BY POWER ELECTRONICS ENGINEERS

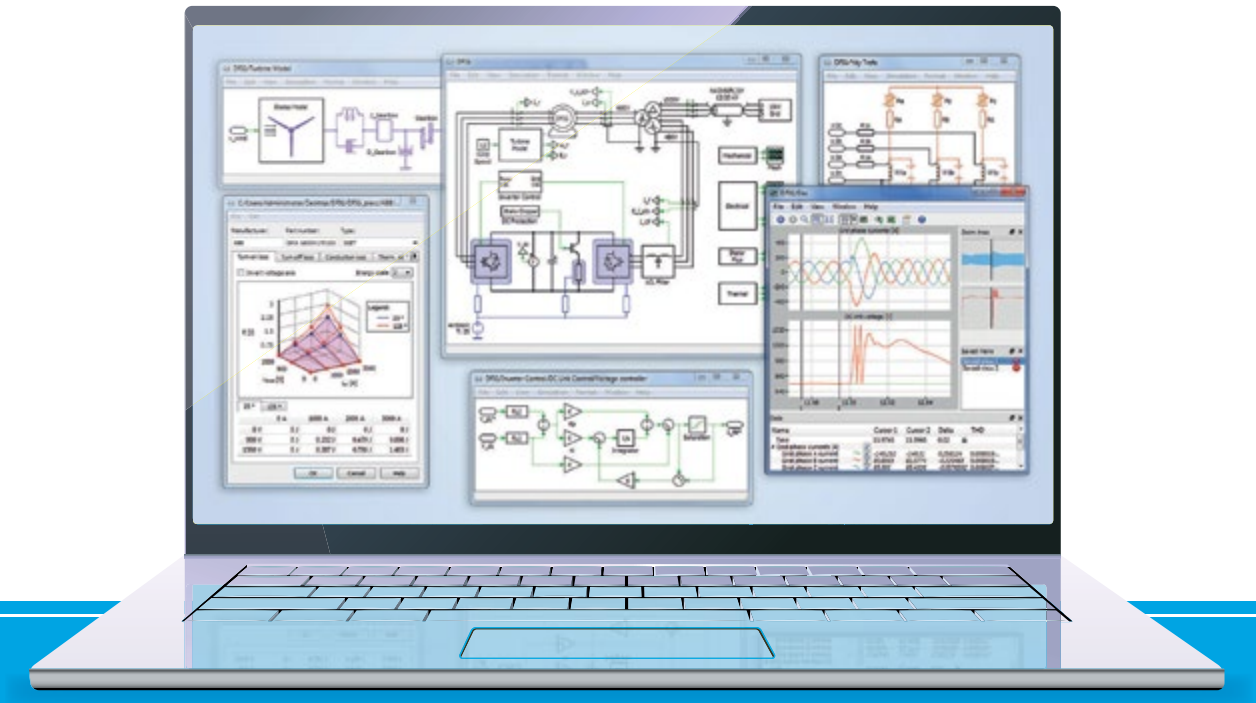

MODELING DOMAINS

- Electrical
- Control
- Thermal
- Magnetic
- Mechanical

KEY FEATURES

- Fast simulation of complex systems
- Code generation
- Frequency analysis
- Available as standalone program or Simulink blockset

Get a free test license
www.plexim.com/trial

Latest Technology

Hitachi continues to apply the latest technology breakthroughs to the nHPD^2 series to continue extending the performance envelope. The application of latest generation Side Gate IGBT, SiC, on board temperature sensing and Copper sintering for improved die attach ensure the best output power, energy losses, control and lifetime.

Low loss, high controllability – motor system cost merit

The Side Gate IGBT reduces energy losses and improves controllability compared to conventional trench IGBT. The loss trade-off can be improved with up to 35% reduction in turn off energy or 15% reduction in saturation voltage as shown in Figure 3a.

Low gate charge reduces the load on the gate driver and low reverse recovery dv/dt and voltage overshoot allows optimization of the turn-on to lower switching losses further and enable easy integration into a converter as shown in Figure 3b. Moreover, shifting to an application level cost benefit, two options may be considered. In place of a full focus on reducing system electrical efficiency (Eon+Err), there is an opportunity to trade-off the full benefit to reducing the cost of the motor or generator. Since the motor and dv/dt filter cost can be linked to the level of isolation provided, by relaxing the turn off and recovery loss performance, the switching dv/dt (kV/us) can be reduced allowing the motor specification to be relaxed and cost down to be enjoyed. For example, an existing design based on a motor with an isolation 7kV/us, by accepting the status-quo Eon+Err efficiency, the motor isolation may be down-graded to 2kV/us. Surveying common motor suppliers, we can translate this to a shift down from a motor with reinforced winding isolation to a motor with standard isolation regarding IEC/TS 60034-17. Cost merit is a factor of 2.5 which correspondents to a cost saving of 1.5k€ for a 30kW motor.

Further to motor cost saving potential, the market leading gate capacitance values (Qg) of side wall gate, offer significant reductions is the power required to drive the gate. A typical GDU rated for conventional IGBT half bridge modules rated 1400A/1700V may consume 2x10W of power per GDU. Adopting low Cres side wall gate requires only 2x5W. Translating to a monetary benefit, the cost down opportunity may be as much as 50% reduction for the GDU solution.

The reduced reverse transfer capacitance (Cres) of Side Gate IGBT leads to improved Short Circuit performance with better-controlled gate voltage and lower peak collector current. This provides a power module that is more robust under short circuit conditions and reduces the current that must be handled in the converter design.

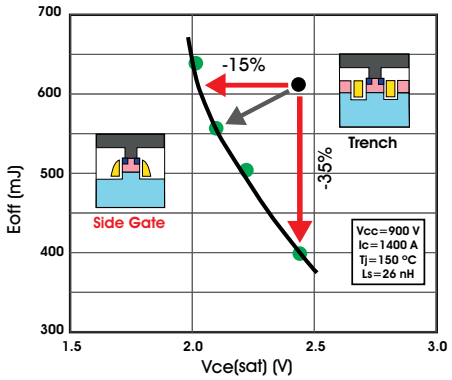

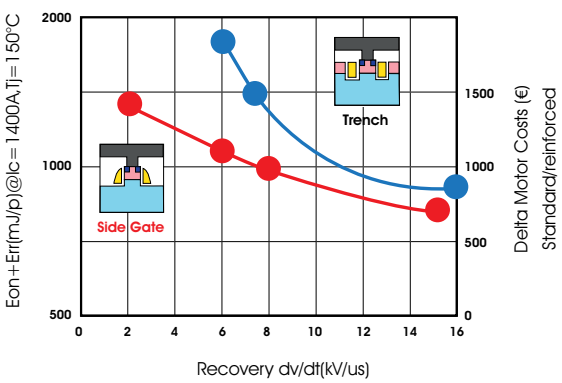

Figure 3: Side Gate IGBT performance

a. (left) Vce – Eff tradeoff

b. (right) Eon+Err –recovery dV/dt- motor costs

Maximum Lifetime and power density

The application of Hitachi's proprietary copper sintering to replace the solder layer between the IGBT chip and the substrate greatly increases the robustness of the module, in particular increasing the power cycle life by 10 times compared to standard solder. It also improves the thermal impedance of all dies and the I2t of the diodes and is providing the highest possible power density. This is particularly suited to high performance traction and wind power designs requiring aggressive acceleration and highly dynamic mission profiles, whilst ensuring total reliability throughout the lifetime of the system. Figure 4 shows the copper nanoparticles sintered to form a strong die attach joint. Figure 5 shows the cross-sectional image after power cycling of more than 400k cycles with Δj=125K and Tjmax=175°C, setting a new durability benchmark in a market used to lesser goals, like ΔTj=<100K and Tjmax=150°C.

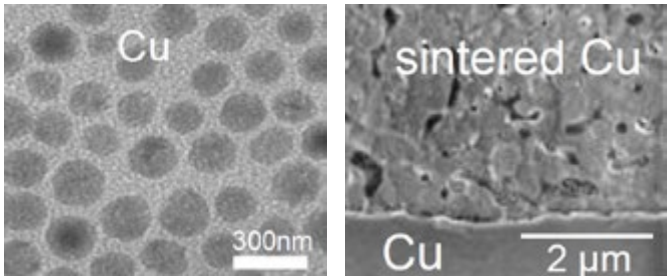

Figure 4: Copper Sintering Die Attach Process

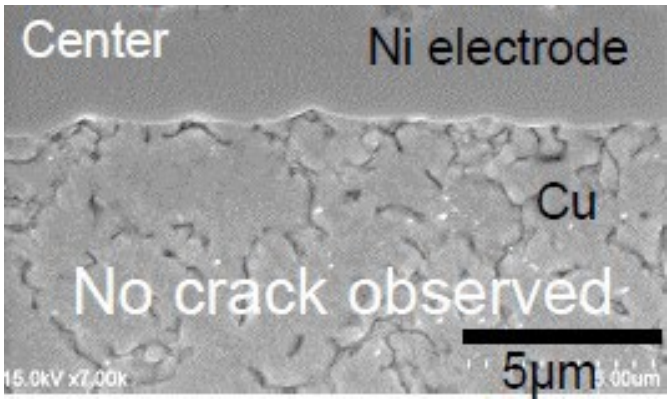

Figure 5: Cross section after Power Cycling

Next generation Silicon IGBT

The nHPD^2 is also optimized for the next generation of Hitachi's Silicon IGBT called Dual Side Gate. It is Hitachi's main strategy to offer best in class performance of Silicon IGBT and SiC MOSFET in the nHPD^2 package to make our customer systems flexible and successful. The dual side gate IGBT breaks through the conventional performance limitation of silicon. By applying dynamic carrier control, the turn off loss can be reduced by 45% compared to conventional trench IGBTs and the Eoff – Vce(sat) trade-off approaches that of SiC MOSFETs but using standard silicon processes. To break though the limitation on IGBT loss reduction, techniques

ONE CAPACITOR DOES THE JOB OF MANY IN A FRACTION OF THE SPACE.

THA: 3,000 hr. life @ 85 °C
THAS: 3,000 hr. life @ 105 °C

Highest energy density in low-profile: 1.1 J/CC

Replaces banks of SMT capacitors

Uses about 70% less board space than alternatives!

YOU CAN DO MORE WITH THA THINPACK ON BOARD.

Using the most advanced aluminum electrolytic capacitor technology, type THA and THAS offer the highest energy density in a low profile. Design-in one component versus banks of alternative SMT capacitors for incredible size and cost savings. Improve reliability with one component versus many.

CDE CORNELL DUBILIER
ENERGIZING IDEAS

For technical information and samples visit cde.com/THA

for controlling carrier concentration right before turn-off switching have been found to be highly effective. Figure 6 shows the simulated stored carrier density distribution and performance of VCEsat and Eoff on a cutting-edge side gate HiGT for high and low hole injection structures. Tuning the p-collector dose concentration enables controllability of conductivity modulation in the drift layer. However, the carrier density near the emitter surface cannot be controlled effectively due to injected carrier from the accumulation layer of the MOS gate. This accumulated carrier leads to large turn-off current during turn-off switching and then limits the IGBT Eoff from being reduced further. As the method of breaking though such a limitation, we consider the ideal stored carrier profile, shown in Figure 7. In the conduction state of the IGBT, a large amount of carriers should be stored for low VCEsat, while right before turn-off switching, the stored carrier concentration near the emitter surface region of the drift layer should be reduced to promote depletion of the drift layer, reducing the turn-off current for low Eoff. By applying this idea, Eoff is lowered while maintaining low VCEsat, thus breaking thorough the conventional limitation of an IGBT: conduction versus switching loss trade-off performance.

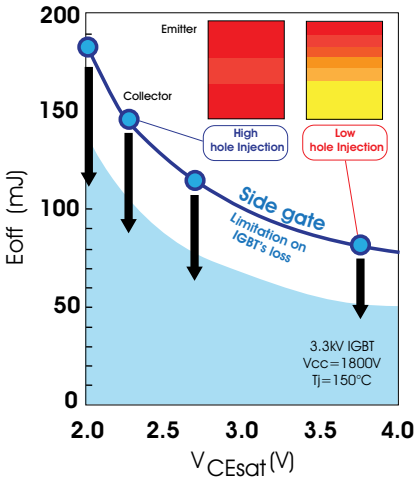

Figure 6: Simulated carrier distribution of hole for leading-edge side gate IGBT

Figure 8 shows a schematic cross-sectional view of the dual side-gate HiGT structure.

Driving the two independent gates enables effective controllability of conductivity modulation. In conductive mode, both side gates act to inject a large amount of electrons, thereby reducing VCE(sat). In advance of a switching event, one of the two side gates are turned off while the other gate remains in the on-state to reduce the amount of stored carriers, thereby enabling faster switching during the final turn off. Aside of the key dual gate channel feature, the merits of the standard side wall gate structure equally apply. This means low Miller capacitance, easy drive and reduced short circuit peak currents, each of which contribute to enhanced device and system durability. Simulating the dual side-gate HiGT, figure 9 shows the simulated stored carrier distribution in the conductive mode (VGsE/VGcE = +15 V/+15 V) and switching mode (VGsE/VGcE = +15 V/-15 V). In the conductive mode, electrons are injected from both gates and the stored carrier concentration near the emitter region is increased by the generated conductivity modulation effect. On the other hand, stored carrier density at the surface emitter region is decreased by one-side gate turn-off control. Figure 10 shows the simulated output characteristics of the dual side gate HiGT. After trial fabrication, the dual side gate solution in conductive mode, realized less than 2.7V VCE(sat), showing a 6.0% reduction compared to the best in class MBN1800F33F trench gate (2.85V @ Tj=150°C), despite conduction loss being the secondary performance target, with switching loss reduction the primary goal.

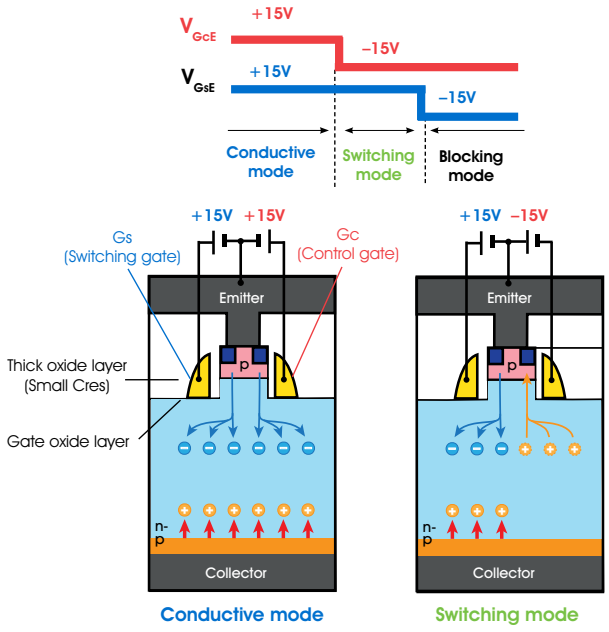

Figure 8: Concept and structure of proposed novel dual side gate IGBT

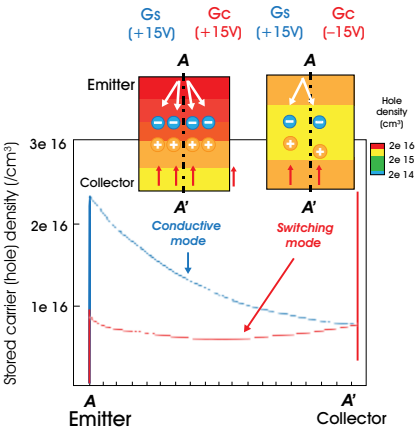

Figure 9: Simulated stored carrier distribution for dual side gate IGBT

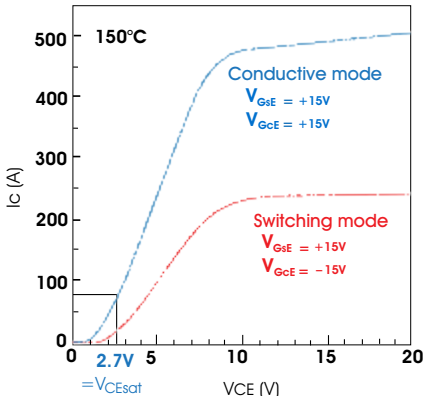

Figure 10: Simulated output characteristic on dual side gate IGBT

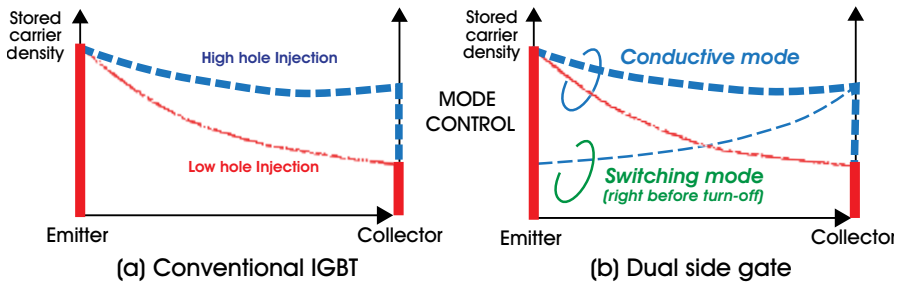

Figure 7: Carrier distribution with low density for low-loss performance

Next, turn-off switching characteristics of the dual side-gate HiGT were simulated. Figure 11 shows the applied gate input signals and the obtained turn-off waveforms the timing delays for Gs and Gc signals (tdelay). As tdelay increased, a higher speed turn-off waveform is obtained. This is the direct effect of reducing the stored carrier concentration using Gc control and tdelay right before the turn off signal of Gs. Table 2 summarizes the simulated stored carrier profiles after the elapsed tdelay i.e. after Gc negative gate bias (-15V) is applied. It also highlights the effect on conduction loss during tdelay (Econd), turn-off switching loss (Esw) and total Eoff (Econd+Esw). As tdelay increases, a decrease of stored carrier concentration and an increase of Econd is observed, whilst showing a dramatic reduction of Esw. Thus, the proposed dual side-gate HiGT had 31% lower Eoff than the conventional single side gate HiGT with a 40µs tdelay drive profile.

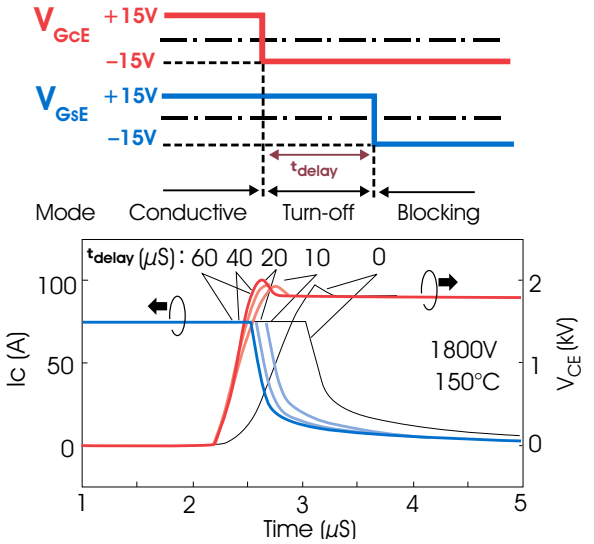

Figure 11: Turn-off drive signal and simulated turn-off waveform of dual side gate IGBT

t_{delay}	0 µs	10 µs	40 µs	60 µs
Stored carrier profile right before turn-off (Hole density (cm³): 2e 16, 2e 15, 2e 14)	Gs (+15V) Gc (+15V)	Gs (+15V) Gc (–15V)	Gs (+15V) Gc (–15V)	Gs (+15V) Gc (–15V)
VCEsat right before turn off (V)	2.7	3.5	4.3	4.4
Increase in conduction loss during delay: Econd (mJ)	0	3	11	18
Switching loss: Esw (mJ)	125	96	76	74
Total turn off loss: Eoff (mJ) (Econd + Esw)	125 (100%)	98 (78%)	87 (69%)	92 (73%)

Table 2: Simulated Eoff dependency on tdelay

Next generation SiC "TED-MOS"

Hitachi also brings SiC MOSFETs to industrial applications to further drive efficiency improvements in the nHPD^2 package. Hitachi's proprietary next trench SiC MOSFET technology "TED-MOS" uses a special trench etched double diffused structure to offer leading performance with low energy losses and improved short circuit durability over standard DMOS and trench MOS.

The structure of TED-MOS ensures a robust and reliable chip that is easy to control. Both Drain-Source resistance and switching losses are reduced compared to SiC DMOS and trench structures. Most notable is the electric field around the trench, reduced compared to conventional trench structures to give a more reliable chip. Short circuit current is also better controlled, resulting in a short circuit durability that is similar to standard silicon IGBTs at ≥10µs. This per-

formance withstand capability is setting new standards in the SiC market, especially when compared to the more modest value of 3-5µs for most existing SiC products in the market today. Rather than shifting from standard proven detection and reaction methodologies developed over the past 20 years of silicon device use, the combination of TED-MOS 10µs short circuit capability and nHPD^2's current sense auxiliary terminal offers to match silicon performance we have become accustomed to. Intensive engineering effort anticipated to overcome the need to turn off a short circuit within 3µs for SiC devices is no longer a requirement by adopting Hitachi TED-MOS.

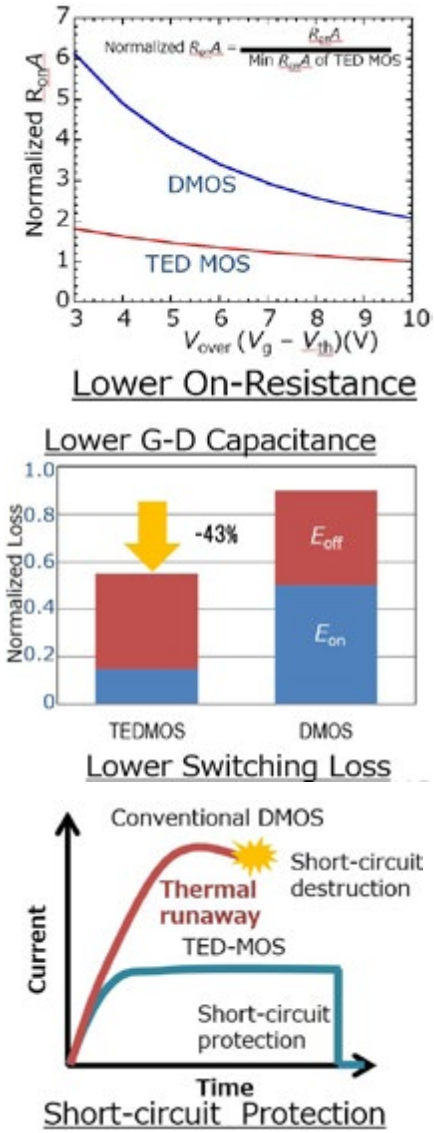

Figure 12: Hitachi SiC TEDMOS performance compared to conventional SiC DMOS

a. *Lower On-State Resistance*
b. *Lower Switching Loss*
c. *Improved Short Circuit Durability*

Modularity and scalability

The nHPD^2 module allows easy paralleling and optimized realization of multi-level topologies regarding stray inductances and system costs.

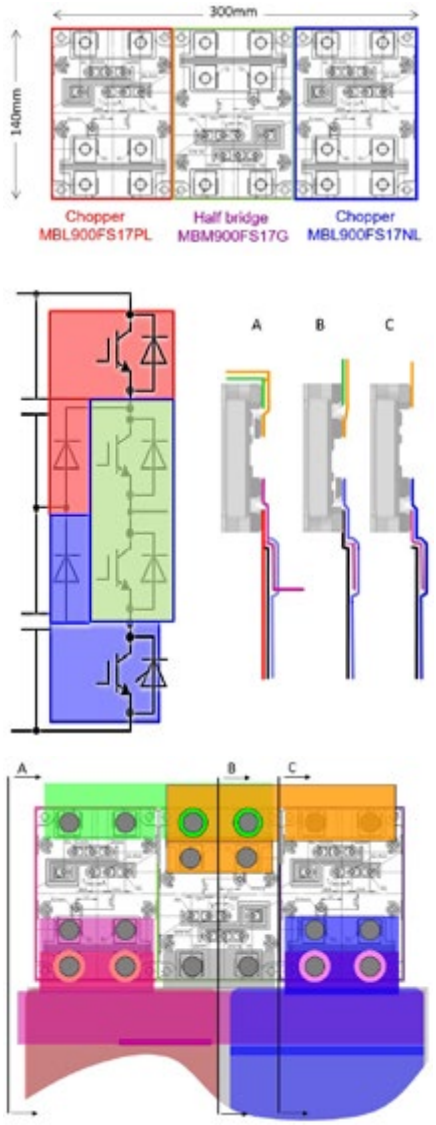

Figure 13: nHPD2 bus bar arrangement on heat sink for 3 level

Figure 14: Example for a compact and compatible inverter configuration

Conclusion

Hitachi is supporting the development of modern and flexible converters by applying innovation and advanced technology to range of industrial focused power modules. The modules are well suited to high performance applications that demand the highest levels of efficiency, lifetime and power output.

The common module outline for the nHPD^2 series facilitates a high level of design re-use and common design across converter power ranges to suit a wide range of applications.

Hitachi's focus on bringing the best performance to the market through innovation and advanced technology is evident in the future roadmap for the nHPD^2 series. The latest generation Silicon IGBTs and SiC MOSFETs line-up already available now will be followed by further advanced Silicon and enhanced SiC MOSFET generations to continually push the boundaries for higher efficiency, better performance and flexibility for the next decades. The integration of copper sintering for SiC MOSFET and side gate IGBT will be the next big step to secure the success of our customer.

Furthermore, Hitachi is offering life time simulations based on customer mission profiles and dedicated measurements in our high-tech lab in Maidenhead, UK related to your requirements.

Michael Sleven, Power Device Division,
Hitachi Europe Ltd

michael.sleven@hitachi-eu.com
+49 2115283-200

www.hitachi.eu

UJ3C Series
650V & 1200V

UnitedSiC
Simply More Efficient

Silicon Carbide FETs – Simply More Efficient

The new UnitedSiC UJ3C series elevates SiC FETs to a whole new level of efficiency, performance and ease of use. Our FETs are compatible with commonly used silicon and SiC gate voltages, come in industry-standard power packages, and allow for easy, drop-in replacement.

- Drop-in replacement for IGBTs, Si and other SiC MOSFETs
- Excellent body diode performance (V_f <2V)
- Lowest $Rds_{(on)}$ in TO-220 (27mΩ)

Get started now. Visit unitedsic.com/cascodes for a complete suite of technical docs written to help make your next design even better.

Find out how easy it is to upgrade your design at **unitedsic.com**

Power Modules in Low Power Drive Applications

IGBT based power modules are used for a wide power range and voltage range. The topic of the following is about system considerations and some effects to the power stage of the inverter. Finally the right choice of power module is discussed.

By Patrick Baginski, Vincotech GmbH, Unterhaching/Germany

Introduction

The number of induction motors operated with a variable frequency inverter (VFD) increases year by year. The range varies from some watts to some megawatts. The biggest market for frequency inverters is between 1 kW and 100 kW.

Most modern VFDs use PWM inverters with very fast-switching power semiconductor devices such as Insulated Gate Bipolar Transistors (IGBTs), which are now the industry standard because of their reliability and low switching losses. The fast change of voltage generated at the output terminals of the frequency inverter causes some effects on the motor cable and also on the motor itself. But is the situation for a power module in a low power different from that of a medium or high power application? Let's have a closer look what the situation for a power module in low power applications is.

To understand some of the effects resulting because of the use of a variable frequency drive the complete system has to be taken into account. Most often applications below 10 kW have a higher tendency to higher switching frequencies compared to applications above some tenth of kW. On the one hand this can be because bigger inverters and motors are located in environments where noise doesn't matter that much whereas low power applications can be placed in noise sensitive environments. On the other hand the mass moment of inertia and the resulting torque ripple might not critical in high power drives cause the mechanical time constant of the application is much bigger than the electrical time constant of the electrical drive.

Switching frequency vs. dead-time

For VFD operation the dead-time has to be takes in consideration. This is the time which is needed to ensure that the complementary switch does not switch on before the other is safely off. Therefore it is important to set the dead-time in a correct way for a reliable operation. A too small dead-time may cause shoot through while an increase leads to higher THD. The dead-time introduces small voltage errors, which are sufficient to produce distorted motor currents, oscillations of the motor torque and therefore even the motor controllability may be lost. Obviously the carrier frequency has to be increased to lower the ripple current and therefore the torque ripple. By increasing the pulse frequency, the switching dead-time takes a remarkable part of the whole modulation period and, thus, it distorts the average load voltage more and more seriously.

The distorted voltage is given by:

$$\Delta v \approx \frac{t_{dt}}{T} \cdot V_{DC} = t_{dt} \cdot f_{sw} \cdot V_{DC}$$

t_{dt} = dead-time

T = period of the carrier frequency

f_{sw} = switching frequency

V_{DC} = DC-link voltage

The voltage V_m at the motor is not like the set reference voltage V_{ref}.

Dependent of the sign of inverter output current i_m the distorted voltage becomes also positive or negative.

In another words, as higher the switching frequency, as more bad is the impact of the dead-time. The result is an offset in voltage which distorts the current in the zero crossing voltage. Therefore to minimize the dead-time is even more important for low power drives where the switching frequency is usually higher compared to higher power rated drives.

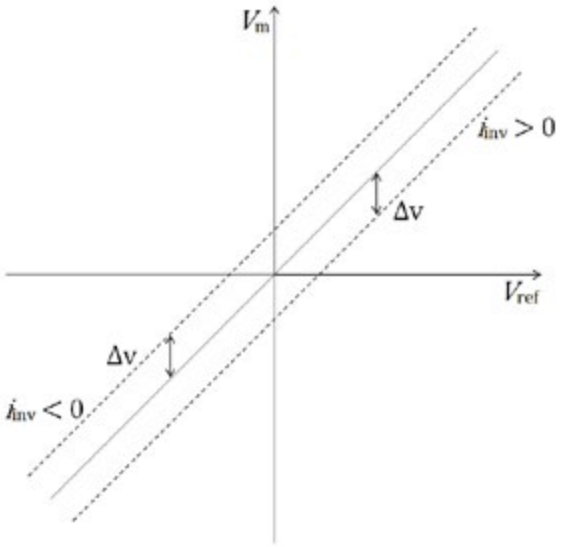

Figure 1: Dead-time effect

Mismatch of cable and motor impedance

Another effect is due to the motor cable and the mismatch of the motor surge impedance to the cable surge impedance. This is known as reflected wave theory. The cable surge impedance can be calculated with given *L*' and *C*' values of the cable manufacturer as

$$Z_C = \sqrt{\frac{L'}{C'}}$$

L' = cable inductance per length

C' = cable capacitance per length

TeamNexperia

"Join TeamNexperia and become part of a leading company that supports, rewards and challenges you equally."

Martin from Hamburg – *Senior Engineer*

For our location in Hamburg we are looking for:

SiC Experts, Application Engineers and Power Package Engineers

Nexperia is a world-class company in semiconductor development and in-house production. We form a global network of talent, with passion and performance, perseverance and professionalism. Talk to us today and learn your true capabilities in an energetic company where you will develop and thrive, the Efficiency Company – Nexperia.

Get in touch with your future: www.nexperia.com/careers or contact joinourteam@nexperia.com.

nexperia

EFFICIENCY WINS.

The inductance and capacitance per length for a usual 3 conductor + ground wire cable with 0.75 mm² would be approx. 0.5 µH and 100 pF per meter which leads to a surge impedance of 70 Ω.

Since smaller power rated motors, have higher surge impedance Z_M, they tend to reflect more of the applied PWM pulses than larger motors cause the mismatch gets greater.

Consider the following relation between the motor rating and the surge impedance.

The motor surge impedance is not an absolute value as a 1 kW motor varied between roughly 800 Ω to 4000 Ω depending on the motor manufacturer.

Motor terminal voltage

As it is obvious that the cable and the motor impedance do not match at all the reflection coefficient can be calculated with the equation

$$\Gamma = \frac{Z_M - Z_C}{Z_M + Z_C}$$

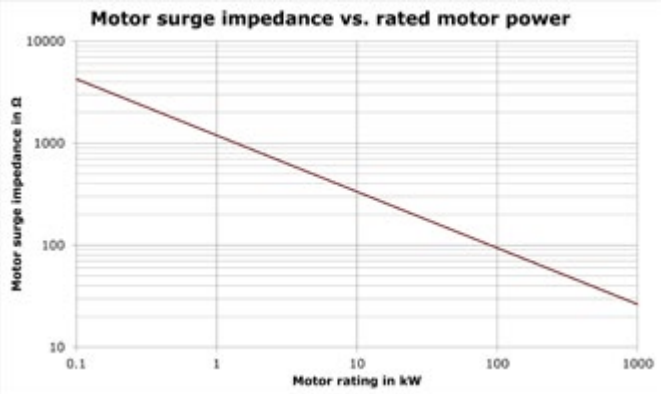

Table 1: Impedance vs. motor rating

Taking a 1 kW motor with 1 kΩ into consideration, this result to a reflection coefficient of 0.87. Means that the theoretical voltage at the motor terminals can be 87 % higher than the original DC-link voltage.

The cable length plays also an important role but this should be not discussed at this stage. It is considered to be a long cable and therefore the full voltage of the wave reflection is present at the motor terminals.

The above figure shows a simulation of a long wire with a DC-link voltage of 565 V and turn on rise time of 100 ns which is roughly 6 kV/µs.

The voltage overshoots are applied with the switching frequency to the cable and to the motor and this has to be considered when choosing the correct cable, especially the isolation of the wires, and also the isolation capability of the motor winding has to be taken into account. Usual motors are only rated up to 1000 V.

One solution to come along this is the use of a 230 V motor and inverter as this gives a good margin to the isolation capability. There are also other effects to the motor and especially to the bearings which are not subject of the discussion here. So this is the basis to understand the effects to the application and finally to the inverter stage in a better way.

Losses of inverter stage

Most tools and equations for loss calculations and simulations do not take the motor cable into consideration. As the IGBTs in the output of the drive switch on and off they have to charge and discharge the parasitic cable capacitances. To keep this in mind is even more important for low power drives.

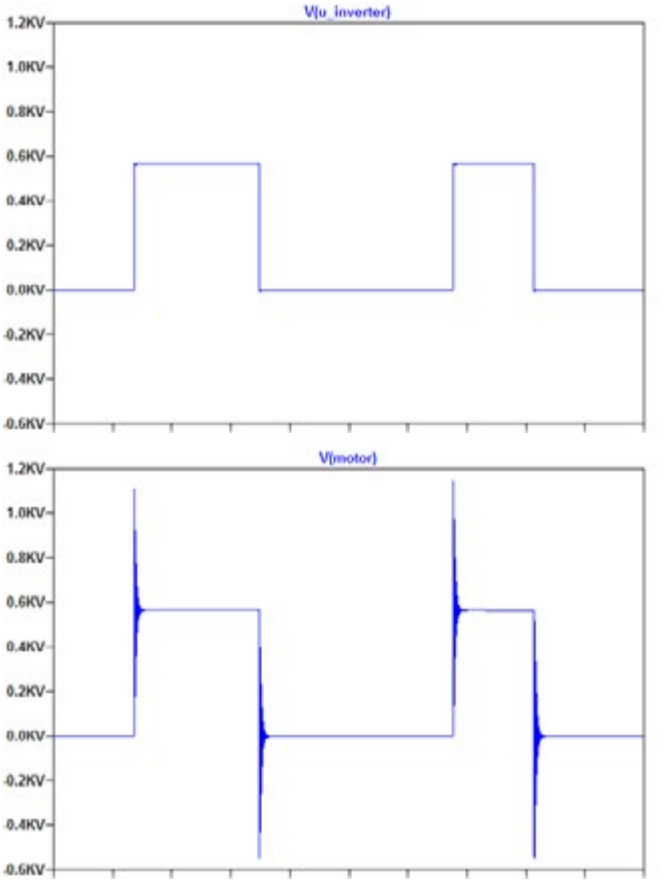

Figure 2: Output voltage of the inverter and voltage at motor terminals

Here comes the cable surge impedance into account. The drive output switches face the cable impedance with the DC-link voltage and in time with the carrier frequency and the dv/dt. So the parasitic capacitances of the cable increase the switching losses in the inverter, and the drive runs hotter. If the cable is too long and the capacitance becomes excessive, the drive may overheat and will trip on over temperature.

The RMS current of a 3-phase 400 V motor with 1 kW is about 1.4 A. But the surge peak current that the inverter has to provide is

$I_p = C_p \cdot \frac{dv}{dt}$ neglecting all other effects.

These additional currents exist whether a motor is connected or not. So much higher turn on energy has to be considered when doing a thermal calculation.

As for the motor terminal voltage this phenomena always exists and is exhibited to a greater degree on 400 V drives than on 230 V drives due to the higher output transition voltage. It is even made worse by having long leads on small kW drives.

Reverse bias safe operation area

It might be that a turn-off pulse comes even before the cable is charged fully. In this case the semiconductor has to be able to switch

the current safely off. The RBSOA is important during these turn off transients. The reverse biased safe operating area curve gives the maximum current and voltage which the device can handle simultaneously during turn off. As most chip suppliers specify the RBSOA to twice the nominal rated current of the semiconductor a bigger chip might have to be considered for the design or the cable length needs to be limited.

Conclusion

Several elements have to be taken into account when designing a low power drive. One major concern is the chip size and current carrying capability of the chip as additional losses will present when it comes to long motor cables and higher carrier frequencies.

Also the quality of cable plays an important role because of the impedance mismatches between the cable and the motor. Transient voltages can easily reach the isolation capability of the cable insulation but also the motor winding insulation.

An additional topic is the THD as the dead-time becomes a remarkable part of the whole modulation period with high switching frequencies.

Finally the turn-off capability of the semiconductor has to be considered as its ability is usually limited to twice the nominal current rating.

www.vincotech.com

High Voltage Thyristors with Self-protection Elements in Situations Beyond Safe Operation Mode

This article addresses the possibility of forming built-in overvoltage self-protection elements in high-voltage semiconductor thyristors with local proton irradiation of the main control electrode area, and shows results of using such solution in development of a new high-voltage thyristor T483-1600-60 after a successful testing.

By Dmitry Titushkin, Alexey Surma, Vladimir Verevkin, Igor Savin, JSC Proton-Electrotex

Introduction

Modern market of power equipment requires highly reliable technical solutions and components, since failure of a power semiconductor under operating conditions can lead to a very costly failure of the entire converter system. With regard to high-voltage conversion devices, which include power semiconductor thyristors (usually designed for a voltage of the order of 6500V), a failure of the power thyristor control driver can cause a situation going beyond safe operation of a standard high-power thyristor, when the thyristor needs to be switched to a conducting state with no external control signal due to the driver failure.

In this regard, an important direction in improving designs of high-voltage power semiconductor thyristors is introduction of overvoltage self-protection elements into the semiconductor structure [1-6]. This solution allows to prevent a failure of a high-voltage thyristor in abnormal mode of operation by imparting the thyristor element with dynistor properties (switching to a conducting state when a certain cathode-anode voltage is applied) [6].

It is known that proton irradiation introduces recombination centers into the structure of a semiconductor device, making it possible to adjust dynamic parameters of thyristors which is often used in production of fast and fast-recovery thyristors and diodes [4]. Similarly, proton irradiation (implantation of hydrogen atoms) induces the emergence of donor centers similar in properties to traditional donors (phosphorus, arsenic, antimony) [4,7]. Local proton irradiation can thus form self-protection elements against overvoltage while accurately adjusting avalanche breakdown voltages, which is especially important for operation of thyristors in serial assemblies of high-voltage switches [5].

Thus, a thyristor in a serial connection can safely switch after its driver fails (with no regular control signals), meaning that the switch remains operational when the driver of one of the thyristors fails [5].

Experiment Samples

This design and technology solution was tested on 2000V thyristors with a diameter of the semiconductor element of 80 mm, where an n' region was formed under the main control electrode region by means of proton irradiation.

The research program included the following:

- measurement of basic electrical parameters and properties and comparing them with measurements taken before formation of the self-protection elements;
- tests for safe switching at low anode currents (up to 35 A);
- tests for safe switching at anode currents up to 1250 A;
- electrical testing (applying surge current) to determine stability of the switching mechanism under operating conditions;
- repeated tests for safe switching at anode currents up to 1250 A.

Measurements of the main electrical parameters and properties before and after forming the built-in self-protection elements demonstrated that introduction of a local region responsible for switching to a conductive state into the thyristor structure did not degrade basic electrical and thermal parameters and properties of the tested thyristors.

Tests of thyristors with self-protection elements for safe switching by the anode were intended to test their ability to withstand current pulses of considerable amplitude when switching under overvoltage in the forward direction. The tests were carried out with both open and shorted control circuit. The tests were carried out in two stages.

In the first stage, the thyristors were subjected to an overvoltage in the forward direction from a high-voltage current source that formed a current pulse of a half-sine wave form of 100 µs duration at a level of 0.5 from the amplitude value throughout switching of the tested thyristor. The output voltage of the source's idle current was no less than 6 kV, the amplitude of the current pulse was set to 35 A. Each sample was subjected to 5 overvoltage pulses. After the tests, values of the repetitive pulsed current in the closed state and the repetitive pulse reverse current were monitored.

In the second stage of the test, samples were subjected to overvoltage in a circuit forming a high-amplitude current pulse of trapezoidal shape with a high rate of rise of the leading edge after switching the thyristor.

The test sample with either short-circuited or open control circuit was installed in the clamping device of the test unit in serial connection with a T173-2000-34 switching thyristor. During the test we used a forming line with a wave impedance of 1 ohm. Before the control pulse of the switching thyristor is applied, voltage on each of the thyristors is approximately equal and makes a half of the voltage on the forming line. After turning the switching thyristor on, all voltage is ap-

plied to the tested thyristor, and since it exceeds the switching voltage of the test thyristor, it switches. The current amplitude was set with additional resistors in serial connection with a resistance of 6.7 ohms or 0.75 ohms. The rate of current rise was controlled with inductance coils in serial connection with a resistor. Voltage on the forming line before turning on the switching thyristor was set to 2300 V. Connection of the test thyristor to the forming line is illustrated in Fig. 1. The voltage on the switching thyristor and on two serially connected thyristors (switching and testing) was monitored with a TPS2024 oscilloscope and voltage dividers Tektronix P5100. The oscillogram of voltage on the tested thyristor with self-protection is obtained with the differential measurement method. The oscillograms of voltage and current at the test sample are shown in Fig. 2 - 6.

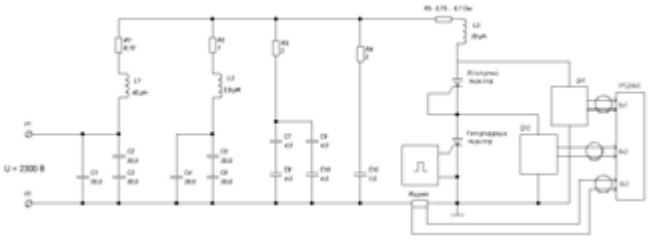

Figure 1: Connection diagram

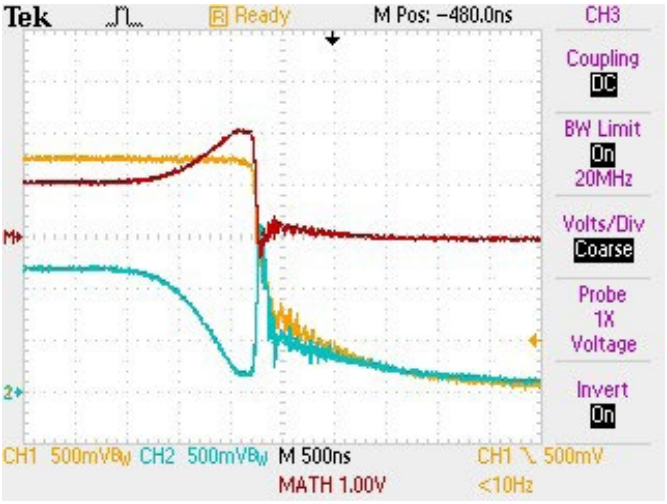

Figure 2: Voltage oscillogram for:
- two serially connected thyristors – yellow;
- switching thyristor – blue;
- tested thyristor with self-protection – red.

With a load resistance of 6.7 ohm, the current amplitude was 290 A, the rising rate of the leading edge at 0.5 level was 75 A/μs, the pulse duration at 0.5 level was 350 μs. The number of exposures per each sample was 300 pulses with a frequency of 1 Hz.

With a load resistance of 0.75 ohm, the current amplitude was 1250 A, the rising rate of the leading edge at 0.5 level was 90 A/μs, the pulse duration at 0.5 level to 125 μs. The number of exposures per each sample was 120 pulses with a frequency of 1 Hz.

As a result, the thyristors have successfully passed the tests for safe switching, that is, at currents up to 1250 A the self-protection mechanism was correctly triggered when switching under overvoltage (Figures 2-6). Resistance of the thyristors against the rate of current rise in the open state when switching over the anode in the test samples is comparable to the typical values of di/dt resistance when thyristors are switched on by the control electrode.

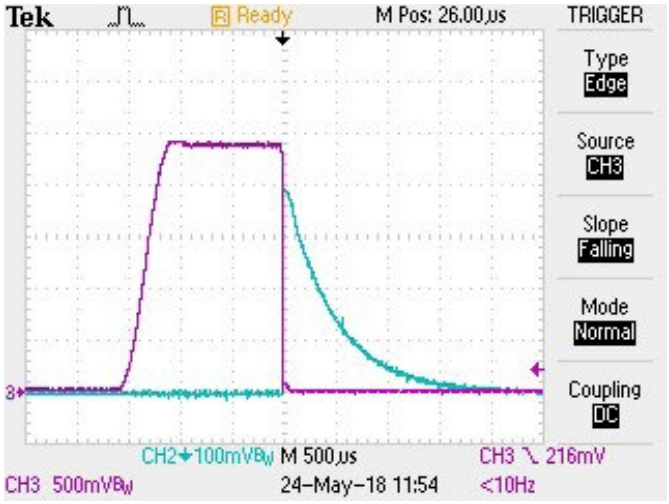

Figure 3: Voltage oscillograms for two serially connected thyristors (violet) and current through the tested thyristor with self-protection (blue) at current amplitude 290 A

Figure 4: Voltage oscillograms for two serially connected thyristors (violet) and current through the tested thyristor with self-protection (blue) at current amplitude 290 A

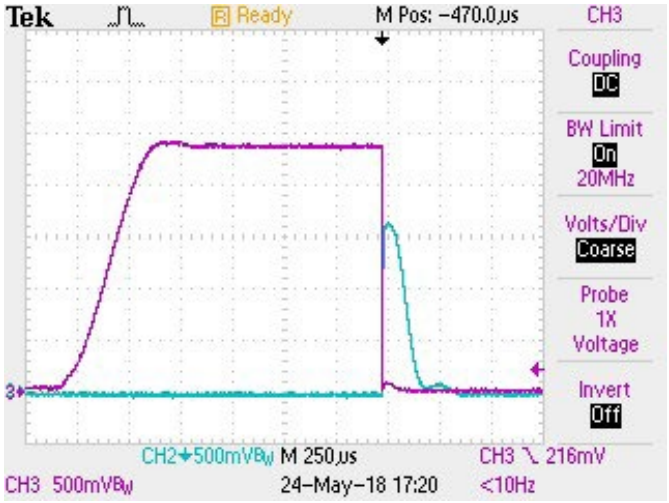

Figure 5: Voltage oscillograms for two serially connected thyristors (violet) and current through the tested thyristor with self-protection (blue) at current amplitude 1250 A

To evaluate a possibility of annealing the effect of local irradiation (in emergency modes of thyristor operation), tests were carried out for resistance to 20 consecutive pulses of surge current with an amplitude of 40 kA at T = 125 and VD = VR = 0. Then we measured the eligibility criteria and repeated the switching test for the thyristor with built-in self-protection mechanism against overvoltage at a current of 1250 A. The tests did not identify changes in thyristor switching voltage in the forward direction, and there were no parametric and catastrophic failures.

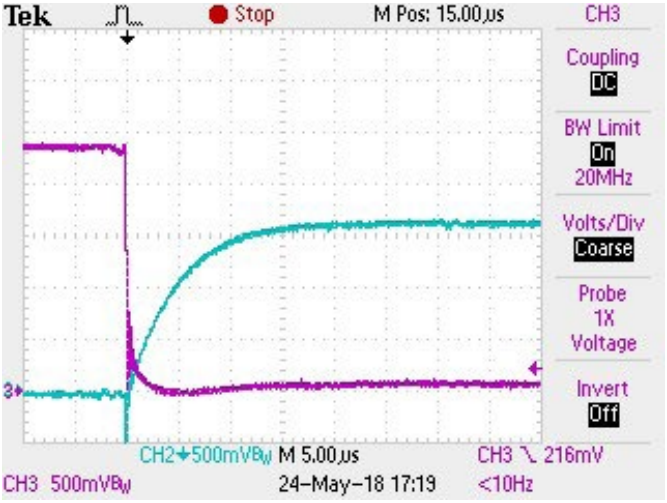

Figure 6: Voltage oscillograms for two serially connected thyristors (violet) and current through the tested thyristor with self-protection (blue) at current amplitude 1250 A

Development of a New High Voltage Thyristor with integrated Overvoltage Self-protection Elements

Based on the experience gained with this solution of forming built-in overvoltage self-protection elements, it was decided to design a powerful high-voltage thyristor T483-1600-60, characterized by:

- optimized diffusion structure and application of a low-temperature sintering technology to reduce dynamic resistance (rT);
- updated topology of the diffusion element and the use of proton irradiation to obtain low (up to 400 µs) thyristor turn-off times;
- precise control of the reverse recovery charge values (Qrr) within ± 5%;
- an integrated element of overvoltage self-protection, eliminating the need for such solutions as installing external voltage limiters (BOD) and, consequently, not having to refine design of the power unit around protection systems. Such solution will reduce the complexity of the power assembly and eliminate associated risks, with a cost level comparable with using external protection elements. In addition, Proton-Electrotex plans to test operation of a protection system integrated in the thyristor structure, i.e. from the customer's point of view certification will cover not only the device itself, but also the protection system integrated in the device structure, which cannot be achieved using the components separately.

The main parameters and properties of the developed thyristor are summarized in Table 1.

Conclusions

We successfully tested an integrated mechanism of self-protection against overvoltage obtained with local irradiation of the control electrode region of the main thyristor, and proved stability of this mechanism in conditions of electrical effects. The obtained results enabled development of a new high-voltage thyristor T483-1600-60 with built-in self-protection elements against the possibility of driver control failure, facilitating construction of power converters and reducing the chance of failure due to higher number of involved system elements.

Parameter	Norm	Measurement conditions
Blocking Voltage V_{DRM}/V_{RRM}	6000 V	-60 °C<Tj<125 °C;
Average Current I_{TAV}	1600 A	Tc =98 °C; two-sided cooling;
Surge On-state current I_{tsm}	40 kA	Tj=125 °C, (tp =10 ms); single impulse; $V_D = V_R$ =0 B;
Critical Rate of Rise of Off-state Voltage $(dV_D/dt)_{CRIT}$	2500 V/µs	Tj =125 °C; V_D = 4000 V;
Peak On-state Voltage V_{TM}	2.4 V	Tj =25 °C; I_{TM} =5024 A
Peak On-state Voltage V_{TM}	2.1 V	Tj =125 °C; I_{TM} =2500 A
Delay Time tgd	2.0 µs	Tj=25 °C; V_D = 600 B; I_{TM} =1600 A;
Turn-off Time tq	400 µs	dV_D/dt=50 B/ µs; Tj =125 °C; I_{TM} =1600 A; di_R/dt=-5A/ µs; V_R ≥100 V; V_D=4000 V;
Total Recovered Charge Q_{RR}	3500 µC	Tj =125 °C; I_{TM} = 1600 A; di_R/dt=-5A/ µCu; V_R ≥100 B
Thermal resistance junction to case Rthjc	0.0075 °C/W	Two-sided cooling

References

1. Niedernostheide F.-J., Schulze H.-J., Kellner-Werdehausen U. Self-protected high-power thyristors. - Proc. PCIM 2001, Power Conversion, Nuernberg, p.51-56.
2. Adjustment method for a thyristor's reverse breakdown voltage uses negative- and positive-doped bases, a collector and an emitter along with hydrogen-induced donors / Reiner Dr. Barthelmess; Uwe Keller-Werdehausen; Franz-Josef Dr. Niedernostheide; Hans-Joachim Dr. Schulze (Infineon Technologies AG EUPEC GmbH (Infineon Technologies Bipolar GmbH and Co KG). – Patent DE10344592B4; filed on 25.09.2003; published on 19.05.2005
3. Sposob regulirovaniya napryazheniya pereklyucheniya silovogo poluprovodnikovogo pribora / Dermenzhi P.G. (Ministry of Industry and Trade of the Russian Federation on behalf of the Russian Federation) – patent RU2474926C1 ; filed on 21.09.2011; published on 10.02.2013
4. Gubarev V. N., Semyonov A. YU., Stolbunov V. S., Surma A. M. Tekhnologiya protonnogo oblucheniya i vozmozhnosti eyo primeneniya dlya uluchsheniya kharakteristik silovykh diodov i tiristorov. – Silovaya ehlektronika no. 5, 2011, p. 4-7.
5. Dermenzhi P.G., Loktaev Y.M. , Surma A.M., Chernikov A.A. - High-Voltage Power Thyristors with Built-In Protective Elements in the Semiconductor Structure in Case of Emergency Mode - Bodo's Power Systems 10, 2011, p. 38-40.
6. Loktaev Y.M., Surma A.M., Chernikov A.A. - New high-voltage power thyristor with built-in protective elements in the semiconductor structure in case of emergency mode excess-voltage protection. - Bodo's Power Systems 11, 2011, p. 44-48.
7. Kozlovskij V. V., Kozlov V.A., Lomasov V.N. Modifitsirovanie poluprovodnikov puchkami protonov // Fizika i tekhnika poluprovodnikov. 2000. vol. 34, issue 2, page 129–147.

Contacts

d.titushkin@proton-electrotex.com
a.surma@proton-electrotex.com
v.verevkin@proton-electrotex.com
i.savin@proton-electrotex.com

power integrations™

electronica 2018

Visit Us! Hall C5 Booth 212

USB Power Delivery

Highly Efficient and Compact

- Constant power delivery at up to 94% efficiency across full line and load
- Ideal for USB PD, fast charging and dynamic output applications
- Compact power supplies to 65 W
- Accurate secondary-side regulation without an optocoupler

www.power.com

ac-dc converters led drivers gate drivers

Current Source Gate Drivers Boost the Turn-On Performance of IGBT

Gate drive design engineers are often forced to use larger turn-on resistors than the IGBT's datasheet proposes in order to slow down the maximum dv_{CE}/dt during the current commutation. Infineon Technologies proposes the new gate driver IC 1EDS20I12SV, which controls a relatively constant dv_{CE}/dt.

By Wolfgang Frank und Holger Hüsken, Infineon

A comparison of two gate driver boards using 1EDS20I12SV and a conventional gate driver IC, which are operated with the same power module, shows the advantages of the new control method. The power module is a 1200 A / 1200 V (FF1200R12IE5) module designed for high power applications.

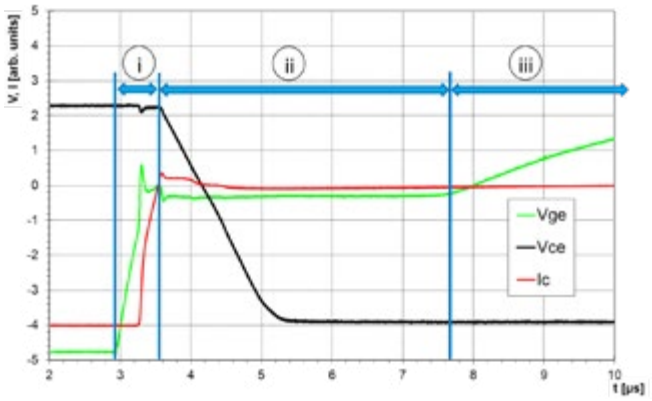

Figure 1: Typical turn-on transient of an IGBT divided into 3 sections

The IGBT´s control equations

It is helpful for the understanding of the control scheme of 1EDS20I12SV to analyze the turn-on behavior of an IGBT as it is depicted in Figure 1 for an inductive load. For simplicity, the commutating diode is a SiC Schottky diode for which reverse recovery is purely capacitive.

The gate current I_g charges both the gate emitter capacitance C_{ge} and the gate collector capacitance C_{gc} according to [4], [5]:

(1) $$I_g = \frac{d}{dt}(C_{ge} \cdot V_{ge} + C_{gc} \cdot V_{gc})$$

The gate emitter capacitance can be assumed to be voltage-independent, whereas the volt-age dependency of C_{gc} is significant. The capacity C_{gc} is low at large values of V_{gc} but large for small voltages.

(2) $$I_g = C_{ge} \cdot \frac{d}{dt} V_{ge} + \frac{d}{dt}(C_{gc} \cdot V_{gc})$$

Note that the gate collector voltage is given by

(3) $$I_g = C_{ge} \cdot \frac{dV_{ge}}{dt} + \left(V_{gc} \cdot \frac{d}{dV_{gc}} C_{gc} + C_{gc}\right)\frac{dV_{gc}}{dt}$$

$$I_g = \left(C_{ge} + V_{gc} \cdot \frac{d}{dV_{gc}} C_{gc} + C_{gc}\right)\frac{dV_{ge}}{dt} - \left(V_{gc} \cdot \frac{d}{dV_{gc}} C_{gc} + C_{gc}\right)\frac{dV_{ce}}{dt}$$

In a simplified picture, the turn-on of the IGBT can then be divided into three phases:

(i) Gate charging at high V_{ce}: first term of eq. (5) dominates
(ii) Miller plateau at constant V_{ge} and changing Vce: second term of eq. (5) dominates
(iii) Gate charging at low V_{ce}: first term of eq. (5) dominates again

The difference between voltage driving and current driving schemes then becomes obvious.
For a voltage driving scheme, the gate current is changing during the switching transition according to

(6) $$I_g = \frac{V_{on} - V_{ge}}{R_g}$$

Where V_{on} is the voltage supplied by the gate driving circuit.

dV_{ce}/dt during phase (ii) and therefore the turn-on energy E_{on} is then determined by the Miller voltage which in turn depends on the load current. Low currents and comparatively low Miller voltages will result in high dV_{ce}/dt during turn-on. On the other hand, the turn-on energy E_{on} when handling larger collector currents is increased both by the higher current level itself and the slower switching speed due to the high Miller voltages and associated lower gate currents. This results in non-linear curves for the turn-on energy as a function of the collector current.

The choice of gate resistors is determined by the need to limit the voltage slope at small currents. This is detrimental for the losses when switching high currents. With a gate current driving scheme, the dV_{ce}/dt during phase (ii) is independent of the load current, thus allowing optimized switching speed for a wide current range. The turn-on energy is therefore only depending on the collector current amplitude at turn-on.

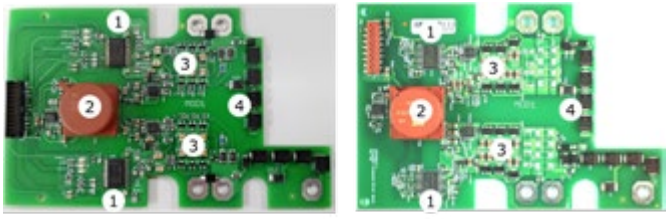

Figure 2: Driver board with current source gate control (left) and voltage source gate control (right)

PROTECTION, COOLING & CONNECTIVITY: SOLUTIONS FOR EV/HEV & BATTERY-RELATED APPLICATIONS

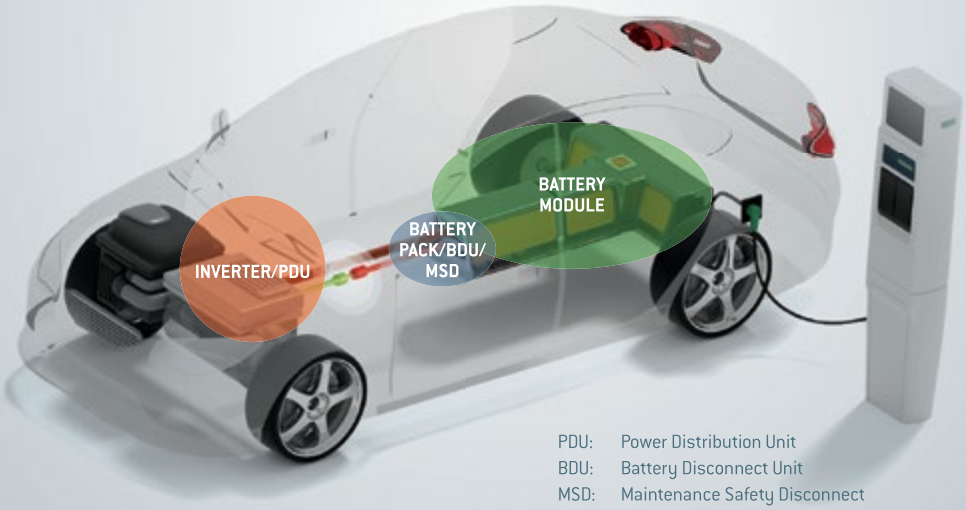

PDU: Power Distribution Unit
BDU: Battery Disconnect Unit
MSD: Maintenance Safety Disconnect

Protection and switching for Battery Pack/BDU/MSD

χp hybrid over current protecting device

χs hybrid DC power relay

EVpack-fuse

Protection, cooling & connectivity for Inverter/ PDU and battery Module

Liquid Cold Plate heat sinks

Flexible monitoring bus bar

M-fuse
DC fuses

EP.MERSEN.COM

MERSEN
Expertise, our source of energy

Gate driver boards

Both driver boards are designed to fit to the power module FF1200R12IE5. They contain external buffers (3), which amplify the driver IC´s (1) output current. The buffer of the conventional realization (left in Figure 2) is based on bipolar transistors, while the current source gate driver board used p-channel MOSFETs for boosting the turn-on. The use of p-channel MOSFETs is mandatory for the gate current control loop. The turn-off boost circuit uses pnp-transistors similar to the conventional gate driver board. An output bias supply (2) provides the gate drive voltages for a +15 V / -8 V supply. Finally, there is also an active clamping function (4), which acts on the gate voltage to avoid overvoltages during turn-off. Since the active clamping is only activated during turn-off, it does not interfere with the constant current turn-on.

The current source gate driver IC contains the option to change the switching speed pulse-by-pulse during operation. This is an important function to reduce the turn-on switching losses furthermore in the application [1].

Gate current control turn-on scheme

The first phase during turn-on is the preboost phase and lasts for 135 ns according to Figure 3. The preboost charges the gate-emitter voltage to a value below the gate-emitter threshold voltage $V_{ge(th)}$. The current during the preboost phase depends on the gate charge and is therefore constant throughout the operation of a given power switch.

The turn-on phase follows the preboost. The turn-on current level can be selected arbitrarily during operation out of 11 levels. The selected gate current level yields in a given turn-on speed. The selection of the switching speed levels is done by applying an analog signal to a specific terminal on the control side of the gate driver IC. The turn-on current level is active until the gate reaches the final gate bias voltage, which is 15 V in this case.

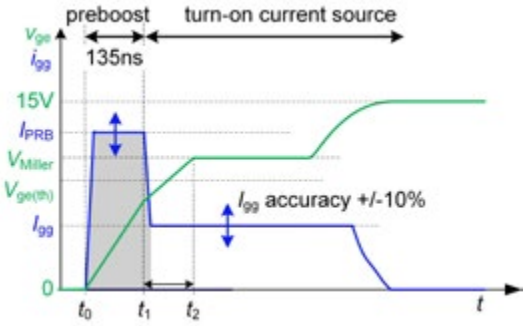

Figure 3: Turn-on sequence of the current source gate driver IC 1EDS20I12SV

Measurement results

Both gate driver systems are evaluated on a double pulse test bench with automated switching parameter calculation. The double pulse technique is explained elsewhere. The boards are operated with various turn-on speeds in order to evaluate as well the trend of each parameter as a function of the switching speed. This is achieved by using the integrated speed selection option of the current source gate driver IC and by variation of gate resistors of the conventional voltage source gate driver board.

Figure 4 shows an example of turn-on waveforms. The gate-emitter voltage v_{GE} (green) and the collector current i_C (red) are smooth with acceptable small oscillations. The voltage slew rate dv_{CE}/dt is evaluated shortly after the reverse recovery of the freewheeling diode (instance “1”). The diode takes over the voltage from the IGBT there and there is in many cases the largest dv_{CE}/dt. Therefore, Figure 5 shows the transient of the diode´s reverse voltage.

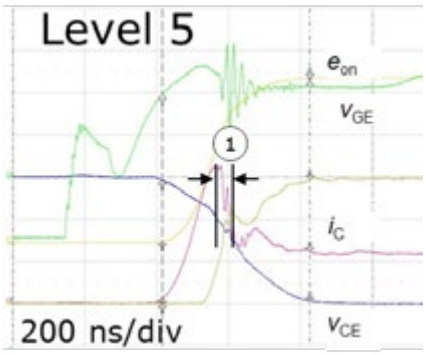

Figure 4: Example waveforms for turn-on at I_C = 120 A (10% of nominal current) and DC-link voltage of V_{DC} = 600 V

Figure 5 depicts the results and contains marks which designate the design point of the gate drive in order to keep the dv_R/dt at 5 V/ns or below. This is in case of the current source solution the curve representing “level 5” and the curve of R_G = 2.2 Ω for the voltage source solution. It can be seen that the dv_R/dt stays relatively constant for the constant current source gate driver board, because the gate current is constant over the whole turn-on-process regardless of the individual

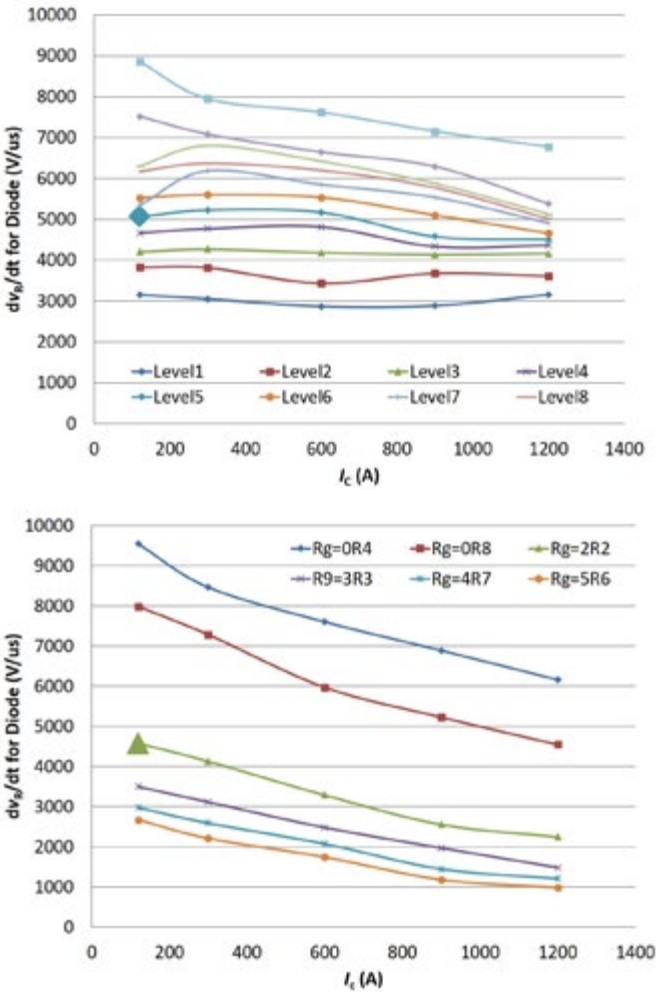

Figure 5: dv_R/dt of the measured power module with current source gate control (top) and voltage source gate control (bottom)

collector current. This yields in a constant dv_R/dt. This is different for the voltage source board. The dv_R/dt is constantly decreasing there, because the increasing miller voltage over the collector current range reduces the driving voltage for the gate current, and thus the gate current itself.

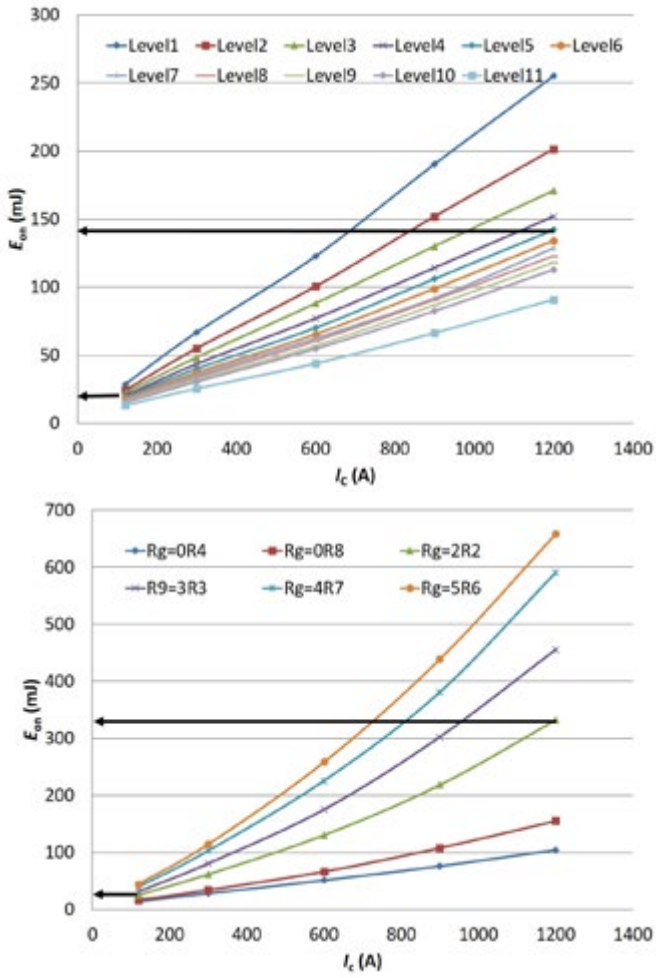

Figure 6: Turn-on energy of FF1200R12IE5 measured with current source gate control with change of switching speed (top) and voltage source gate control (bottom)

Figure 6 represents the turn-on energy E_{on} of both solutions. The same starting conditions at 5 V/ns indicate also similar turn-on energy, which is approximately 20 mJ. However, the situation changes at high collector currents. Here the constant gate current source yields in a turn-on energy of only 140 mJ compared to the voltage source driver board with approximately 340 mJ. Thus, the turn-on energy of the constant gate current driver is only 41 percent of the voltage source gate driver solution at rated collector current.

Conclusion

The gate current source turn-on shows much lower turn-on energy at similar dv_{CE}/dt com-pared to voltage source gate drivers over the rated collector current range. Therefore, the current source gate control board is superior to conventional voltage source gate driver sys-tems, which operate with a fixed turn-on gate resistor. A higher performing system can be achieved at a competitive cost compared to a conventional system. The adjustment of switching speed during operation results a new degree of freedom for the gate current gate driver, because it can adapt the turn-on with respect to other operat-ing conditions, such as the IGBT temperature or the load condition. [6] This advantage translates of course into larger tem-perature margins or output current margins on a system level, as well.

References

[1] W. Frank, et al.: Real-time adjustable gate current control IC solves dv/dt problems in electric drives, Proceedings of PCIM 2014, Nuremberg, Germany, 2014.
[2] Infineon: 1ED020I12-F2, datasheet, Infineon Technologies AG, Germany.
[3] Infineon: 1EDS20I12SV, datasheet, Infineon Technologies AG, Germany.
[4] J. Lutz, Semiconductor Power Devices, Springer Verlag Berlin Heidelberg, 2011, ISBN 3-540-34206-0.
[5] D. Schröder, Leistungselektronische Bauelemente, Springer Verlag Berlin Heidelberg, 2nd Edition, ISBN 3-540-28728-0.
[6] S. Mahmodicherati, N. Ganesan, L. Ravi, R. Tallam: Application of Active Gate Driver in Variable Frequency Drives; Proceedings of 10th IEEE-ECCE Conference; Portland, USA, 2018

www.infineon.com

Temperature Stability Assessment of GaN Power Amplifiers with Matching Tantalum Capacitors

Wide band gap GaN and SiC devices are expected to experience high levels of growth in applications ranging from power conversion to RF transistors and MMICs. End users recognize the advantages of GaN technology as an ability to operate under higher currents and voltages. RF GaN market is expected to grow at 22.9 % CAGR over 2017-2023, boosted by implementation of 5G networks. [1]

By T.Zednicek, European Passive Components Institute, Lanskroun, Czech Republic;
R.Demcko, M.Weaver, D.West, AVX Corporation, Fountain Inn, SC, USA;
T. Blecha, F.Steiner, J.Svarny, R.Linhart, RICE, University of West Bohemia, Pilsen, Czech Republic

During the past years, the wide band semiconductors have reported achievement of >1000 V BDV that opens new challenges for high power industrial applications such as electric traction systems in trams, trolley buses or high-speed trains etc.

Decoupling and BIAS matching tantalum capacitors are used due to its stability of capacitance value over wide temperature range, stable capacitance with BIAS, no piezo noise sensitivity at small, low profile case sizes. They are not prone to wear out associated with Aluminum electrolytic capacitors and exhibit high reliability & stability across temperature, voltage and time.

Figure1: RF GaN Power Amplifier; image credit: Cree

GaN Power Amplifiers with matching Tantalum Capacitors

GaN RF Power Amplifiers

Requirements for the best linearity of RF GaN power amplifiers, as one of the key parameters, can be achieved by two ways: 1] use of optimum output impedance of the optimum linearity, this could however limit the output power and decrease efficiency.

Or 2] use optimum output impedance for maximum power output and define the working linearity region by the proper BIAS point setting and optimization. This requires a proper design of BIASing circuits and its stability in wide operating conditions. [1]. Tantalum capacitors in number of referenced designs are used to keep the working point within the high linearity region.

RF GaN reference designs with tantalum capacitors:

- Nitronex NPTB00004 GaN 28V, 5W RF Power Amplifier for CW, pulsed, WiMAX, W-CDMA, LTE, DC to 6 GHz. 10µF 16V gate decoupling capacitors.

- Qorvo QPD1008 125W, 50V, DC – 3.2 GHz, GaN RF 10µF 16V gate BIAS decoupling capacitors.

  The other Qorvo designs:
  QPD1008L DC - 3.2 GHz, 125 Watt, 50V GaN RF Power Transistor
  QPD1009 DC - 4 GHz, 15 Watt, 50V GaN RF Transistor
  QPD1010 DC - 4 GHz, 10 Watt, 50V GaN RF Transistor
  QPD1015L DC - 3.7 GHz, 65 Watt, 50V GaN RF Power Transistor

- Cree / Wolfspeed CGHV50200F 200W, 4400 - 5000 MHz, 50-Ohm Input/Output Matched, GaN HEMT with 10µF 16V capacitors

The other Cree references:
CGH40006P 6 W, RF Power GaN HEMT
CGH40010 10 W, DC - 6 GHz, RF Power GaN HEMT
CGH40025 25 W, RF Power GaN HEMT
CGH40045 45 W RF Power GaN HEMT
CGH55030F1 / CGH55030P1 30W, 5500-5800 MHz, 28V, GaN HEMT for WiMAX

GaN High Power PFC Compliant Systems

The main power supplies used in telecom, server, and industrial power supply unit (PSU) systems convert AC line power to an isolated constant DC voltage output suitable for the loads the power: typically, 1 kW to 5 kW 12V for server PSUs, 48V for telecom rectifiers, and 24V for industrial PSUs. These systems require a front-end power factor correction (PFC) circuit to shape the input current of the power supply, so as to meet the power factor and current total harmonic distortion (THD) norms defined in IEC61000-2-3.

Requirements for PFC to meet >80 % standards calls for very-high efficiency over wide operating ranges of input and output. This need has generated interest in bridgeless PFC topologies that push the efficiency above 99%. [3]

Capacitors are among the critical components that in case of SC failure may cause a fatal error. Tantalum capacitors are providing high capacitance efficiency in small dimensions with stable electrical parameter over its long lifetime:

SEMIKRON
innovation + service

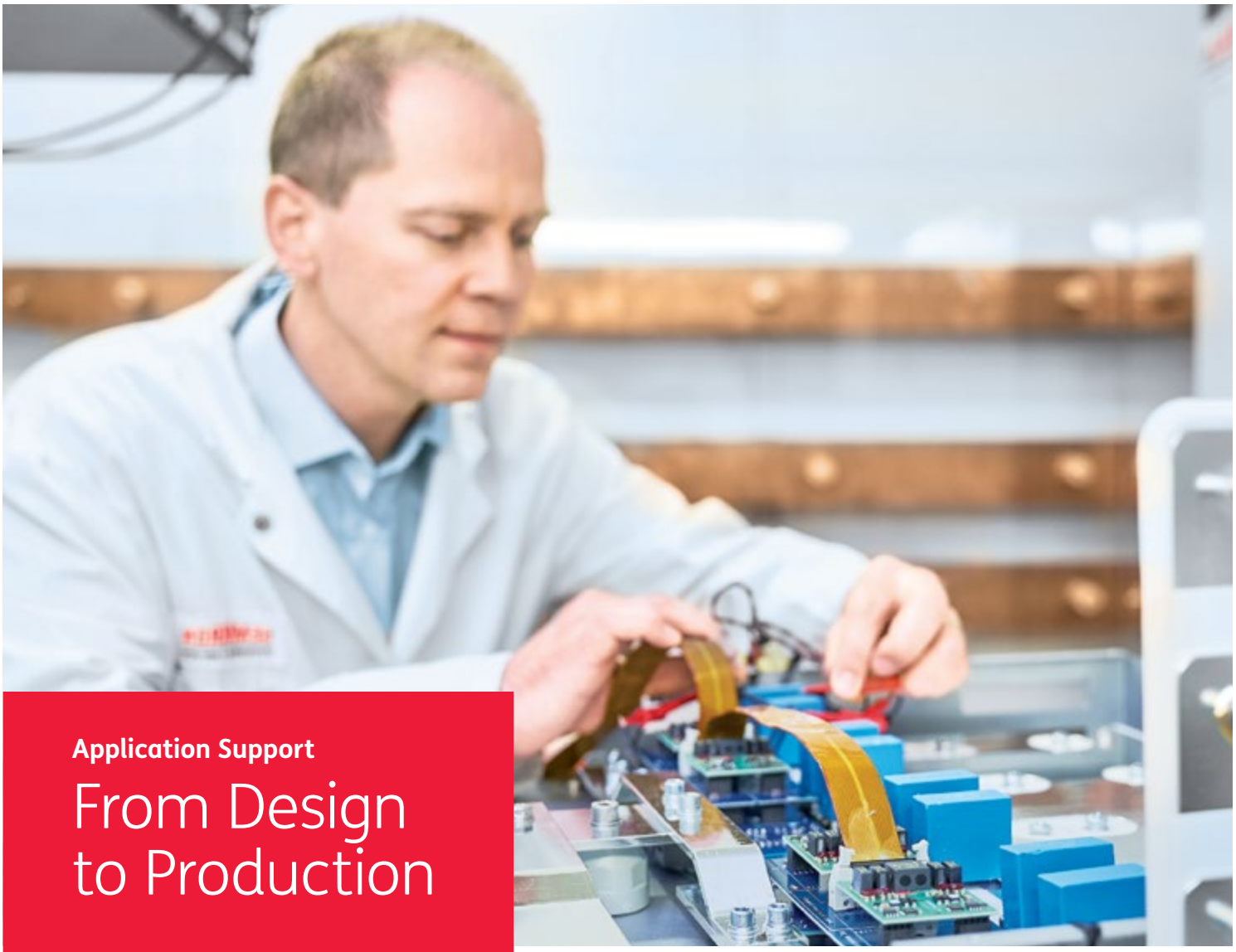

Application Support

From Design to Production

Application engineering support, lab space and reference designs.

Today, increased product diversity in power semiconductors calls for customer support that goes far beyond the information contained in data sheets. Only comparison under application-specific conditions – such as voltage, switching frequency or cooling conditions – can demonstrate the differences in performance in the devices available.

How can we help you with inverter design?

- → Heatsink selection and TIM application
- → DC link design and capacitor selection
- → Isolation coordination
- → Lifetime calculations
- → Measurement support
- → Application samples and reference designs

AC | DC

Learn more: Application Test Bench video
wwww.semikron.com/video/application-test-bench

- Texas Instrument TIDA 00961 GaN 12V, 1.5kW for telecom, servers and industrial power supplies 100µF 16 V, 220µF 16 V tantalum capacitors for bulk 12V line stabilization [1], 4.7µF 10V on 3.3V output stabilization.
- Texas Instrument LMG3410 600V 12A Integrated GaN Power Stage for solar power, battery chargers with 33µF 16V as 5V output capacitor.

GaN Hi Point of Low Controller

TI half-bridge point-of-load 80V 10A GaN controller LMG5200 evaluation board implements the 48-V to 1-V converter as a single-stage hard-switched half-bridge with current-doubler rectifier. This topology efficiently supports a high step-down ratio while providing significant output current and fast transient response. GaN offers superior switching performance to traditional silicon MOSFETs due to its lack of reverse-recovery effect and reduced input and output capacitance. By using a GaN module, this application achieves high efficiency while operating in a hard-switched configuration.

Four low ESR B case 150µF 6.3V polymer tantalum capacitors are used as high efficient, high power filtering output small size capacitors.

GaN Board Temperature Stability Assessment

GaN board selection

ORVO QPD1008 has been selected as a typical representative board with input tantalum capacitors subjected to a temperature stability measurement at RICE, University of West Bohemia. The QPD1008 is a 125 W (P3dB) wideband unmatched discrete GaN on SiC HEMT which operates from DC to 3.2 GHz with a 50 V supply rail. The device is in an industry standard air cavity package and is ideally suited for military and civilian radar, land mobile and military radio communications, avionics, and test instrumentation. The device can support pulsed, CW, and linear operation. [2]

In measurement set up, this transistor was connected in the test board as an amplifier for frequency range from 0.96 GHz to 1.215 GHz. The aim was to observe an influence of the C2 capacitor on the transistor behaviour for different ambient temperature level. The C2 capacitor is tantalum capacitor (10 µF/16 V) recommended by the manufacturer in its reference datasheet – see Figure 3 and Figure 4.

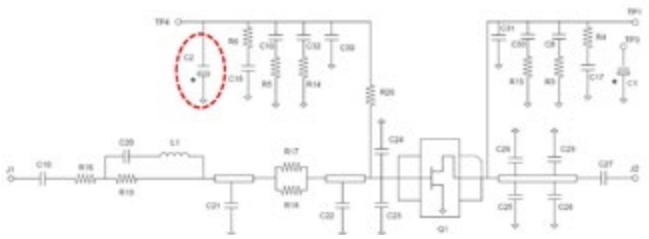

Figure 3: Circuit diagram of GaN QPD1008 connection as an amplifier for frequency range from 0.96 GHz to 1.215 GHz

Figure 4: GaN QPD1008 evaluation test board with C2 tantalum capacitor

Measurement Setup

The measurement was performed at standard conditions within the referenced datasheet operating conditions recommendations:

Bias and voltage setup: according to datasheet

Input signal: sin wave, frequency of 1 GHz, power of 15 dBm

Ambient temperature: -30 °C; +25 °C and +70 °C

Measurement equipment:
- Spectrum analyser Agilent N9320B
- Oscilloscope Tektronix MSO4104B

Spectrum analyser was connected to the test board output via the 30 dB attenuator. C2 tantalum capacitor waveforms were measured by oscilloscope and compared at different temperatures. The test board was inserted into the climatic chamber. Before the measurement, the test board was conditioned at least 30 minutes at the desired temperature (-30 °C, +25 °C and +70 °C). Spectrum of output signal was measured and compared.

Measurement Results

Figure 5, 6 and 7 presents measured waveforms and its FFT analyses on C2 tantalum capacitor position at temperatures: -30 °C, 25 °C and +70 °C. Spectrums of the output signals of GaN test boards – see figure 8.

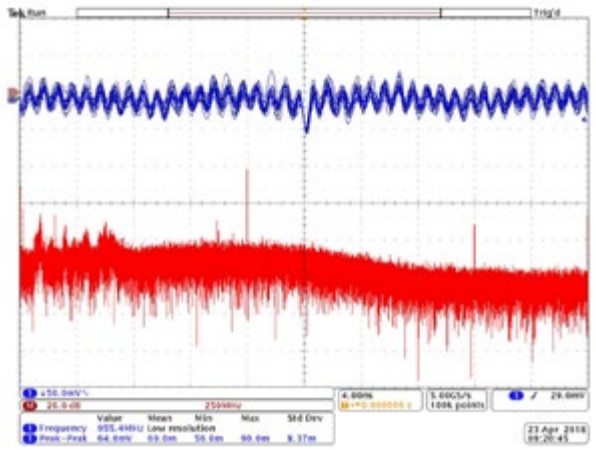

Figure 5: Waveform on C2 tantalum capacitor at -30 °C and its FFT analysis

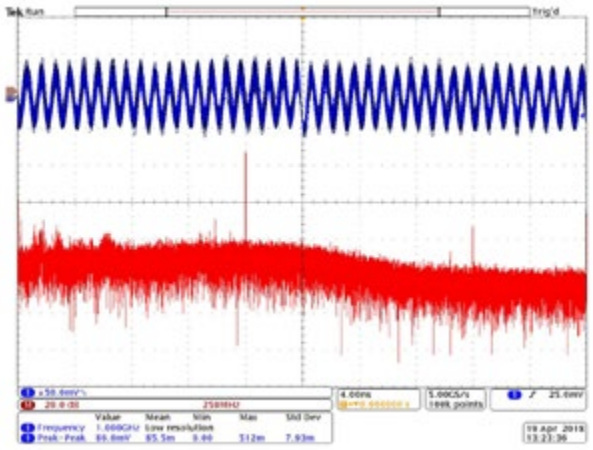

Figure 6: Waveform on C2 tantalum capacitor at +25 °C and its FFT analysis

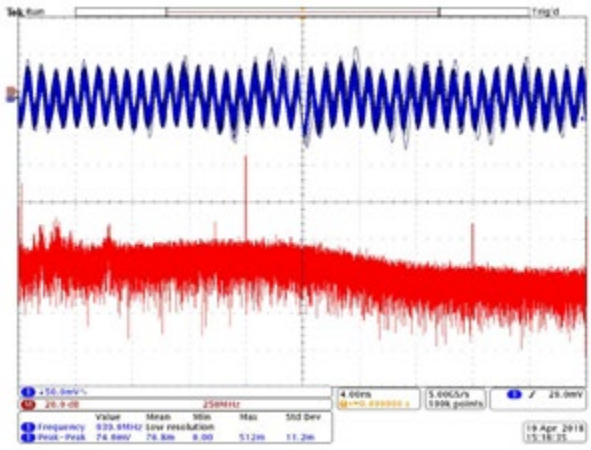

Figure 7: Waveform on C2 tantalum capacitor at +70 °C and its FFT analysis – tantalum capacitor.

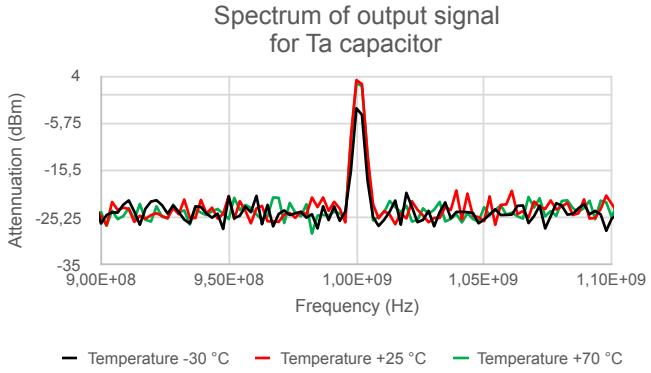

Figure 8: Spectrums of the GaN test board output signals for different temperatures.

Measurement Summary

There are practically no measurable differences in output signal stability of the tested RF amplifier board at +25 °C and +70 °C temperatures. Some output signal drop about 5 dBm test frequency attenuation is visible in the measured spectrums at ambient temperature of -30 °C. Nevertheless, such shift within 5 dBm can still be considered as a very good stability performance of the tested GaN RF power amplifier at the referenced conditions.

Conclusions

Rate of improvements of conventional MOSFETs has levered off, as their performance is now close to its theoretical limits as determined by the underlying fundamental physics of these materials and processes.

GaN is featuring a higher critical electric field strength than silicon that is resulting in a smaller size for a given on-resistance and breakdown voltage than a silicon semiconductor. GaN also offers extremely fast switching speed and excellent reverse-recovery performance, critical for low-loss, high-efficiency performance.

The above feature pose GaN as an ideal choice for RF systems and the upcoming fast growing 5G networks development as well as growing market of high power ~1 kV industrial applications such as renewable energy, EV/HEV vehicles, power traction systems, servers etc. GaN advantages can bring also new applications that have not been possible to make within such small size and simplified architecture so far such as the 48-V to 1-V single-stage hard-switched converter.

Stability at wide temperature range and harsh conditions are one of the design challenge for number of industrial applications. Linearity, efficiency, stability and high-power outputs are mostly driven of a good impedance matching and stable gate BIAS working point setting. Tantalum capacitors have been the favourite solution for BIAS decoupling circuits in the latest GaN power amplifiers.

The reference measurement on GaN RF power amplifier Qorvo QPD 1008 with tantalum 10 µF 16 V decoupling capacitor confirmed its very good stability at whole temperature range from -30 °C to +70 °C.

References

[1] Texas Instrument TIDA 00961 GaN 12V, 1.5KW design-in note; January 2018; http://www.ti.com/lit/ug/tidudt3/tidudt3.pdf
[2] Markos.A.,Z.; "Efficiency Enhancement of Linear GaN RF Power Amplifiers Using the Doherty Technique"; 2009; Kassel university press GmbH; ISBN online: 978-3-89958-623-7
[3] Qorvo QPD1008 125W, 50V, DC – 3.2 GHz, GaN datasheet; https://www.qorvo.com/products/p/QPD1008

Development of a Wideband High-Precision Current Sensor

In the field of power electronics, especially within the automotive and railway segments, the miniaturization and heightened efficiency of inverters that represent the primary structural component of motor drive systems is one of the most important tasks for developers. Wideband gap power semiconductors such as SiC and GaN are expected to feature smaller passive components due to higher switching frequencies and lower loss due to low on-resistance, thus leading to their use.

By Masayuki Harano, Product Manager – Sensors, HIOKI E.E. Corporation

The switching frequency of inverters built with power semiconductors will continue to heighten, which will necessitate power measurement at even wider bandwidths and higher precision. This article discusses the key features of a recently developed wideband high-precision current sensor and provides performance comparisons with competing products.

Classification of current sensors by principle of operation

Table 1 shows HIOKI's current sensor products classified into six operation principles. The Hioki CT6904 represents the flux gate element type.

High precision power measurement using the current sensor method

In order to achieve high precision power measurement with high repeatability using the current sensor method, it is important to use the following standards as conditions for selecting the appropriate current sensor [1].

(1) The rated current of the current sensor matches the current level of the DUT.
(2) The DUT's switching frequency of the current and all of the frequency components including harmonics are within the measurable frequency bandwidth of the current sensor.
(3) Measurement accuracy of the current sensor is defined across its entire measurable frequency bandwidth, and that the accuracy is sufficiently high.
(4) Uncertainty with respect to the current sensor's output noise, temperature characteristics, effect of conductor position, effect of external magnetic fields, magnetic susceptibility, effect of common-mode voltage, etc., are clearly defined and sufficiently small.

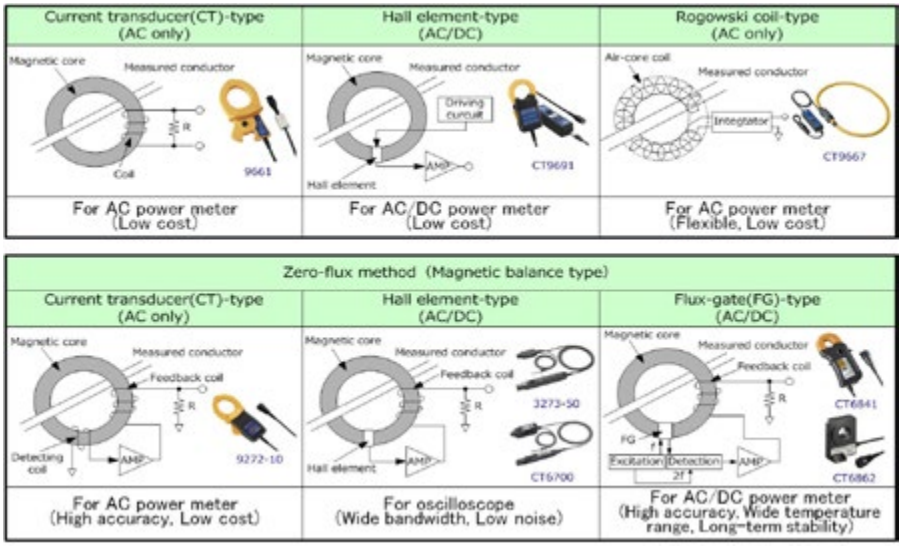

Table 1: Current sensors classified by operating principle

In particular, it is important to note that with regard to condition (3), many general current sensors define accuracy solely for DC and 50/60Hz signals, while accuracy for all other frequencies are only stated for typical reference. When using the current sensor method to measure power with high precision, careful attention must be paid to select both a power analyzer [2] and current sensor that exhibit the appropriate performance levels.

Developing wide bandwith high precision current sensor for next generation power electronics

Over a span of more than 40 years, HIOKI has developed high performance current sensors using proprietary technologies [3]. Its most recent development is the CT6904 AC/DC Current Sensor that delivers even higher performance in order to meet the needs of next generation power electronics applications. Table 2 provides the key specifications of the CT6904 (800A).

A) New CT Coil Structure

Figure 2 illustrates new CT coil structure of the newly developed Opposed Split Coil Technology. That technology increases the measurement band for current by utilizing a split winding in an opposed arrangement around a magnetic core. By optimizing the coil winding, the parasitic capacitance between wires is reduced and the frequency characteristic is improved.

B) Circuit Architecture

Figure 3 shows the architecture of the CT6904 AC/DC current sensors. Like conventional products (e.g., Hioki CT6862), the instrument uses the flux gate method, which takes advantage of the nonlinearity of a magnetic material's B-H characteristics to detect magnetic fields. This method, which offers

Production code generation

Development

Testing

Simulation

Electromobility – Complete Development and Testing with dSPACE

With advanced function development and test systems, dSPACE products make it possible to develop, simulate and test electronic control unit (ECU) software for all areas of electromobility and generate production code for it. Whether it's for electric motors, power electronics, batteries, electrical networks, or the charging infrastructure – You get everything from a single source. Trust in dSPACE's years of experience and one-stop solutions.

Be a pioneer – with development tools by dSPACE.

www.dspace.com/go/emobility

Embedded Success dSPACE

high sensitivity and extremely high temperature stability, is generally used to detect direction based on terrestrial magnetism.

Rated Current	800 A
Maximum Input Current	Within frequency derating characteristics (Fig. 1), up to ±1200 A peak is allowable if within 20 ms (design value).
Frequency Bandwidth	DC to 4 MHz (±3 dB Typical)
Linearity	±12.5 ppm Typical (23 °C)
Offset Voltage	±10 ppm Typical (23 °C, no input)
Accuracy	±0.025 % rdg. ± 0.009 % f.s. (45 Hz ≤ f ≤ 65 Hz, 23 °C ± 5 °C, max. 80 % RH)
Common-Mode Rejection Ratio (CMRR)	Minimum 140 dB (50 Hz / 60 Hz) Minimum 120 dB (100 kHz)
Measurable Conductor Size	Max. φ32 mm
Output Voltage	2 mV/A
Output Resistance	50 Ω ± 10 Ω
Maximum rated voltage to ground	1000V CAT III Expected transient overvoltage 8000V
Dust-proof and Waterproof	IP20 (EN 60529:1991+A1:2000+A2:2013)
Standard Compliance	Safety EN 61010-2-030:2010 EMC EN 61326-1:2013 Class B
Operating Temperature and Humidity	-10 °C to 50 °C, Max. 80 % RH (no condensation)
Power Supply	Via PW6001, PW3390, CT9555

Table 2: Key specifications of CT6904 (800A)

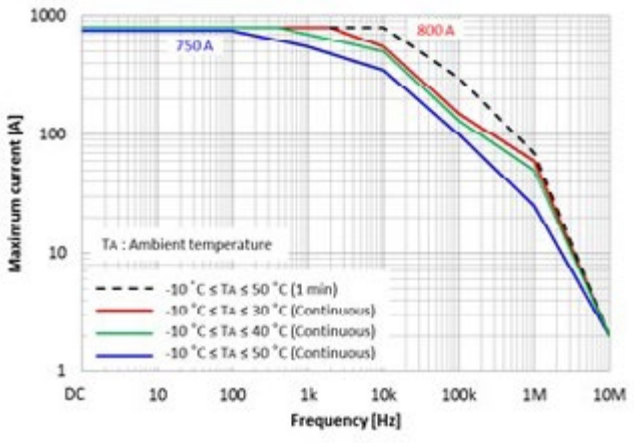

Figure 1: Frequency derating characteristics.

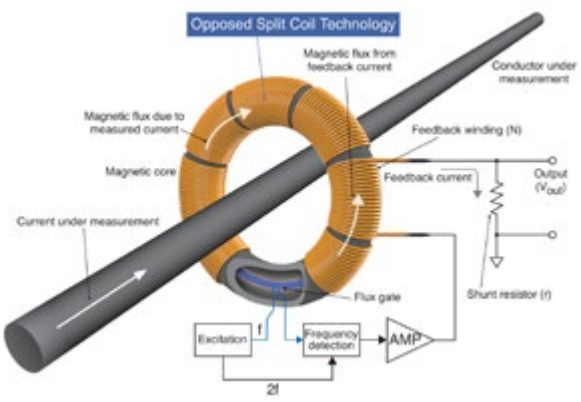

Figure 2: CT coil structure

[Solid Shield] Aluminum shield machined into a unique shape to eliminate influence on current measurements

An excitation current (f = 10.4 kHz) consisting of a triangle wave is generated so as to saturate a magnetic core around which a feedback coil is wrapped. When the current to be measured flows under these conditions, the instrument performs differential detection of changes in the voltage waveform induced in the winding by the resulting magnetic flux. By performing synchronous detection of this detection signal using a 2f signal that is synchronized with the excitation current, it is possible to obtain an output signal that is generally proportional to the current being measured. However, because the flux gate suffers from degraded sensitivity in the presence of large magnetic fields that cause its magnetic core to become saturated, we incorporate a design known as the zero-flux method by adding a negative feedback circuit. This enhancement allows the instrument to measure large currents.

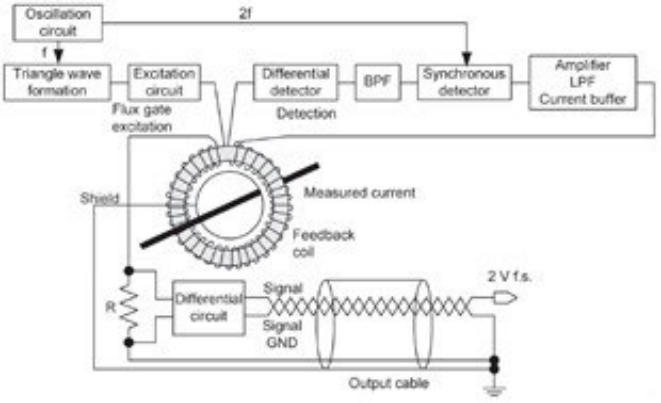

Figure 3: Circuit architecture

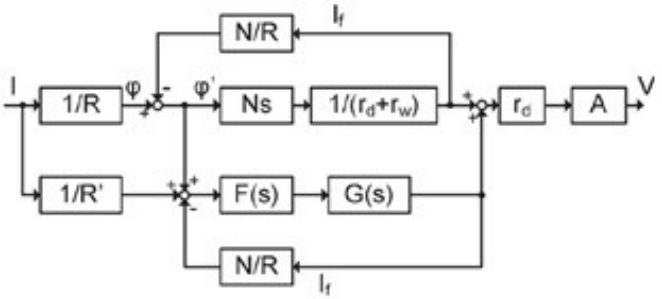

N: Number of feedback coil turns
R: Reluctance of magnetic circuit
R': Reluctance of leakage magnetic circuit
r_d: Detection resistance
r_w: Winding resistance
A: Output circuit gain
F(s): Transfer function for flux gate sensor
G(s): Transfer function for feedback circuit
I: Input current
V: Output voltage
I_f : Feedback current

Figure 4: Block diagram

C) Block Diagram

Figure 4 provides a block diagram. To achieve the instrument's basic current measurement accuracy, which significantly exceeds that of conventional sensors, we reduced noise by carefully selecting the magnetic material and optimizing the design of the flux gate excitation circuit's filter. Furthermore, stability was improved by adopting new electronic components with excellent temperature characteristics and long-term stability for use in the output block's differential circuit.

High-performance power

1.8kW

400 - 700V_{IN}

98% efficiency

Isolated fixed-ratio

Ultra-high voltage DC-DC converter

4.4 x 1.4 x 0.3in
110.5 x 35.5 x 9.4mm

HIGH POWER

500W

200 - 420V_{IN}

93% peak efficiency

Isolated regulated

DC-DC converter

1.8 x 0.8 x 0.2in
47.9 x 22.8 x 7.2mm

NEW RELEASE

98% efficiency

750W, 12/48V bidirectional

Non-isolated bus converter

0.9 x 0.6 x 0.2in
23 x 17 x 7.4mm

Up to 96% efficiency

8 – 60V_{IN}

10 – 50V_{OUT}, 140W

Cool-Power ZVS buck-boost switching regulator

10 x 14 x 2.6mm

Qualify for a free evaluation product at **vicorpower.com**

VICOR

D) Shield structure

Figure 5 shows the shield structure of the CT6904. By completely shielding the opposed split coil with a uniquely shaped solid shield crafted from aluminum, we are able to achieve both broad bandwidth and superior noise resistance. That allows accurate measurement without influence from surrounding voltage.

Figure 5: Shield structure

Example characteristics

Figure 6 through 14 illustrates the CT6904's example typical characteristics. The instrument delivers extremely favorable characteristics compared to conventional products or competing products, including in terms of frequency characteristics (versus gain and phase), CMRR, and effect of conductor position.

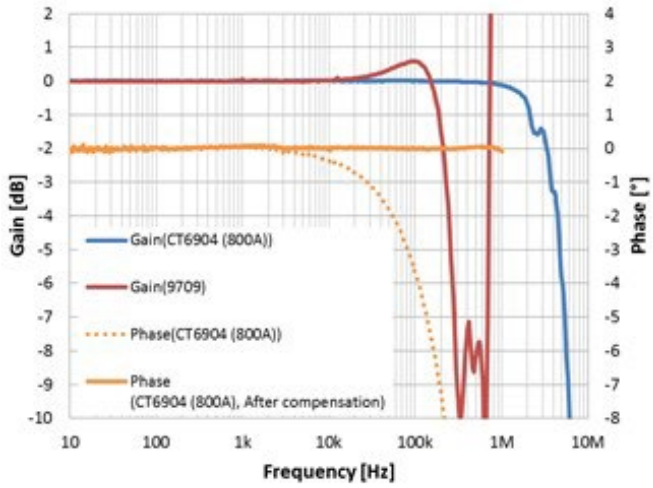

Figure 6: An example frequency characteristics

A) Frequency Characteristics

Figure 6 shows an example of its frequency characteristics. By utilizing a new CT coil structure in a closed-loop current sensor in which feedback current is made to flow to a feedback winding so as to continuously zero out the magnetic field generated by the current under measurement, we were able to achieve a wide 4MHz frequency bandwidth.

The phase values appearing in Figure 6 illustrate the difference when the HIOKI PW6001 Power Analyzer's phase shift function is activated. The phase shift function of the current sensor will be described below. High-accuracy current sensors tend to exhibit a phase error component that increases gradually in proportion to frequency in the high-frequency portion of the frequency domain, with the result that measurement accuracy may deteriorate for high-frequency measurement targets with a low power factor. The PW6001's phase characteristics shift block performs proprietary signal processing in real time to correct the phase characteristics of the 5 MS/s current waveform.

Current sensor phase characteristics information is configured by entering values for frequency and phase error from the sensor's test results. The instrument determines time lag, which is calculated from the input frequency and phase difference, and performs processing to shift to the equivalent time. This approach makes it possible to perform optimal correction for HIOKI's various current sensors based on each sensor's characteristics [4].

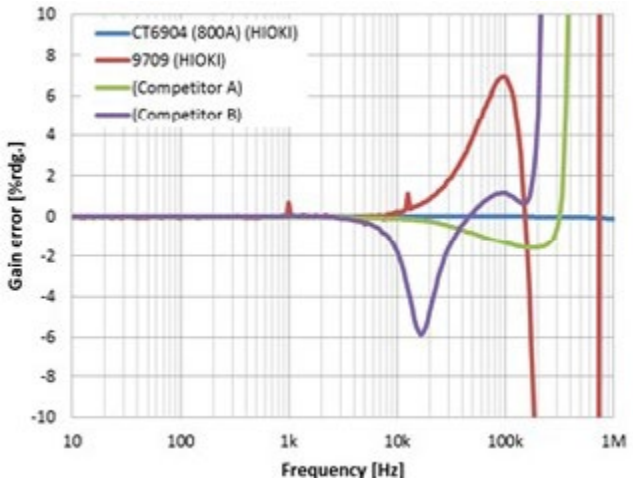

Figure 7: Frequency characteristics comparison of gain uncertainties

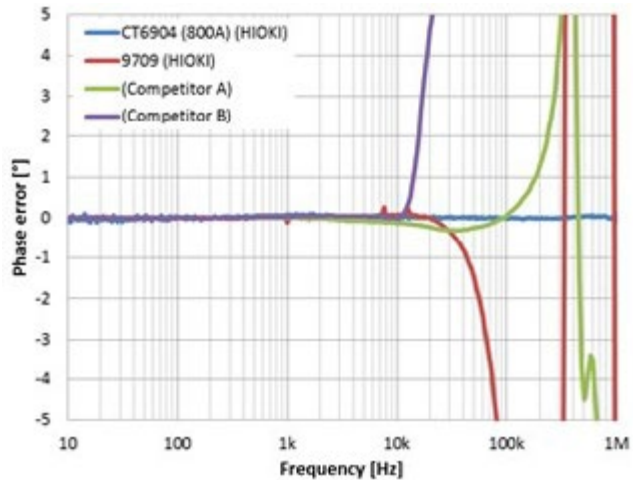

Figure 8: Frequency characteristics comparison of phase uncertainties

B) Performance Comparisons with Competing Products

The frequency characteristics graphs in Figure 7 and Figure 8 provide a comparison of the gain and phase uncertainties between the CT6904 and the HIOKI 9709 (500 A rated current, 100 kHz frequency bandwidth), Competitor A (600 A rated current, 500 kHz frequency bandwidth), and Competitor B (600 A rated current, 300 kHz frequency bandwidth), respectively. Because the competing sensors are both current output sensors, I-V conversion via a wideband shunt resistor is required. The frequency characteristics were measured using an FRA (Frequency Response Analyzer). As shown in the comparison results, the CT6904 exhibits extremely superior flatness up to 1 MHz over its competitors. ([Phase Shift Points] CT6904: 300 kHz; 9709: 20 kHz; Competitor A: 100 kHz; Competitor B: 10 kHz)

C) CMRR and Superior Noise Resistance

Figure 9 shows the frequency characteristics with respect to common-mode rejection ratio (CMRR). By completely shielding the opposed split coil with a solid shield crafted from aluminum, we were able to achieve exceptionally wide measurement bandwidth and noise

resistance. For example, the sensor delivers a CMRR of 120 dB (1/1 million) at 100 kHz, enabling it to measure accurately with low susceptibility to surrounding electric fields. Compared with traditional pass-through current sensors, it provides superior CMRR of at least 40 dB (1/100).

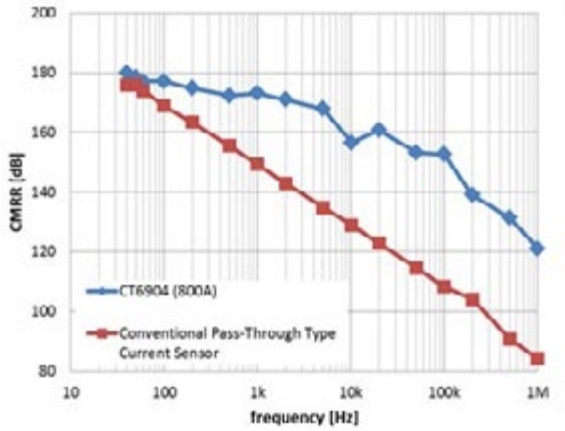

Figure 9: Frequency characteristics with respect to CMRR

In order to prove its high noise immunity, an experiment was conducted with the configuration shown in Figure 10, and an example of the measurement result is shown in Figure 11. In Figure 11, the uppermost yellow waveform is a voltage waveform, and the other four waveforms are three-phase output current waveforms. From the results, it was clear that the CT6904 exhibits significantly less noise than competitors A and B. For reference, the characteristics of HIOKI PW9100 are also shown. PW9100 is a direct-wiring type current sensor [5].

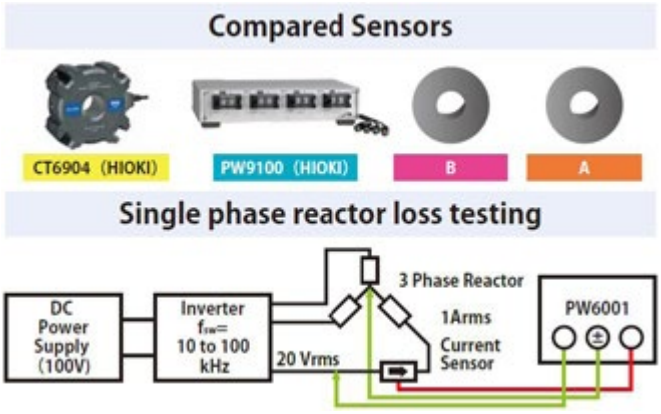

Figure 10: Experimental configuration for noise resistance comparison

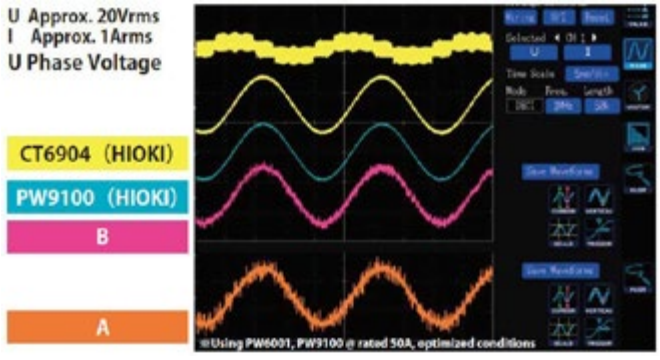

Figure 11: Results of comparison of noise resistance

D) Measurement Repeatability Not Affected by Conductor Position

Figure 12 illustrates conductor position on the inner core (A to F : position). Figure 13 and Figure 14 compare the effects of conductor position of the CT6904 with those of competitor sensors A and B. As illustrated, the CT6904 delivers superior gain and phase characteristics for input current at 100kHz.

Figure 12: Conductor position on inner core

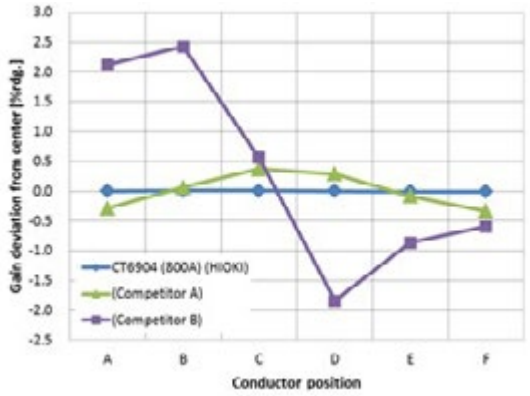

Figure 13: Effect of conductor position (Gain)

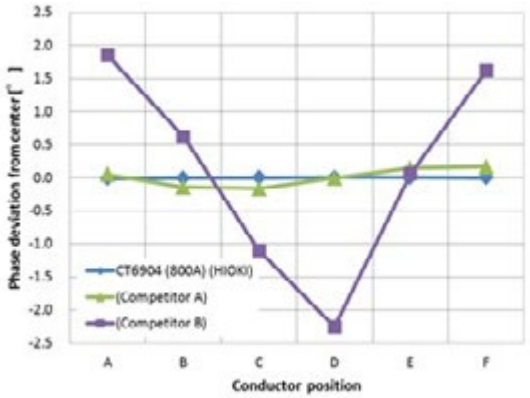

Figure 14: Effect of conductor position (Phase)

Performance required for high-precision measurement of high-frequency reactors

Inductance is the principal component in determining a reactor's impedance. From a power measurement standpoint, the measurement is characterized by a low power factor. In short, the phase difference between the voltage and current is close to 90°. As illustrated in Figure 15, the effect of the phase error between the instrument's volt-

age and current measurement system on measured values is greater than when measurement is carried out with a high power factor. Consequently, the measurement system must exhibit a high degree of phase precision.

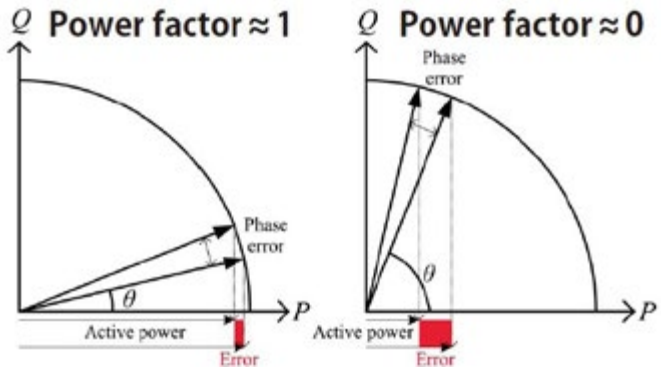

Figure 15: Relationship between phase error and active power error at different power factors

In addition, reactors are switched at frequencies ranging from several tens of kHz to several hundreds of kHz. As described above, commercialization of SiC and GaN elements has resulted in a tendency toward rising switching frequencies, and it is necessary to use measuring instruments with high phase precision at such high frequencies. Furthermore, when using current sensors, it is necessary to consider the current sensor's phase error.
Moreover, for measurements such as reactor loss of a step-up chopper circuit in a DC/DC converter, when testing voltage and current, a large common-mode voltage will be generated. As a result, it is necessary to use an instrument with a high CMRR. In addition, conventional wisdom holds that measuring reactor loss is a difficult process because it requires an instrument that exhibits a high level of performance in numerous areas. These requirements can be met by using the PW6001.

Example applications

A) High-Precision and Efficiency Testing of Inverters
Figure 16 provides an experimental configuration on how to measure the efficiency of the inverter-driven motor, and how the PW6001 and current sensors are configured. Principal components of inverter output power include a fundamental frequency component (up to 2 kHz), its harmonic components, the switching frequency (5 kHz to 100 kHz), and its harmonic components. Of those, the fundamental frequency component is dominant. Figure 17 illustrates an inverter output's line voltage waveform, line current waveform, and associated FFT results for a typical motor drive system.

Looking at the voltage FFT results, it is possible to observe the fundamental wave that is the principal component of the line voltage PWM waveform and its harmonics, along with the switching frequency and its harmonic components. A spectrum of at least 0.1 % f.s. exists up to approximately 2 MHz. The fundamental wave, its harmonics, the switching frequency, and its harmonic components can also be observed for the current waveform. However, the observed spectrum at frequencies of 100 kHz and above falls below 0.1 % f.s., and the current level falls abruptly as the frequency increases. This phenomenon can be explained by considering the equivalent circuit of a motor that is connected to an inverter as a load. The motor's winding can be thought of as an R-L load consisting of a resistance and inductance connected in series. Consequently, impedance grows at high frequencies, making it harder for current to flow.

Similarly, if we look at the power factor (cos θ) for the power of an R-L load, the power factor approaches a value of 1 when the frequency is low, for example for the fundamental wave and its harmonics. However, inductive reactance becomes dominant at high frequencies such as the switching frequency and its harmonics, so current exhibits lagging phase, resulting in a low power factor.

The bottom half of Figure 18 provides an enlarged view of the time axis for the inverter output voltage and current waveforms up to the switching frequency region. The voltage waveform is triangular. It is apparent that their phase relationship is characterized by the current's lagging phase, as described above, resulting in a low power factor.

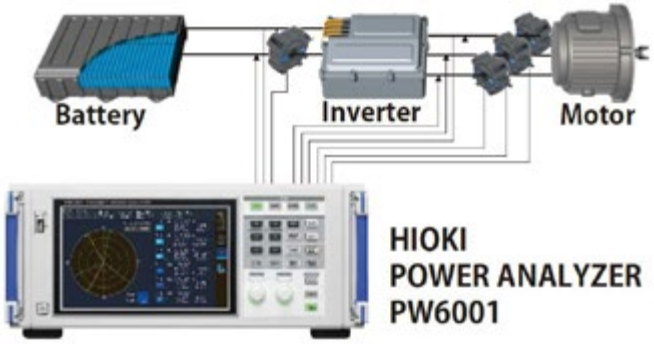

Figure 16: Experimental configuration on measuring an inverter-driven motor

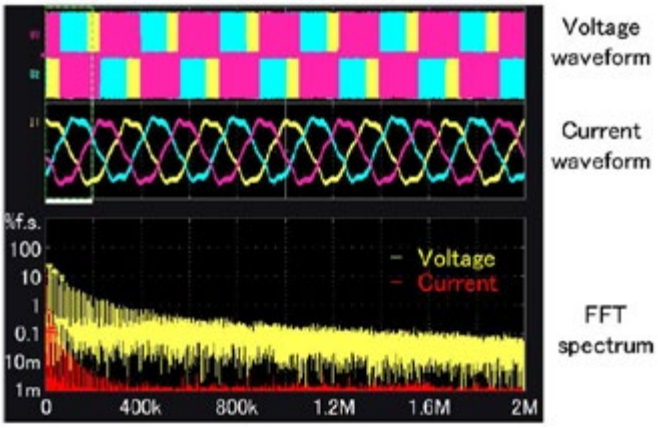

Figure 17: Waveform and FFT results

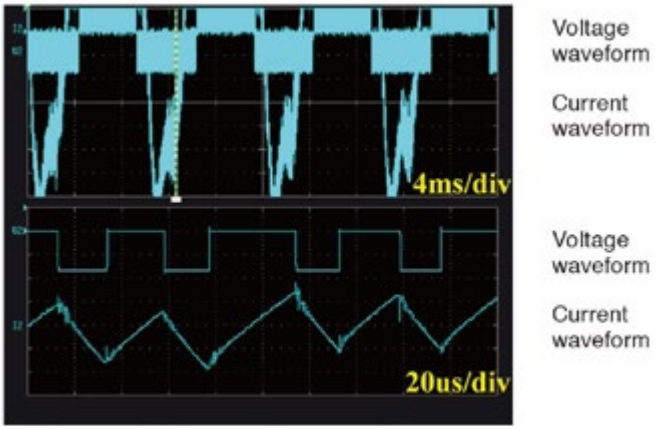

Figure 18: Enlarged view of inverter output waveforms

The characteristics of the main components of the active power of the inverter output are summarized as shown in Figure 19.

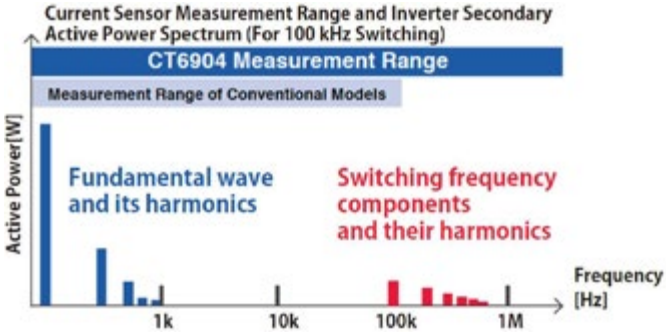

Figure 19: Principal components of inverter output active power and their characteristics

B) Reactor/Transformer Loss Analysis

Figure 20 provides an experimental configuration on how to measure the reactor loss of a step-up chopper circuit in a DC/DC converter, and how the PW6001 and current sensors are configured. Voltage and current applied to the reactor are directly measured by the PW6001, and power and loss are calculated. Power measured using this method represents the sum of the power consumption of the reactor coil and core, making it possible to measure the loss of the entire reactor [6].

Figure 21 shows an example of measuring the voltage and current waveforms of a reactor when it is switching at 100 kHz. Current waveforms measured using traditional current sensors (9709 or Competitor B) may be superimposed with high-frequency common-mode voltage noise at the time of the switching, but with the CT9604, such common-mode voltage noise does not appear, resulting in the ability to see exceptionally clear triangular current waveforms. Conventionally, in order to maximize the bandwidth, we use a LC resonance phenomenon near 100 kHz, which gives rise to the oscillating signal and common- mode noise. In contrast, the sufficient margin in the 4MHz bandwidth of the CT9604 and excellent noise resistance of at least CMRR=120dB are extremely effective in avoiding this issue without the need for a filter.

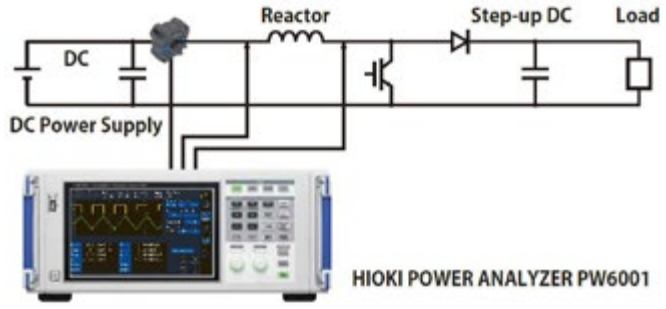

Figure 20: Experimental configuration on measuring the reactor loss of a step-up chopper circuit in a DC/DC converter

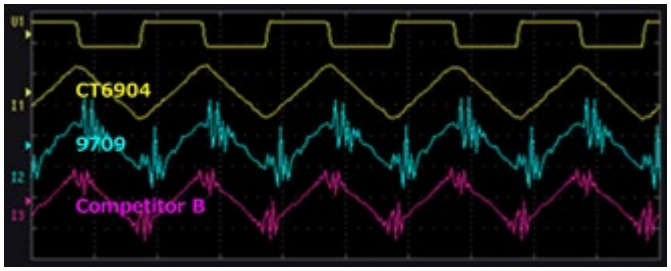

Figure 21: Example of measuring the switching waveforms of a reactor (100kHz switching frequency)

Finally, the configuration images of PW6001 and CT6904 are shown in Figure 22. In addition to the application of this paper, our products are expected to be useful for solving many customer problems.

Figure 22: PW6001 and CT6904

Conclusion

This article discussed the development of a current sensor that bears pioneering performance capabilities and its usefulness. As an application example, the loss measurement of a DC/DC converter reactor was described. Traditionally, it has been extremely difficult to measure reactor loss with high precision, but using the PW6001 and the current sensor, high precision testing can now be easily achieved. In the power electronics field, frequencies will continue to increase, along with the need to perform high precision analysis of power efficiency and other factors. HIOKI is confident in our ability to contribute to the development of industrial society through the development of advanced measuring instruments [7].

References

[1] H. Yoda, H. Kobayashi, and S. Takiguchi, “Current Measurement Methods that Deliver High Precision Power Analysis in the Field of Power Electronics,” Bodo’s Power Systems, pp.38-42, April 2016.

[2] H. Kondo, C. Yamaura, Y. Saito and H. Kobayashi, “Effectiveness of Phase Correction When Evaluating High-Efficiency Motor Drive”, Bodo’s Power Systems, pp.44-49, November 2017.

[3] K. Ikeda and H. Masuda, “High-precision, Wideband, High Stable Current Sensing Technology”, Bodo’s Power Systems, pp.22-28, July 2016.

[4] H. Yoda, “Power Analyzer PW6001”, HIOKI Technical Notes, Vol. 2, No. 1, 2016.

[5] H. Yoda, “AC/DC Current Box PW9100”, HIOKI Technical Notes, Vol. 3, No. 1, 2017.

[6] K. Hayashi, “Measurement of Loss in High-Frequency Reactors”, Bodo’s Power Systems, pp.18-22, February 2017.

[7] Masayuki Harano, Hajime Yoda, Kenichi Seki, Kazunobu Hayashi, Tetsuya Komiyama and Shuhei Yamada, “Development of a Wideband High-Precision Current Sensor for Next Generation Power Electronics Applications”, in Energy Conversion Congress and Exposition (ECCE), 2018 IEEE, pp. 3565-3571.

Heat Dissipation Challenge in Automotive High-Power Integrated Magnetics

In 2016, Premo Group launched 3DPower™, the first product to integrate two magnetics components that share the same core and feature two orthogonal magnetic fields at all points within the core. As a result, the increased power density in the component makes heat dissipation a tough challenge for our designers.

By Hector Perdomo Díaz, R&D Engineer, PREMO Group and Juan Manuel Codes Troyano, R&D Engineer, PREMO Group, in collaboration with MSMP Power GmbH

This article focuses on discussing the advances achieved by PREMO regarding heat dissipation techniques in 3DPower™. The biggest impact of magnetic integration is volume reduction when compared to a discrete solution for the same component. A consequence of increasing the power density is a temperature rise of the part.

Introduction

3DPower™ Pot-Core uses a custom pot-core shape where 2 inductive components are integrated. One of them is placed in the pot-core itself and the other one outside the pot-core as if it were a toroid. This product allows us to solve the engineering challenge of integrating magnetics: in this case it consists of a choke and a transformer. Unlike other magnetics integration technologies, both components share the whole core volume in the 3DPower™. For this purpose, the magnetic field of one component is orthogonal to the other, resulting in 2 independent and fully uncoupled magnetic elements.

As it can be seen in Figure 1, there is one winding inside the ferrite core (70a); while the other orthogonal winding is outside (70b/c/d). Designers of magnetics for mass production know that ferrite cores break easily, particularly when the winding is machine-made. Hence, it was necessary to cover the core with a coil. The readers can imagine how hot a core can be when it contains a winding with a few tens of amps, and it is covered by a plastic coil that has also wires around it; plus, this adds up to the core self-heating due to core losses.

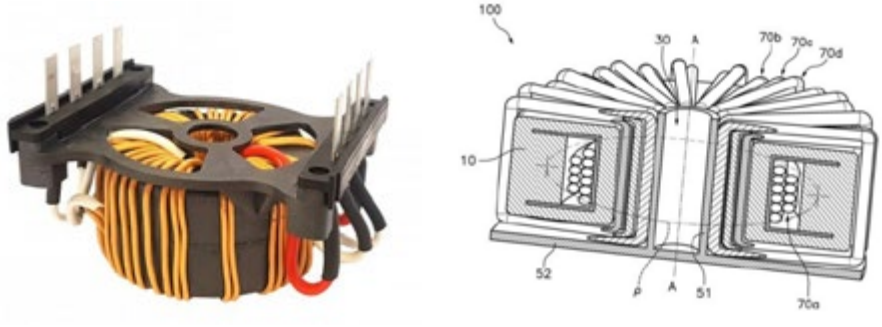

Figure 1: Pot-core solution (left); detailed cross-section (right)

Most of the times overheating failures are caused not only by the overall temperature increase, but also by hot spots. Hot spots can create temperature gradients in the ferrite core that could lead into breaks or a poor performance. Therefore, the main goal in a product is to avoid hot spots by creating good thermal link between all the components and then ensure a proper cooling system to remove heat.

Premo can provide fully customized solutions of the 3DPower™. However, due to its geometry, the main applications are Phase-Shifted Full-Bridge and Resonant LLC DCDC converters. The output power range spans from 1 kW to 11 kW, but higher powers can be reached on demand. One of our latest developments can be seen in Figure 2, where three magnetics components are combined in one single core (1 transformer and 2 inductors). This is just one example of how easy is to integrate magnetics by using our technology.

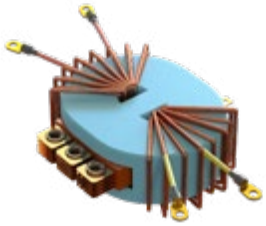

Figure 2: Step-down transformer + series inductor + parallel inductor for a 3.5kW LLC converter

Thermal Link

A proper design and a wise selection of materials are key for thermal performance. The picture below shows an 11kW transformer where windings were made using stereolithography 3D printing technology and cooled with water in the bottom core. The wire is much hotter than the core, particularly on the bottom.

The solution consists of using thermal conductive plastics on the coils to create a thermal link between the wire and the core, for example with thermal pad or thermal liquid gap filling material. In the 3DPower™, thermal liquid gap filler was dispensed to guarantee a reliable thermal link between coils, windings and core.

Core Adhesive

Core sets are supplied in halves. The easiest and cheapest way to join two cores is to use tape, which is common for cheap and small transformers. Although the magnetic path is not affected, the thermal resistance is high

Driving the Best Efficiency

The SA110 is the first half H-Bridge with silicon carbide MOSFETs and integrated digital gate drive to provided reduced switching losses, reduced conduction losses and a low temperature dependency of $R_{DS(on)}$

With the use of silicon carbide (SiC) MOSFETs, the SA110 drives a significant increase in performance and reliability compared with silicon or IGBT alternatives while providing 40 A of peak output current on supply voltages up to 400 V. The integration of a gate drive with full digital control makes it easier to control and reduce the impact of parasitics on switching frequency. As a result, the SA110 can switch at a very high 400 kHz MAX frequency. Protection features include under voltage lockout and active Miller clamping. The SA110 is available in a very compact 12-pin Power SIP to save on valuable board space.

Target Applications:

- Sonar
- AC/DC Inverters
- Brushless DC Motors

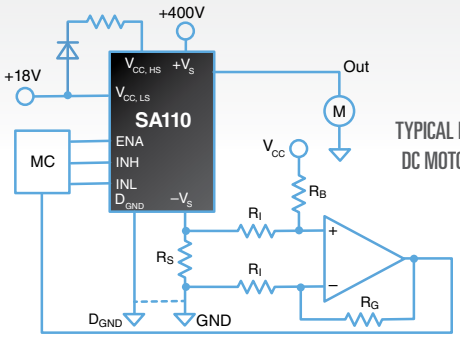

TYPICAL BRUSHLESS DC MOTOR CIRCUIT

12-PIN, POWER SIP, STYLE DP WITH HEAT TAB

Footprint 31mm x 29.5mm

https://apexmic.ro/bpsSA110

APEX MICROTECHNOLOGY

ISO9001

between the two cores. Thus, when one of the cores is attached to a heatsink, the temperature gradient in the other one is so high that could lead into ferrite breaks.

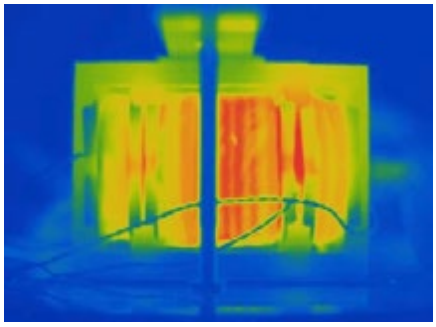

Figure 3: IR image of a 11kW transformer with load (left); overview of the 11kW transformer (right)

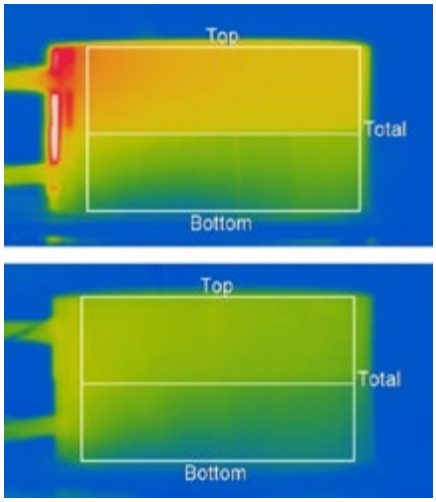

Figure 4: Temperature gradient of core sets with different adhesives: standard adhesive (top), high thermal conductive adhesive (bottom)

We performed tests in our R&D facilities and the results highlighted that when using a standard adhesive, the gradient of temperature between the two cores halves is twice than using a high thermal conductive adhesive. The ferrite not only can break, but also due to an inductance variation with temperature the reluctance of both cores will be different and can create unwanted performance.

Coil Plastics

As explained, the pot core will be covered with a plastic coil to protect the ferrite during the winding process and to provide electrical isolation. This coil will be exposed to the air if natural or forced convection is used and in contact to a cooling plate if water cooling is used instead.

Three different plastics were tested for natural convection. The first plastic was a commonly used Liquid-Crystal Polymer (LCP) ~0.5 W/m·K thermal conductivity, the second one was a PA6-based compound (polyamide) with 1.2W/m·K thermal conductivity, while the third one was also a PA6-based plastic with 4W/m·K thermal conductivity. The three samples were prepared with thermocouples inside and tested at the same operating point. The temperatures measurements were logged and fitted according to the method of least squares (Equation 1). This equation simplifies the thermal model, which becomes a lumped capacitance model.

$$T = T_f \cdot \left(1 - e^{\frac{t}{\tau}}\right) \quad \text{(Equation 1)}$$

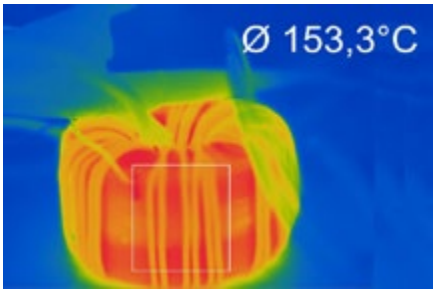

Figure 5: IR image of the LCP sample during the test

Results showed that the final temperature was the same for the three sample. Nevertheless, the PA6 with the higher thermal conductivity reached the steady temperature twice as fast as the other samples. This means that the “tau” coefficient of the PA6 4W/m·K sample in the lumped capacitance model equation is halved when compared to the rest.

A fast response system will show a faster ‘reaction’ to temperature variations, spreading the heat faster and therefore lowering the risks of ferrite cracks or hot spots. So, in this case the use of high thermal conductive plastics had a significant impact in the thermal behavior of the part. In the next section we will see if this also applies for the forced conduction approach.

Resins

In EV/HEV vehicles, all high-power magnetics must be cooled down by means of a forced cooling technique. Since semiconductor power modules are attached to a cooling plate, this is used also to mount the magnetic components on it. Most of our clients use only thermal pads, but there is a growing trend in the industry towards the use of resins to pot the whole on-board charger or the power converter. The size of the power electronics units is reduced thanks to the better thermal dissipation and electrical isolation of the resin.

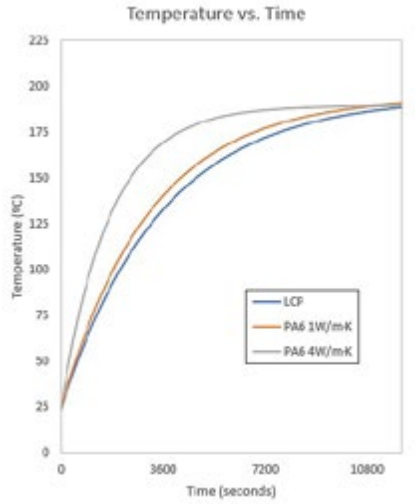

Graph 1: Test results for different coil plastics

We conducted a test with PA6 4W/m·K and LCP samples, both inside an aluminum case and potted with automotive silicone resin. The cases were mounted on a cooling plate with thermal pad in between as shown in Figure 6. The purpose of this test was to check if thermal conductive plastics improve the design when potted with resins.

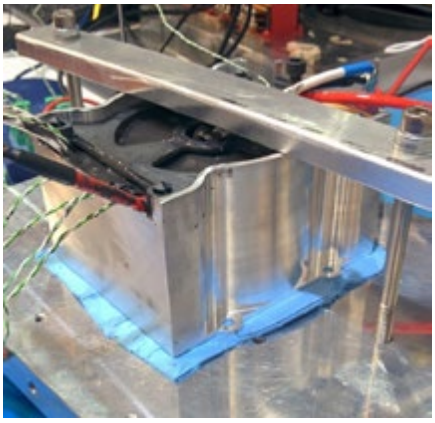

Figure 6: Test setup with cooling plate

Results confirmed that the final temperature of the samples was similar, with a difference of only 4ºC, which is negligible if we consider thermocouples accuracy and manufacturing

divergences among samples. The time response of the system was slower for the PA6 sample (25% slower).

High Power Test Setup

To test the electrical and thermal performance of the 3DPower™ magnetics under all load conditions a high-power test setup from MSPM Power GmbH was used. A TTG1000SIC square wave generator is the main part of the test equipment and it generates the square wave signal of up to 1000V. The square wave frequency can be set within a range of 10 kHz to 450 kHz and it is also possible to set the duty cycle from 0 to 100%. An external full-wave rectifier module (PCK-Module) is connected to the secondary side of the transformer or the resonant circuit to convert the AC signal into a DC voltage. With this test setup it was easy to characterize the magnetic components under real-life conditions.

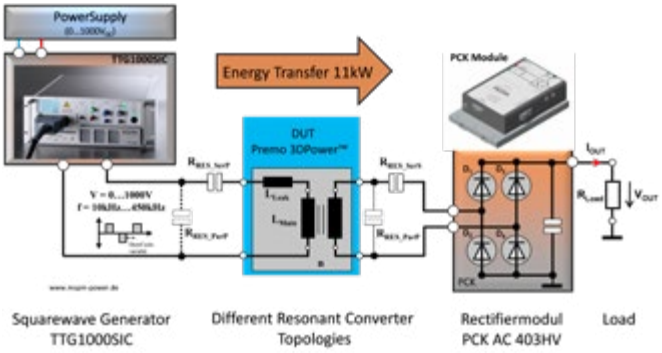

Figure 7: High-power test equipment

Conclusions

Reliability of the components is a performance point often forgotten; we only care about it when there is an issue. Most of reliability issues are related to temperature: fire, parameter variation, ferrite cracks, low performance, etc. For this reason, engineers must design and select the best materials to improve the thermal behavior.

This article has shown how relevant is selecting the optimal materials in different scenarios. First, it emphasizes the creation of good thermal links between all the components of a transformer to achieve a continuous path for the heat to the cooling source.

Then we checked how a simple thing like the adhesive of the cores could reduce the temperature gradient from 18ºC to 9ºC in our test.

Finally, we confirmed that also good thermal conductor plastic can improve the heat dissipation in some cases; however, in other cases, it may not be worth. When the part is potted with resin, a high thermal conductive plastic does not improve at all on a standard Liquid-Crystal Polymer plastic. The cost of the resin is higher, so the final decision is, as usual, a cost-performance tradeoff.

www.grupopremo.com

Inrush Current Limiters - Combined Current Control

High-power loads are a major stress factor when fuses and components are switched on, as they cause very high currents to flow. To avoid this, TDK offers ceramic EPCOS inrush current limiters (ICLs), based on NTC and PTC thermistors – a strong duo when used in combination.

By Christoph Jehle, Manager Technology Communications, TDK

When high power loads such as power supplies, frequency converters or on-board chargers are powered up, currents that can be many times the rated current occur for a short period. This can result in undesirable effects, such as the tripping of fuses, or even damage to the system. Two types of load in particular are responsible for high inrush currents: On the one hand, these are inductive loads such as motors and transformers, which require very high currents in order to create the magnetic fields. The other group are high-capacitance capacitors in DC links, which cause very high charging currents at the moment of connection, which represents a considerable stress factor for the capacitors themselves, as well as for the rectifiers. Figure 1 shows the current flow with and without inrush current limiters (ICLs).

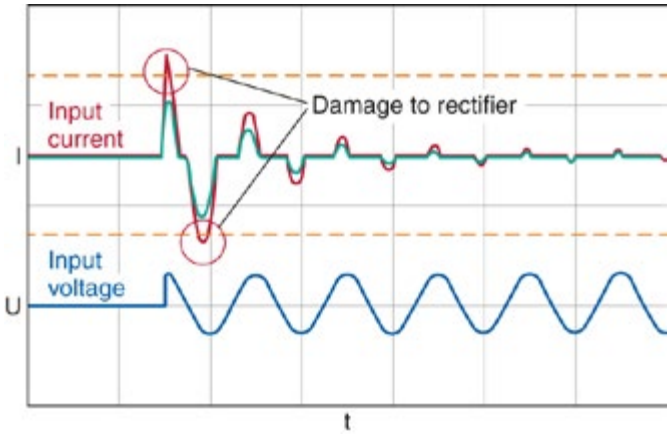

Figure 1: Current flow in a rectifier without inrush current limitation (red) and with inrush current limitation (green).

The simplest way is for inrush currents to be limited using low-ohmic power resistors. This does however have the disadvantage that in normal mode a power loss occurs at these resistors that should not to be ignored. A considerably better solution is the use of thermistors in their function as ICLs. NTC or PTC thermistors, which exhibit different thermal characteristics and thus offer different possibilities for use, are used for this purpose. One way of exploiting all the benefits of these components is to use them in combination. First let us look at the NTC thermistors:

Elegant solution with NTC thermistors

One very elegant solution for limiting high input-side inrush currents is the use of EPCOS NTC thermistors. Functional principle: These ceramic components are temperature-dependent resistors whose resistance drops as the temperature rises. At room temperature (25 °C) they exhibit a specific resistance value (R25) which limits the inrush current. When current continues to flow through the component it heats up and the resistance falls to very low values which, depending on the type, can be significantly below one ohm. The losses at the rated current are correspondingly low. Figure 2 shows typical resistor characteristic curves of various NTC ICLs relative to temperature.

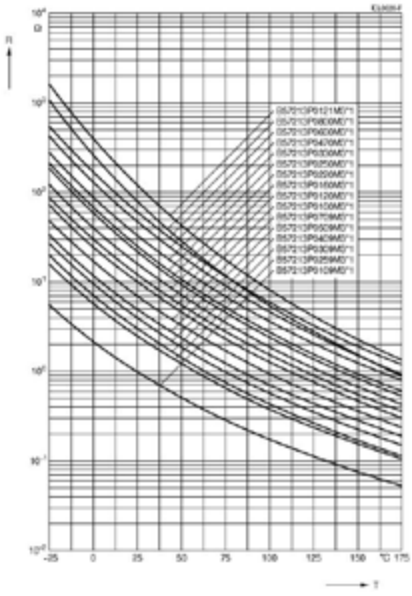

Figure 2 (a+b): Typical characteristic curves of EPCOS NTC ICLs. Right: NTC inrush current limiter with a starting resistance R25 of 10 Ω.

Selection criteria for NTC ICLs

The two most important criteria for determining the suitable NTC thermistor are the initial resistance (R25) and the maximum current. First, the required R25 is determined. It must be selected high enough so that, by connecting it in series with the load, it limits the current to a

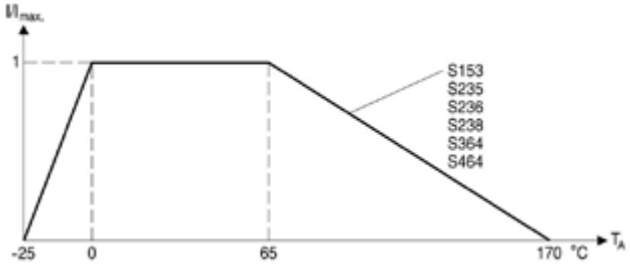

Figure 3: Typical derating characteristic of NTC ICLs.

electronica
2018
Hall B3
Booth 542

Solutions for your Power Modules from One Source

AMB and DAB Substrates

AMB Substrates with lowest thermal resistance and superior bending strength. DAB Substrates with excellent reliability and PD properties.

Integrated Substrate

High innovative substrates, embedded in Al-baseplate or Al-heatsink, enabling >25% improved heat-transfer and > 50% reduction in weight on module level.

Cu Baseplates

Balanced material combination for high thermal conductivity and minimized warpage for high reliability in comparison to conventional Cu baseplates.

Cu-Graphite Composite Baseplates *Co-Development with The Goodsystem Corp.*

Effective material combination of higher thermal conductivity and lower thermal expandability (CTE-adjusted to Al2O3) for excellent reliability, smaller size and lighter weight.

Find out more details:
www.dowa-europe.com / info@dowa-europe.com

DOWA
DOWA HD Europe GmbH

value that does not yet cause the fuse to trip, and so that no damage occurs to components of the load such as rectifiers.

The second criterion is Imax, which is determined by the power rating of the load. The important thing here is the derating of the NTC thermistor. A typical example of this is shown in Figure 3.

TDK offers a wide range of NTC thermistors with an R25 of between 0.5 Ω and 33 Ω and permissible currents of 1.3 A to 30 A.

When using the ICLs, a cooling time of about 90 s depending on type should be ensured, which can be problematic in the case of loads that are frequently switched on and off at short intervals, as a warmed-up NTC thermistor is very low ohmic and thus offers almost no current limiting. A remedy is provided here by the bypassing of the NTC thermistors using a relay or a thyristor. This can take place just a few seconds after switching on, as most loads are then already

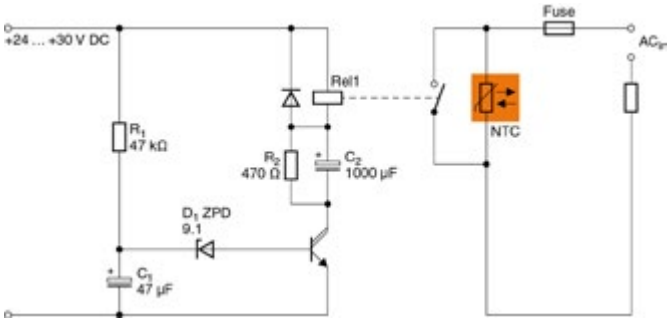

Figure 4: Time-controlled bypass circuit for ICLs.

being operated with the rated current. Thanks to the bypass, there is no warming of the NTC thermistor. Figure 4 shows a time-controlled bypass circuit for ICLs.

The response time of the bypass circuit is determined by the time constants of R1 and C1 as well as the value of the Zener diode. In the example circuit the relay responds after about 3 or 4 seconds – depending on the tolerances of the components. On the relay used (24 V DC, 8 A AC) the holding voltage of the coil is around 0.5 UN. Due to the charging current of C2 the relay responds and is operated

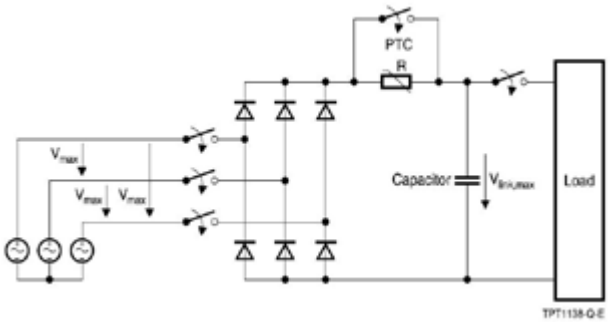

Figure 5: DC link circuit with charging current limitation by PTC thermistor. Right: PTC thermistors in housed and standard disk designs.

at half the rated voltage after C2 has been charged, which halves the current requirement. Particularly if the loads have high rated currents, the power demand of this circuit is less than the losses caused by the continuous current flow through the NTC thermistor.

Reliable capacitor charging by PTC thermistors

High-capacitance capacitors and capacitor banks in DC link circuits represent a short circuit at the moment of switching on. In order to achieve reliable current limitation here, PTC thermistors should be used instead of fixed resistors. The high current flow causes these components to heat up and – contrary to NTC thermistors – become high-ohmic, which makes them intrinsically safe. This behavior offers the advantage that, in the case of a short-circuit in the DC link, the current is limited to harmless values, something that fixed resistors cannot offer. Figure 5 shows the DC link circuit of a 3-phase system with PTC thermistor which is used, for example, in frequency converters.

For DC link circuits, TDK offers a series of special PTC thermistors that are designed for voltages of between 260 V DC and 560 V DC, offering resistances between 22 Ω and 1100 Ω at 25 °C and, depending on their type, have approvals compliant with UL, IECQ and VDE, as well as being qualified in accordance with AEC-Q200.

Particularly in the case of larger banks of capacitors, care should be taken that the maximum thermal capacitance and maximum permissible temperature of the PTC thermistors are not exceeded. The necessary thermal capacitance can be achieved by connecting the PTC ICLs in parallel. The required minimum number of components is calculated as follows:

$$n \geq \frac{k * C * V^2}{2 * C_{th} * \left(T_{Tref} - T_{Amax}\right)}$$

Where:

n	Number of PTC elements required
k	Factor is dependent on the power supply (k = 1 for DC; k=0.96 for 3-phase rectifier; k = 0.76 for single phase rectifier)
C	Capacitance of the DC link capacitor in F
V	Maximum charging voltage of the capacitor in V
C_{th}	Thermal capacitance of the PTC thermistor
T_{Ref}	Reference temperature of the PTC thermistors used
T_{Amax}	Maximum ambient temperature

In normal operation the PTC ICL, or several PTC ICLs connected in parallel, must be bypassed after charging the DC link capacitors in order not to produce any power losses. There must be no bypass, however, if there is a short circuit in the DC link – caused perhaps by damaged capacitors. The most significant parameter for a bypass

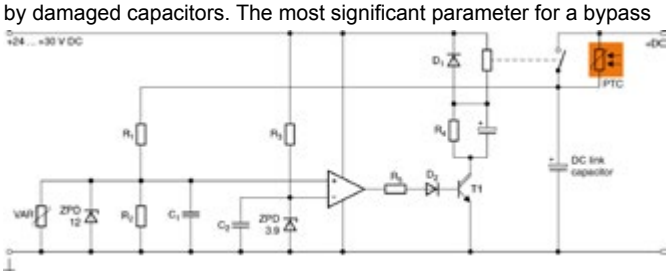

Figure 6: Voltage-controlled bypass for PTC thermistors.

circuit therefore is the DC link voltage. If, after charging, it reaches the setpoint, there is no fault; if, on the other hand, it remains at a very low value for a longer period, there is a short circuit. This enables a

comparator circuit to be implemented with little effort, which bypasses the PTC thermistor only after charging of the DC link (Figure 6).

Notes on the function: The inverting input of the comparator is controlled via the Zener diode ZPD3.9. As long as a voltage of less than 3.9 V is applied to the non-inverting input, a voltage of almost 0 V appears at the output and T1 blocks the relay. Only when a voltage of more than 3.9 V is applied via the voltage dividers R1/R2 to R2 does the comparator at the output trip to positive potential and T1 switches the relay, causing the PTC thermistor to be bypassed. The voltage dividers R1/R2 should be dimensioned in such a way that the relay switches at about 80 percent of the rated DC link voltage. As DC link voltages can be several hundreds of volts, high-impedance types must be used for R1 and R2. Example: At a rated DC link voltage of 500 V DC the value of 80 percent is reached at 400 V DC. At this point, the value for R1 is about 990 kΩ and for R2 it is about 10 kΩ. The varistor and the Zener diode ZPD12 serve to protect the non-inverting input of the comparator against overvoltages.

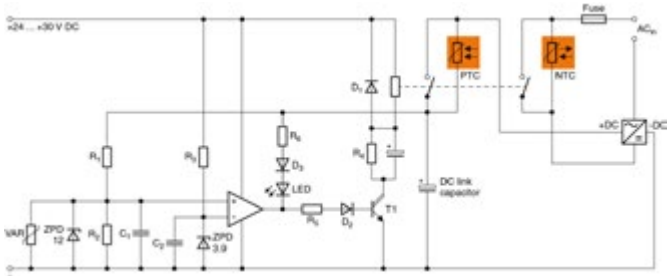

Figure 7: Voltage-controlled combination of NTC and PTC inrush current limiters.

Combining the advantages

Especially in the case of high-power loads that have high DC link capacitances, such as those in industrial power supplies and converters, it is advisable to combine the advantages and functions of NTC and PTC inrush current limiters.

It is sensible therefore to use the voltage-controlled ON time described here also for bypassing the NTC thermistor on the power input side. For this purpose, a relay with two changeover contacts is required in the circuit shown in Figure 6. Figure 7 then shows the complete circuit, in which the NTC and PTC thermistors are switched simultaneously. In addition, an LED has been integrated which indicates that the jumper has not yet been applied.

The advantages of such combined inrush current limitations are the protection of components, the avoidance of unintentional tripping of supply-side or device-internal fuses, and reliable current limiting in the event of short-circuits in the DC link.

www.epcos.com/icl

High B_s Ferrite Material for High Power Application

There is no doubt that power electronics is playing a critical role in the evolution of the overall infrastructure of energy supply, from motion control and drives to industry automation and traction techniques. However, unlike decades of impressive developments in the semiconductor technologies, the developments in the passive components arena, especially magnetic components, has been rather slow and seen as power system bottleneck in terms of efficiency and miniaturization.

by J.C. Sun, founder of Bs & T Frankfurt am Main GmbH

To fully tap the benefits of next generation semiconductors, namely silicon carbide (SiC) and gallium nitride (GaN) power devices, the next generation passive components, particularly magnetic components, must be compatible with these emerging devices, especially at high frequencies and under high pulse excitation. In essence, high saturation and low power losses under pulse excitation and relatively high temperatures are required. Current power converters using manganese-zinc (MnZn)-ferrite magnetic materials possess saturation induction Bs around 530 mT at room temperature that decreases down to 430 at 100 oC. It is to be noted that the Bs is measured according to IEC standard for polycrystalline ferrite under room temperature, at field strength of 1194 A/m and 10 kHz, which is far beyond the application range. The applicable field strength varies between 100 and 200 A/m depending on the industry (aerospace, industrial and consumer electronics). Accordingly, the power losses of these materials at 1MHz and 50 mT vary from around 350 mW/cc at room temperature to approximately 1W/cc at 100 oC. The measuring condition is still under sinusoidal mode.

High Bs Material Development

The Ferrite material given by high resistivity is limited by the saturation flux density due to its polycrystalline nature compared to their counterpart metal alloyed material [Figure 1]. Since magnetic parameters are highly nonlinear, direct comparison is often misleading. Consequently, the decisive parameter, to express the softness of materials, is definitely the coecivity under same temperature, field strength and frequency.

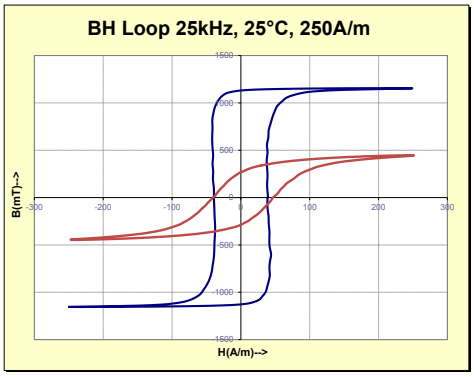

Figure 1: A comparison of AC FeSiBNbCu Finemet type alloy vs. ferrite material @ 25 °C , 25 kHz and 250 A/m, measurement performed by Bs&T Frankfurt am Main GmbH

The very recent development of polycrystalline MnZn-ferrite material with saturation induction can be stated at least 600 mT at room temperature and at least 500 mT at 100oC, which are almost 20 % higher than reference power ferrite material for 120 kHz application.

It is well known that the saturation induction (Bs) of a polycrystalline MnZn-ferrite component is proportional to the magnetization per unit volume and, as such, it depends on the chemical composition of the crystalline unit cell and on the density of the material. It is, therefore, less dependent on the morphological characteristics of the microstructure, such as grain and pore size, or the chemical nature of the grain boundaries. Since MnZn-ferrites are crystalline materials of the cubic (only partially inverse) spinel structure with ferrimagnetic behavior, the saturation induction maximization will most probably proceed according to the rules of the maximization of the magnetization difference between the B (octahedral) and A (tetrahedral) sublattice. Presumably, the iron content of the composition should be maximized under the conditions that the spinel phase is retained and no secondary phases are formed (i.e. hematite-Fe2O3 or wustite-FeO). Thus, materials with the highest possible iron concentration will be synthesized, the conditions for doing that will be specified and the magnetic properties will be measured (with focus on saturation induction as a function of temperature).

The synthesis process is mostly applying so-called mixed-oxide method, according to which a powder mixture of the raw materials (Fe2O3, Mn3O4, ZnO) at the appropriate proportions is prefired, shaped by uniaxial pressing and sintered at elevated temperatures, which is finally supposed to produce the new material grade in large scale. On the other hand, the power losses of components made of MnZn-ferrite materials depend strongly, besides the composition of the unit cell, also on the morphological properties of the microstructure. The fraction of the losses depending on the crystal is termed “hysteresis losses”, while the fraction that depends on the morphology is termed “eddy current” losses. There is also a third fraction termed “resonance losses” that is related with ferrimagnetic resonance of the material and is both crystalline and random microstructure dependent. At high application frequencies (~1MHz), such as those targeted in this proposal, the “eddy currents” dominate and constitute more than 50% of the total power losses. The very first strategic step in the methodology would be the reduction of the main power loss source. Subsequently and at a later optimization phase, attempts to reduce the other source losses will be included.

The eddy current losses are losses because of the development of ohmic type eddy currents when operation takes place under alternating magnetic fields. Since these currents are of ohmic character, the most efficient way for their reduction is to increase the specific resistivity of the material. This can be done by executing the final sintering step in such a way so that a high density and, at the same time, a fine-grained microstructure will form. Fine grained microstructures have a high grain boundary concentration and since the specific resistivity of a grain boundary is significantly higher than the specific resistivity of the crystal, the total resistivity of the polycrystalline microstructure increases. It is well known within ceramic powder technology that the achievement of fine grained microstructures requires active powders with small particles and relatively low temperatures, so that grain growth will not take place during sintering. These low temperatures do not favor densification. Moreover, the presence of excess iron in the composition (as required for the achievement of high saturation induction) is another factor that delays densification. This happens because excess Fe3+ ions on divalent iron positions create positively charged defects, which are compensated by negatively charged cation vacancies. This, in turn, through the Schottky equilibrium, decreases the concentration of positively charged Oxygen vacancies. In ionic solids, the diffusion of the relatively large oxygen ions through oxygen vacancies is the rate controlling step and the existence of oxygen vacancies is essential for mass transfer and densification.

Conclusively, there is an inherent interaction between crystal composition and processing towards the development of the appropriate polycrystalline material. The main challenge is that process parameters that favor high saturation induction (i.e. iron oxide content), also retard sintering and densification that are also desirable both for high saturation induction and high frequency performance. This is exactly the region where innovation through recent engagements will be achieved, bringing about a breakthrough in MnZn-ferrite materials and extending significantly the frequency application region of MnZn-ferrites. Those previously mentioned obstacles are also the reason that all currently existing high frequency materials have low saturation inductions. The proposed concept is to study the densification of MnZn-ferrites and identify the process parameters that affect the two individual but simultaneously occurring processes: densification and grain growth. The results will be used to design firing schedules, allowing densification and grain growth at the most possible separated and consecutive temperature regions rather than in overlapping regions. This will give a lot of freedom to the materials engineer to design compositions and microstructures towards the desired magnetic performance. In a later stage, material optimization due to fine tuning will occur. This may include slight composition adjustment to locate the Curie point at appropriate temperature and, thereby, to mediate the saturation induction decrease with temperature. Likewise, addition of certain selected dopants can increase the resonance frequency and therefore reduce the resonance fraction of the losses. Similarly, addition of dopants with high resistivity (eutectic) phases the grain boundaries and increases the specific resistivity of the material and decreases even further the eddy current fraction of the losses.

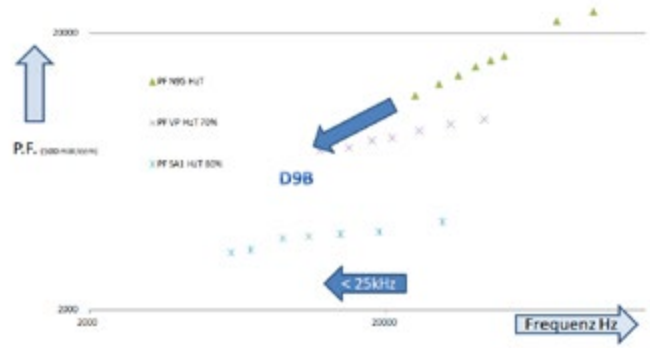

Figure 2: A comparison of performance factor with 500 mW/cm3 for SiC high power application. Iron based amorphous and nanocrystalline alloy (with consideration of packing factor) vs. standard power ferrite and ultra high Bs ferrite VP for Vitroperm, a trademark of iron based nanocrystalline alloy from VAC Hanau Germany, SA1 is trademark of iron based amorphous alloy from Hitachi/Metglas South Carolina, USA, D9B is trademark of ferrite from DTT Shandong China, and N95 is trademark of ferrite from EPCOS/TDK Munich, Germany

Given the importance of loss, which means inefficiency, the loss mechanism is still not fully understood. Consequently, it deserves a separate phrase to describe loss more clearly. Since the only physical origin is damping of domain wall by induced eddy current and relaxation process, the investigation of excitation mode becomes increasingly important to quantify the loss under desired conditions. This enables more insight into loss mechanism for material scientists, as well as for inductive component designers.

Messe München

Connecting Global Competence

electronica

Medical Electronics Conference (eMEC)

November 15, 2018, electronica.de/eMEC

International Conference on Electronics in Medicine and e-health

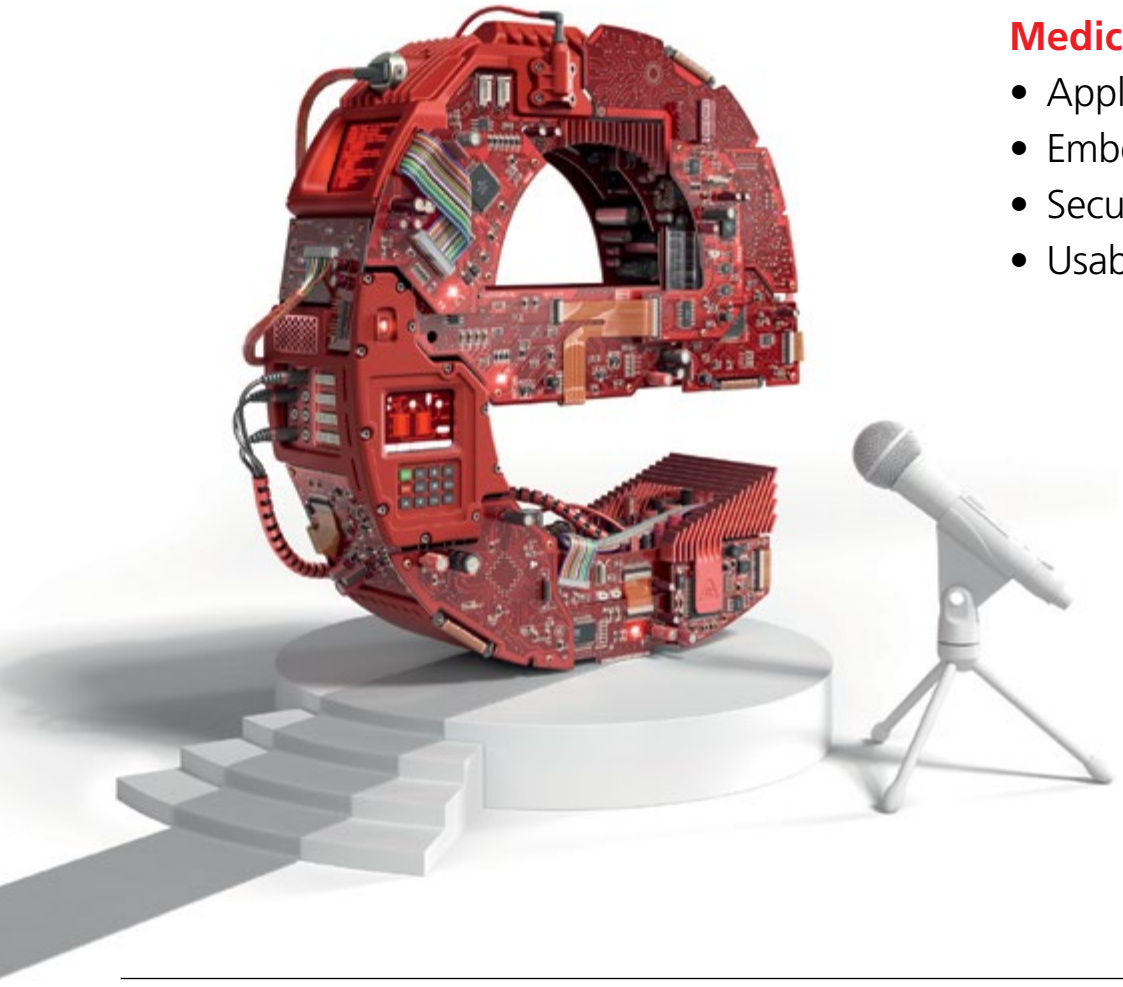

Medicine meets Electronics

- Applications
- Embedded technologies
- Security
- Usability

MEDIZIN elektronik
Fachmedium für Elektronik in der Medizintechnik
medizin-und-elektronik.de

electronica 2018
components I systems I applications I solutions
World's leading trade fair and conference for electronics
Messe München I November 13–16, 2018 I electronica.de

Large sized shaped Ferrite Core

For real application, the magnetic flux is important. The theoretical comparison of flux density is not necessarily helpful for particular application design. In case of thin tape wound core, the whole dimension of large sized alloyed tape wound cores are suffering from the packing factors (~ 20% for thinner tape like 23 µm) (please explain more clearly?). With increasing thinner tape, to lower eddy current loss, the polycrystalline ferrite shaped core has a porosity about some percent.

VP for Vitroperm, a trademark of iron based nanocrystalline alloy from VAC Hanau Germany, SA1 is trademark of iron based amorphous alloy from Hitachi/Metglas South Carolina, USA, D9B is trademark of ferrite from DTT Shandong China, and N95 is trademark of ferrite from EPCOS/TDK Munich, Germany

It is clearly illustrated from Figure 2 that for mid frequency application, like traction, wireless charging and solid state transformer for DC grids, large sized shaped ferrite cores with high Bs characteristics is very interesting alternative for wide range mass application.

Compared to alloyed tape wound material, the size of ferrite core shape is limited by powder metallurgical process. Nowadays the majority of MnZn-ferrite cores have small dimensions, not far away from the dimensions of the laboratory samples. The emerging market driven by SiC for photovoltaics, electrification for automotive and installations like wireless charging infrastructure require large sized MnZn-ferrite cores (https://product.tdk.com/info/en/catalog/datasheets/ferrite_mz_large_e_en.pdf) in order to be able to serve the market needs. Because of high power demands, these cores must have meaningful dimensions, which on average is more than 10 cm. This is associated with certain technological problems that need to be addressed in the development phase and before the transfer of the technology to production.

In every solid component made by compaction and sintering of a particulate powder, numerous gradients may arise. Powder flowability and compaction technology may not be ideal and generate local density gradients in the compacted specimen. During heating and cooling, temperature gradients may develop between the surface and the center of the specimen. Also during sintering, intermediate phases may form, oxidations and reductions may also occur with influence on the unit cell sizes. These phenomena may result in stress generation within the polycrystalline body of the product. In laboratory samples or in small size products, the stresses generated by these gradients usually do not exceed the fracture strength of the material and will not be noticed. However in large size products, as those intended to be produced within this project, the fracture strength can be easily exceeded and internal cracks will appear. The magnetic performance is extremely sensitive in the presence of microcracks. It is therefore proposed to investigate the mechanism of raw materials reaction during the prefiring step and the influence of process parameters (such as prefiring atmosphere, particle size of raw materials etc.) on the phase composition of the final prefired powder. Subsequently, the various weight, expansion shrinkage and phase changes during sintering will be monitored as a function of the phase composition of the prefired powder and of the partial pressure of oxygen in the sintering atmosphere. The recent engagement is the development of the smoothest firing schedule so that eventual temperature gradients will not give rise to gradual oxidations/reductions or other chemical reactions and stress generation.

Conclusion

The most recent ferrite development is illustrated in material and in core shape. The focus is on the highest Bs material for high power i.e. SiC driven application in high power for motion, automotive and traction applications associated with mid voltage dc grid propagation and high power density. The high Bs is desired according to Snoek law. While Bs is predominately influenced by chemistry, the loss mechanism is crystallized with investigation of morphological nature, its processing parameter, i.e. densification process. Another trend in large sized core shape, about 8-inch in height and 4-inch in width, is also described, overcoming challenges to deliver perfect artificial ferrite ceramic to fulfill the needs of newest developments in power electronics.

Today ferrite, after nearly 100 years of development, is manufactured with capacity of about 500,000 metric tons per year for diverse industries. This recent innovation is rooted in Snoek formulation. Both high power density and high power application requires high Bs characteristics. To understand this magnificent artificial ceramics, it is not only the chemical composition, the understanding of morphology process engineering is also essential.

Thévenin Equivalent Circuit and Maximum Power Transfer

The objective of this article is to verify Thévenin's theorem by obtaining the Thévenin equivalent voltage (V_{TH}) and Thévenin equivalent resistance (R_{TH}) for the given circuit, and then to verify the maximum power transfer theorem.

By Antoniu Miclaus and Doug Mercer, Analog Devices

Background

Thévenin's theorem is a process by which a complex circuit is reduced to an equivalent circuit consisting of a single voltage source (V_{TH}) in series with a single resistance (R_{TH}) and a load resistance (R_L). After creating the Thévenin equivalent circuit, the load voltage VL or the load current IL may be easily determined.

One of the principal uses of Thévenin's theorem is to replace a large portion of a circuit, often a more complicated and uninteresting part, with a simple equivalent. The new simpler circuit enables rapid calculations of the voltage, current, and power than the more complicated original circuit is able to deliver to a load. The theorem also helps to choose the optimal value of the load (resistance) for maximum power transfer.

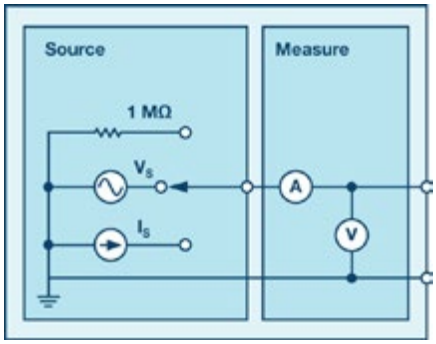

Figure 1: A schematic of the ADALM1000.

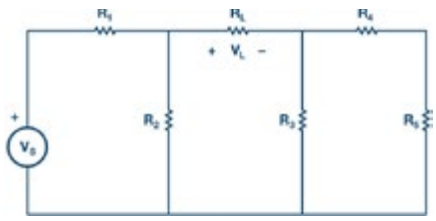

Figure 2: Thévenin equivalent circuit of Figure 1.

The maximum power transfer theorem states that an independent voltage source in series with a resistance, RS, or an independent current source in parallel with a resistance RS delivers a maximum power to the load resistance, R_L, when R_L = RS.

In terms of a Thévenin equivalent circuit, maximum power is delivered to the load resistance R_L when R_L is equal to the Thévenin equivalent resistance, R_{TH}, of the circuit.

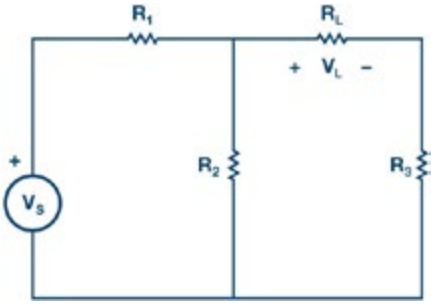

Figure 3: Maximum power transfer.

Materials

- ADALM1000 hardware module
- Various resistors (100 Ω, 330 Ω, 470 Ω, 1 kΩ, and 1.5 kΩ)

Procedure

Verifying Thévenin's theorem:

Construct the circuit of Figure 2 using the following component values:
R_1 = 330 Ω
R_2 = 470 Ω
R_3 = 470 Ω
R_4 = 330 Ω
R_5 = 1 kΩ
R_L = 1.5 kΩ
V_S = 5 V

b) Accurately measure the voltage VL across the load resistance using the ALM1000 voltmeter tool. Use the voltmeter tool by connecting channel CA to the positive node of V_L and connect channel CB to the negative node. V_L will be the difference between CA volts and CB volts. This value will later be compared to the one you will find using the Thévenin equivalent.

c) Find VTH: Remove the load resistance, R_L, and measure the open circuit voltage, V_{OC}, across the terminals. Use the voltmeter tool by connecting channel CA to the positive node of V_{OC} and connect channel CB to the negative node. VOC will be the difference between CA volts and CB volts. This is equal to VTH. See Figure 4.

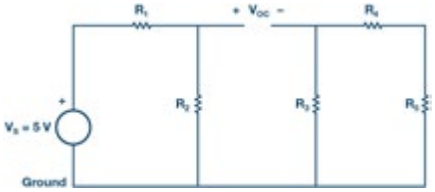

Figure 4: Measuring the Thévenin voltage.

d) Find R_{TH}: Remove the source voltage V_S and construct the circuit as shown in Figure 5. Use the ALM1000 ohmmeter tool to measure the resistance looking into the opening where R_L was. This gives R_{TH}. Make sure there is no power applied to the circuit before measuring with the ohmmeter and that the ground connection has been moved as shown.

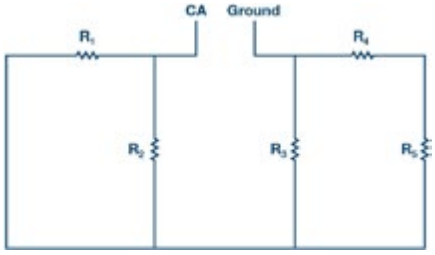

Figure 5: Measuring the Thévenin resistance, R_{TH}.

e) Obtaining V_{TH} and R_{TH}, construct the circuit of Figure 2. Create the value of R_{TH} using a series and or parallel combination of resistors from your parts kit. Using the meter-source tool, connect channel CA for the V_{TH} source and set the value to what you measured for V_{TH} in Step c.

f) With R_L set to the 1.5 kΩ used in Step b, measure the V_L for the equivalent circuit and

compare it to the V_L obtained in Step b. This verifies the Thévenin theorem.

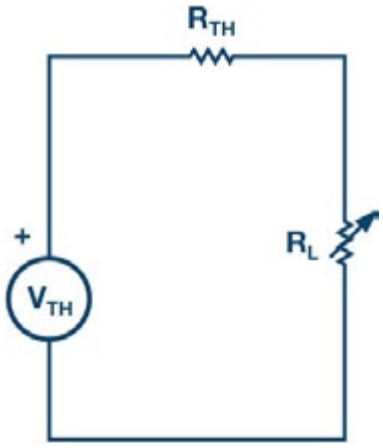

Figure 6: Thévenin equivalent construction.

g) Optional: repeat Step 1b to Step 1f for R_L = 2.2 kΩ.

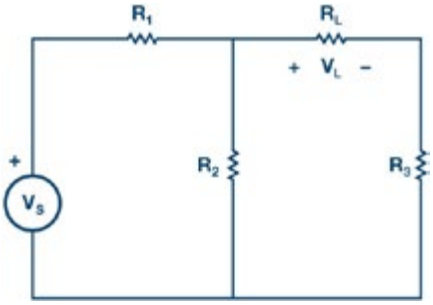

Figure 7: Circuit for maximum power theorem.

Verifying the maximum power transfer theorem:

Construct the circuit as in Figure 7 using the following values:

V_S = 5 V

R_1 = R_2 = 470 Ω

R_3 = 1 kΩ

R_L = combinations of 1 kΩ and 100 Ω resistors (Figure 8)

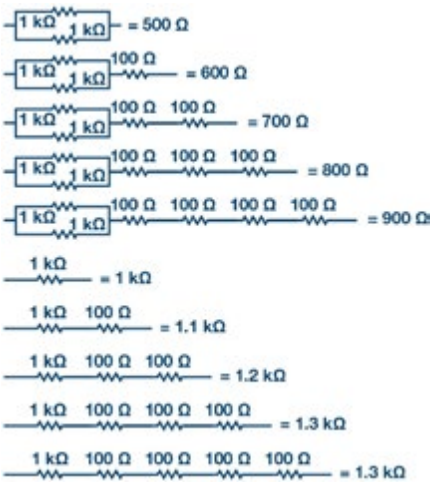

Figure 8: RL configurations.

b) Use the voltmeter tool by connecting channel CA to the positive node of V_L and connect channel CB to the negative node across R_L. V_L will be the difference between CA volts and CB volts.

c) To find the value of R_L for which maximum power is transferred, vary the load resistances by constructing series/parallel combinations of 1 kΩ and 100 Ω for R_L between 500 Ω to 1400 Ω in 100 Ω steps, as shown in Figure 8. For each value of R_L, write down V_L.

d) Calculate the power for each load resistor value using $P_L = V_L^2/R_L$. Then, interpolate between your measurements to calculate the load resistor value corresponding to the maximum power (P_L-max). This value should be equal to R_{TH} of circuit in Figure 7 with respect to load terminals.

Notes

As in all the ALM labs, we use the following terminology when referring to the connections to the ALM1000 connector and configuring the hardware. The green shaded rectangles indicate connections to the ADALM1000 analog I/O connector. The analog I/O channel pins are referred to as CA and CB. When configured to force voltage/measure current, –V is added (as in CA-V) or when configured to force current/measure voltage, –I is added (as in CA-I). When a channel is configured in the high impedance mode to only measure voltage, –H is added (as in CA-H).

Scope traces are similarly referred to by channel and voltage/current, such as CA-V and CB-V, for the voltage waveforms, and CA-I and CB-I for the current waveforms.

We are using the ALICE rev 1.1 software for those examples here.

File: alice-desktop-1.1-setup.zip. Please download here.

The ALICE desktop software provides the following functions:

- A 2-channel oscilloscope for time domain display and analysis of voltage and current waveforms.
- The 2-channel arbitrary waveform generator (AWG) controls.
- The X and Y display for plotting captured voltage and current vs. voltage and current data, as well as voltage waveform histograms.
- The 2-channel spectrum analyzer for frequency domain display and analysis of voltage waveforms.
- The Bode plotter and network analyzer with built-in sweep generator.
- An impedance analyzer for analyzing complex RLC networks and as an RLC meter and vector voltmeter.
- A dc ohmmeter measures unknown resistance with respect to known external resistor or known internal 50 Ω.
- Board self-calibration using the AD584 precision 2.5 V reference from the ADALP2000 analog parts kit.
- ALICE M1K voltmeter.
- ALICE M1K meter source.
- ALICE M1K desktop tool.

For more information, please look here.

Note: You need to have the ADALM1000 connected to your PC to use the software.

www.analog.com

Antoniu Miclaus [antoniu.miclaus@analog.com] is a system applications engineer at Analog Devices, where he works on ADI academic programs, as well as embedded software for Circuits from the Lab® and QA process management. He started working at Analog Devices in February 2017 in Cluj-Napoca, Romania. He is currently an M.Sc. student in the software engineering master's program at Babes-Bolyai University and he has a B.Eng. in electronics and telecommunications from Technical University of Cluj-Napoca.

Doug Mercer [doug.mercer@analog.com] received his B.S.E.E. degree from Rensselaer Polytechnic Institute (RPI) in 1977. Since joining Analog Devices in 1977, he has contributed directly or indirectly to more than 30 data converter products and he holds 13 patents. He was appointed to the position of ADI Fellow in 1995. In 2009, he transitioned from full-time work and has continued consulting at ADI as a Fellow Emeritus contributing to the Active Learning Program. In 2016 he was named Engineer in Residence within the ECSE department at RPI.

Reduce Size and Increase Efficiency with GaN-based LLC Solutions

GaN High Electron Mobility Transistors (GaN HEMT) have lower driving loss and shorter deadtime circuit benefits due to significantly reduced gate charge (Q_g) and output capacitance (C_{oss}) compared to Silicon MOSFETS. Therefore, GaN HEMTs show significant advantages over Silicon MOSFETs in high-frequency soft-switching resonant topologies such as an LLC resonant converter. With increased switching frequency (fsw), the transformer core size can be reduced. Furthermore, a 3-D PCB structure is employed to increase the power density. A 190-Watt, 400V-19V GaN Systems E-HEMT based LLC DC-DC resonant converter is carefully designed, and the transformer is optimized for high-end adapter applications operating above 600kHz. The converter shows a complete design with a power density over 63W/inch^3, including the 400V bus capacitor, with a peak efficiency of 96%.

By Yajie Qiu, Senior Power Electronics Applications Engineer, GaN Systems Inc.

Introduction

High power density is one key motivation for GaN HEMTs to be widely used in low power consumer applications such as laptop adapters, flat screen TVs, and all-in-one desktop computers. The LLC resonant converter topology is effective in improving efficiency, especially for high-input voltage applications where the switching loss is more dominant than the conduction loss. The series and parallel inductors are often integrated into the transformer using the leakage and the magnetizing inductance, thus reducing the component count. The purpose of this article is to demonstrate a high-power density and high-efficiency DC-DC LLC solution using GaN HEMTs.

	Si CoolMOS CFD2	Si CoolMOS CFD7	GaN HEMT	
	IPx65R110CFD	IPP60R105CFD7	GS66504B	Unit
V_{DS}	650	600	650	V
$R_{DS(ON)}$	110	105	110	mΩ
Q_G	118	42	3	nC
$C_{O(ER)}$	118	60	44	pF
$C_{O(TR)}$	582	616	72	pF

Table 1: Q_G and C_{OSS} comparison

The Capability of GaN HEMTs operating at high-frequency soft-switching LLC application

Compared to Silicon MOSFETs, GaN HEMTs feature significantly reduced gate charge (Q_g) and output capacitance (C_{oss}), resulting in lower driving loss and shorter turning-on/off periods. Therefore, GaN HEMTs show significant advantages over Silicon MOSFETs in high-frequency soft-switching resonant topology such as the LLC resonant converter.

In order to take a closer look at the potential advantages of GaN in high-frequency soft-switching resonant converters, we have to compare the key parameters of GaN HEMTs to those of the conventional Si MOSFETs. As an example, GaN Systems' GS55504B is selected

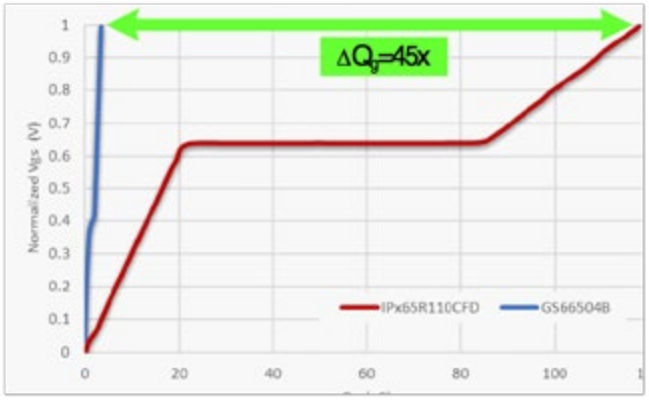

Figure 1: Q_g comparison

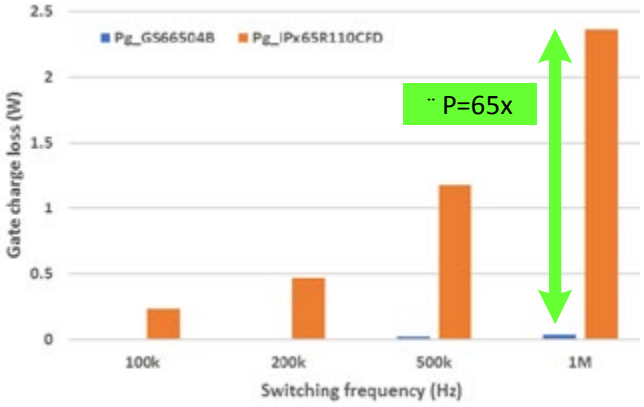

Figure 2: Gate-driver loss comparison

to be compared to the active Si MOSFETs (IPx65R110CFD and IPP60R105CFD7) because they have comparable $R_{DS(ON)}$ values. The following table shows the comparison of the key parameters: V_{DS}, $R_{DS(ON)}$, Q_G, $C_{O\ (ER)}$ and $C_{O\ (TR)}$.

A. The Qg advantage of GaN

As shown in Figure 1, the GS55504B features significantly reduced gate charge (Q_g) compared to both the IPx65R110CFD and IPP60R105CFD7, resulting in a lower driving loss. Figure 2 shows the comparison of gate-driver loss at different switching frequencies. The loss difference between two devices increases dramatically with the increase of the switching frequency, demonstrating the advantage of GaN HEMTs working at the high switching frequency.

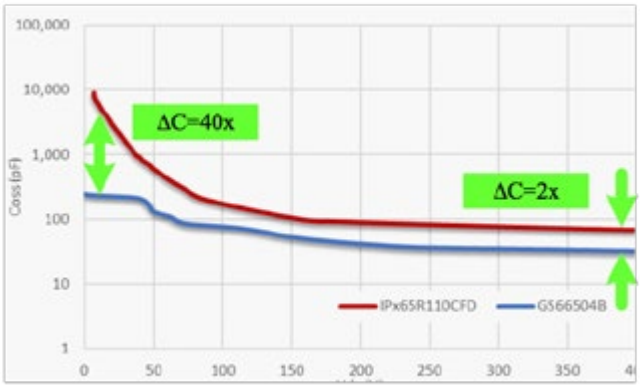

Figure 3: C_{oss} comparison

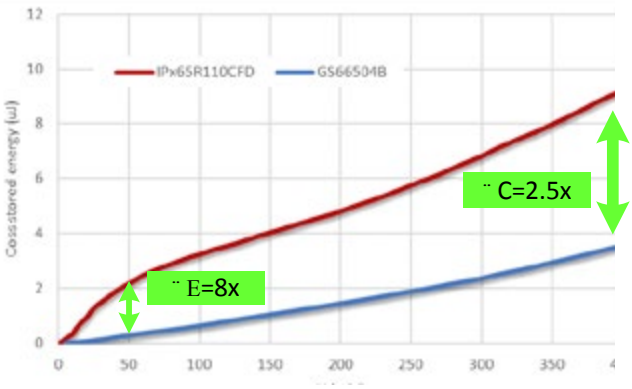

Figure 4: C_{oss} energy comparison

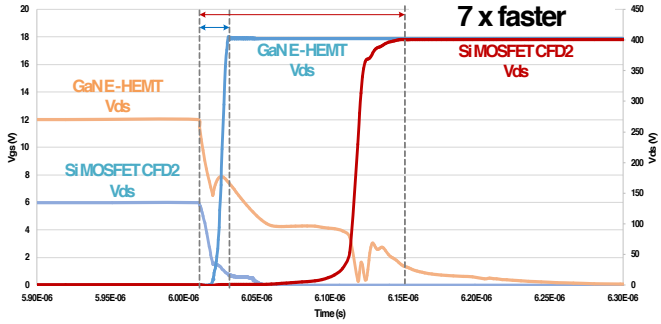

Figure 5: C_{oss} charging time comparison at the turn-off

B. The C_{oss} advantage of GaN

C_{oss} of a Si MOSFET is highly nonlinear at low voltage. The C_{oss} values of a GaN HEMT and a Si MOSFET are compared in Figure 3 and Figure 4. The GaN HEMT features significantly reduced output capacitance (C_{oss}) and C_{oss} energy, resulting in shorter turning-on/off period, as shown in Figure 5. This characteristic allows the shorter deadtime and higher switching frequency operation to be achieved.

C. The GaN advantage in LLC resonant converter

The schematic of GaN-based half bridge LLC converter is plotted in Figure 6.

For the LLC resonant converter working in the below-resonance region and at resonance point, primary side half-bridge switches, S1 and S2, always safely turn on without incurring switching loss (Zero-voltage Switching). The total loss resulting from the power switches is composed of three parts: 1) driving loss (decided by Q_g), 2) conduction loss (decided by $R_{DS(ON)}$) and 3) switching off loss (decided by C_{oss}). It has been analyzed that the GS55504B has the all three mentioned advantages over the Si MOSFETs when applied to the high-frequency soft-switching frequency LLC converters.

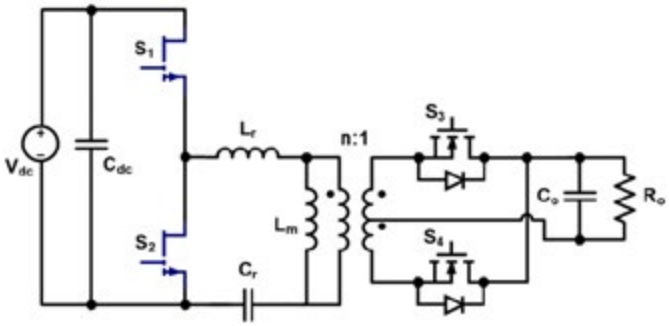

Figure 6: GaN-based half-bridge LLC converter

The design specification of the LLC converter is shown in table 2, which is very popular in two-stage adapter applications. The LLC tank is designed, and the parameters are listed in Table 3.

V_{in}	350-400	V
V_o	19	V
I_o	10	A
P_o	190	W

Table 2: Design Specifications

L_m	80	µH
L_r	5	µH
C_r	6	nF
F_r	726	kHz

Table 2: LLC Resonant Tank Parameters

3-D PCB structure solution for high-power-density LLC resonant converter

A. 3-D Structure Concept

In order to push the power density of the GaN HEMTs based LLC prototype, the “3-D PCB” concept is also utilized, where all the active switches, power diodes, and MCU are assembled on the PCB daughter cards.

B. Implementation

The whole LLC system design is composed of the following four parts:

PCB board #1:

Primary side half-bridge daughter card with two GaN HEMTs (GS66504B) and bootstrap driving circuitry (32mm (L) × 19mm (W)). Since GS66504B are a bottom-side-cooling device, one 17mm × 17mm square shape heatsink is connected to the bottom side of PCB to cool the two GaN HEMTs.

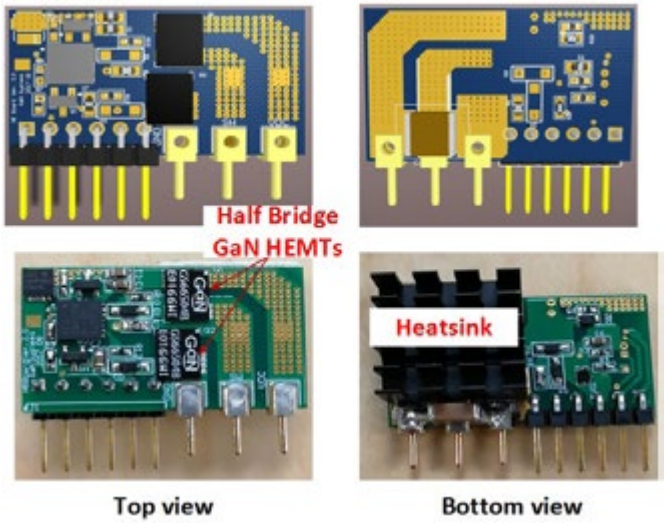

Figure 7: Primary side half bridge daughter card PCB layout (top) and pictures (bottom)

PCB board #2:

Primary side digital controller with peripheral circuits (26mm (L) × 20mm (W)). The topology employs a digital control solution integrating an output voltage regulation, OVP, and OCP function into one low-cost MCU (DSPIC33FJ06GS202A from Microchip).

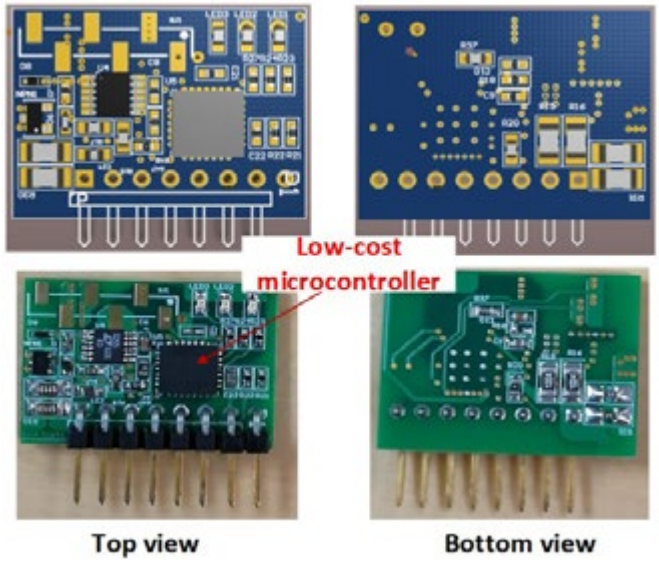

Figure 8: Primary side digital controller daughter card PCB layout (top) and pictures (bottom)

PCB board #3:

Secondary side synchronized rectifier daughter card (20mm (L) × 17mm (W)). All the components are soldered on only the top side. One 20mm × 20mm square shape heatsink is connected to the bottom side of PCB to cool the four Synchronized Rectifier MOSFETs (2 × 2 paralleled MOSFETs).

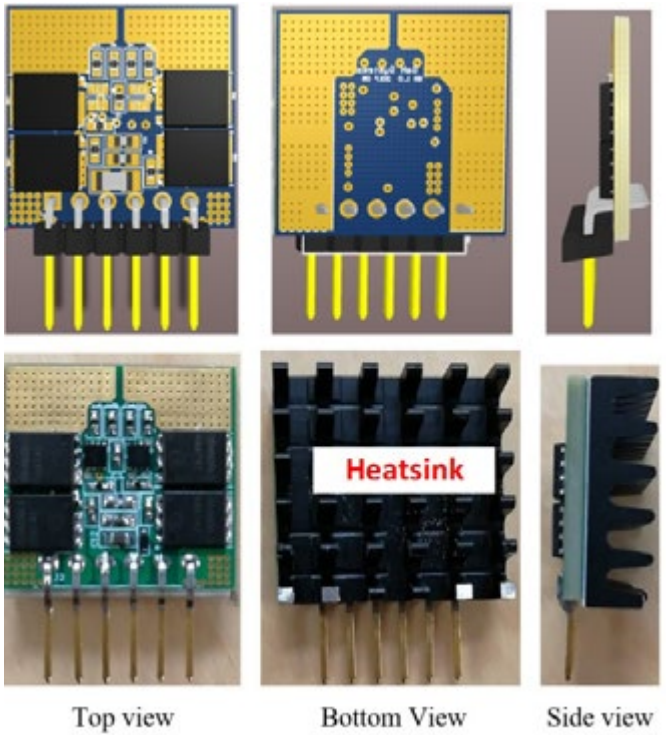

Figure 9: Secondary side synchronized rectifier daughter card PCB layout (left) and pictures (right)

PCB board #4:

Mother board with input capacitor, output filter, and integrated transformer (69mm (L) × 34mm (W)) is shown in Figure 10. Three slots are provided on the mother board for PCB board #1, PCB board #2, and PCB board #3 to be inserted.

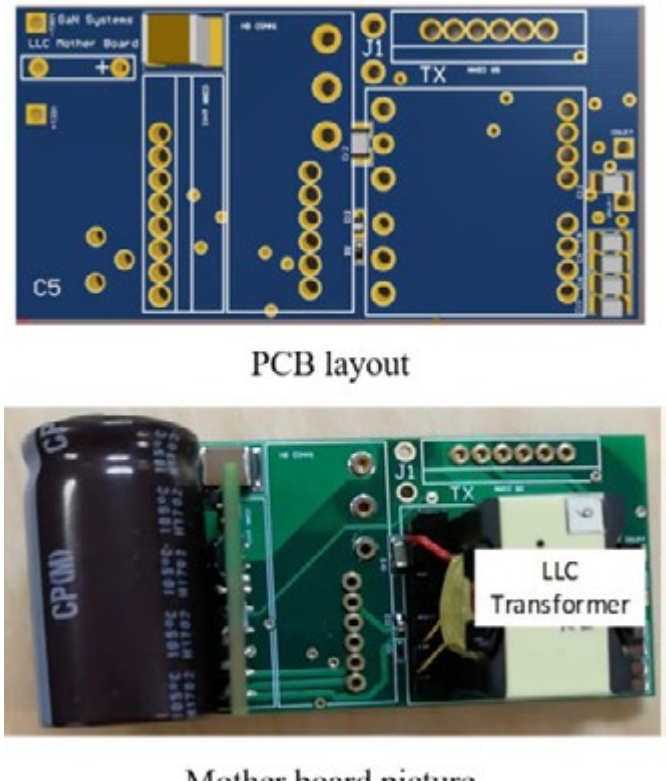

Figure 10: Designed GaN-based LLC Resonant Converter Prototype

C. LLC prototype and its power density

The finished prototype and its dimension are shown in Figure 11. All the heatsinks are connected to the bottom side of the daughter cards, which is effective for the bottom-side cooling devices, such as GaN HEMT, GS66504B, on the PCB board #1 and secondary side synchronized rectifiers PCB board #3.

$$V = 69mm\ (L) \times 21mm\ (H) \times 34mm\ (W) = 3\ inch^3 \quad (1)$$

$$Power\ density = \frac{190W}{3\ inch^3} = 63.3W / inch^3 \quad (2)$$

The key waveforms of designed high-frequency LLC converter working at half load and full load are shown in Figure 11 and Figure 12.

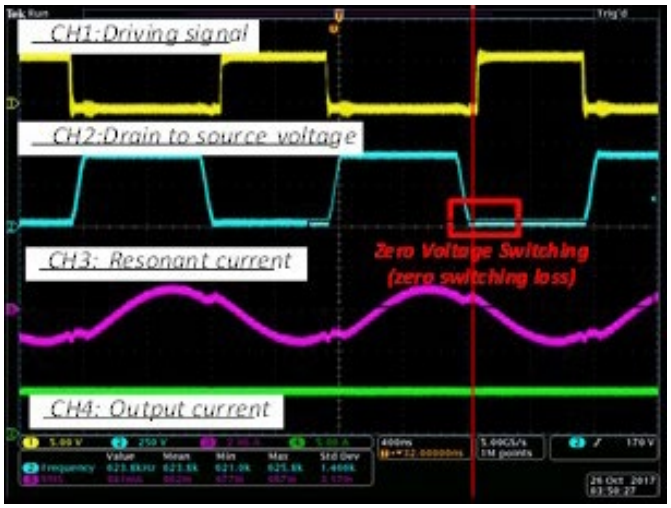

Figure 11: The key experimental waveforms of the proposed high-power-density GaN HEMT LLC converter when V_{in}=400V, V_{out}=19V, I_o=5A Po=95W, F_s=623kHz (50% load)

The efficiency at different loads is tested and shown in Figure 13, the power loss from the auxiliary winding is not included. The peak efficiency has achieved 96.1% at 95W (50% load) while the efficiency at 190W (100% load) is 95.6%.

Conclusion

The GaN HEMTs features a superior figure of merit (low Q_g, $R_{DS(ON)}$ and C_{OSS}) which enables the resonant converter such as the analyzed LLC allowing operating at a high switching frequency over 600kHz. The smaller core using high-frequency magnetic materials can then be employed to increase the power density. Furthermore, with the help of 3-D PCB structure as well as the combined digital control solution, the prototype shows a complete 400V DC-19VDC design with a power density of 63W/inch3 while its peak efficiency has achieved 96.1%.

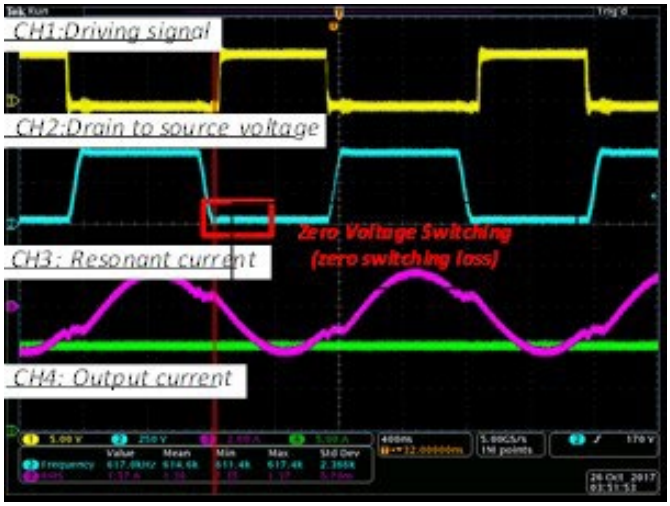

Figure 12: The efficiency performance at different load when V_{in}=400V, V_o=19V, I_o=1A (19W) to 10A (190W)

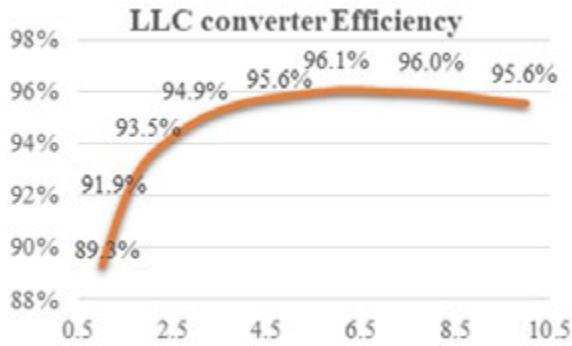

The Linear Charger in Wearable Applications

Wearable devices have become increasingly integrated into our lives. In addition to being used in fitness devices, they have also worked their way into other fields, including medical care, entertainment, security, and finance. In all applications, battery life and component size are two key concerns.

By Hank Cao, Applications Engineer, Monolithic Power Systems

In regards to component size, applications require the main board within the wearable device to have a small size and low BOM, which means a small package and high integration are required for each IC on the main board. For example, smart bands, a very popular wearable device, require a small main body size (usually 20mm×20mm). The main board within the body is even smaller. The battery pack takes up a large portion of the board space, leaving components to be mounted on the other sides of the board and severely limiting the size and height of components.

For this reason, the chip scale package (CSP) is an ideal package choice in wearable applications, since this package is at a chip scale level with a low height (see Figure 1). With regards to the chip size, an optimized circuit design and process take an important role.

Figure 1: Chip in a CSP Package

High integration of power MOSFETs and control circuitry is another way to reduce board size in wearable applications. Higher integration reduces the number of external components of the IC on the main board, reducing the total size (see Figure 2).

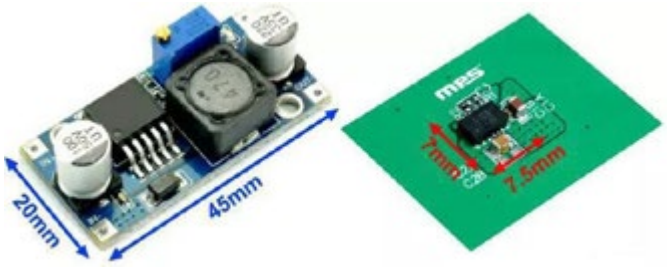

Figure 2: Traditional Solution vs. Highly Integrated Solution

Programmability is also an important feature in wearable applications. For example, the charging parameters can be programmed in real application scenarios, which provide a better customer experience. Battery charger ICs with an I2C interface are ideal for customers needing to meet various requirements and can also allow the host to flexibly monitor any status and fault during charging.

The battery is a critical component of wearable equipment. The charger IC should charge the battery safely and ideally have a separate bidirectional control between the system and the battery. This way, the charger IC can power the system even with a dead battery by regulating the system to a minimum voltage level and operating the battery switch as a linear regulator. When the system load exceeds the input source capability, the battery can supplement power to the system to enable higher power draw for brief periods of time. Normally, the charger IC can implement power path management with input voltage and current loops to achieve the above functions (see Figure 3).

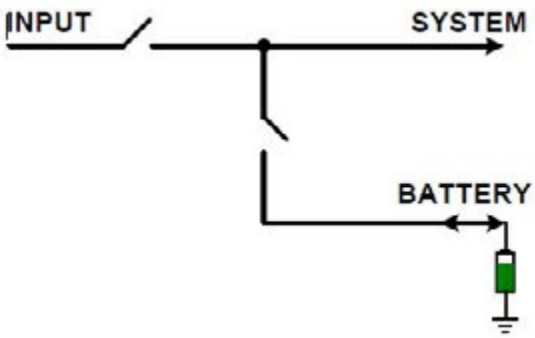

Figure 3: Separate System and Battery Control

With the help of the power path, the charger IC can also provide battery discharge protection, such as over-current protection (OCP) and battery under-voltage lockout (UVLO) when only the battery is present. In applications where the system runs in and out of control, it is important to reset the system to prevent any unexpected damage. With the help of the power path, the charger IC can reset the system safely, even during shipping mode.

The battery in wearable applications is small (in the range of several tens of mAh to 100+ mAh), while customer usually expect several days of runtime. The charger IC should also have a low quiescent battery discharge current to extend the battery runtime. Using a 70mAh battery as an example, three days of runtime is typically required, so the average consumption current is less than 1mA. Achieving a quiescent current less than 10µA is challenging for a charger IC while it is enabled with only a battery connected. This is because a

low quiescent current impacts system response and accuracy. For example, battery under-voltage lockout (UVLO) is a key parameter in preventing a battery over-discharge, which requires high-accuracy circuits to be active to monitor the battery voltage and control the battery MOSFET.

In addition to an accurate charging control, such as accurate charging current and charging voltage, the charger IC should also have battery over-voltage protection (OVP), temperature monitoring, and other robust safety features.

An ideal solution for wearable devices would have a small size, low BOM, high integration, flexible charging configurations, and a number of protection features. MPS has that ideal solution in the MP266x family of linear chargers. MP266x devices come in ultra-compact WCSP packages while maintaining fully integrated power switches with no external block MOSFETs required and less than 7μA quiescent current in standby (battery only) mode.

Conclusion

Small size and low quiescent current are key concerns for battery chargers in wearable applications. An ideal solution can achieve these two requirements while being highly integrated and offer programmable charging parameters for use with a wide variety of batteries. The MP266x linear charger family from MPS is an excellent solution for charger ICs in wearable applications. These devices take advantage of MPS's industry-leading power MOSFET and programmable analog technology to optimize wearable designs.

www.monolithicpower.com

Quasi-Class E Achieves Power Control and ZIS/ZVS

This is the first in a 3 part series describing a novel approach to high frequency (27 MHz) power conversion and control. This part describes the basic Quasi Class E circuit. Part 2 will describe voltage controlled reactance means to vary power. Part 3 will describe rectification to DC using SiC diodes, and EMI issues.

By David Pacholok, Paul Reich and Jim Spangler

Introduction

To meet the increasing need for ever smaller power supplies, wireless chargers, and other devices, resonant power converters are being driven to ever higher frequencies.

Off-line operation of MHz power converters presents unique challenges with regulatory agency EMC standards. Choosing a frequency of operation at random may lead to severe limits for conducted and radiated EMI, as mandated by FCC Part 15 rules, for example. Operating the converter at one of the Part 18 industrial/scientific/medical frequencies may simplify EMC compliance.

However, fixed frequency operation reduces design freedom in terms of topology. For example, the popular LLC converter is controlled by altering switching frequency to change output power/voltage. Fixed frequency operation is not an option for the LLC and some other topologies.

About 40 years ago Nathan Sokal taught the world his class E RF power amplifier technology1,2. This topology, while very efficient and cost effective, has one major issue for HF switch mode power supply application, or any application where power/voltage output needs to be varied. This requirement covers perhaps 90% of possible applications. In order to vary the output, whether rectified-to-D.C. or simply RF, the D.C. input voltage to a class E amplifier must be varied. Hence a pre-converter stage of some form is needed, such as a buck converter. For some applications the size, cost, and efficiency penalties of the pre-converter are tolerable, but for cost sensitive consumer applications they are not desirable.

We have developed a GaN-based quasi-class E topology that allows power output control over a 10:1 range while maintaining efficient commutation. This may be defined as Zero Current Switching (ZIS) at device turn-on and Zero Voltage Switching (ZVS) at turn-off. This opens the door for high efficiency DC-DC converter applications. As an RF generator, besides variable output, the advantage of operation over a wide range of load impedances is provided, while maintaining efficient commutation.

Our concept is to vary the reactance of a control element to vary power. A variable reactance tunes a series or parallel reactive network up and down its resonance curve to control power output.

The variable reactance element may take the form of a voltage variable capacitance, a saturable reactor, or a digitally switched array of capacitors or inductors as we will show in the Part 2 of this series.

In this article, we simply vary the value of C2 as shown in Table 1 to achieve power control.

The Basic Resonant Flyback Circuit

Referring to the resonant flyback converter topology of Figure 1, L1 and C1 (including Cds) provide a resonant frequency higher than the drive frequency. The half-sine drain voltage waveform returns naturally to zero before the next “on” time. With very light loading, the inductor current tends toward a sawtooth (Figure 2).

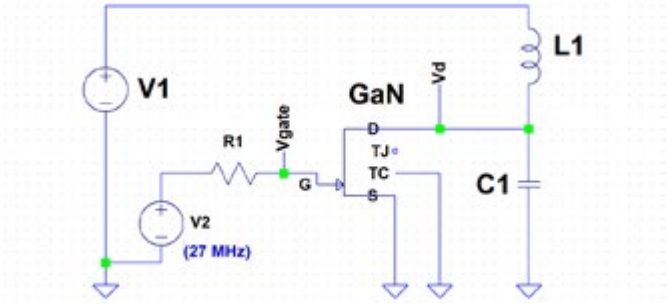

Figure 1: Basic Resonant Flyback Circuit

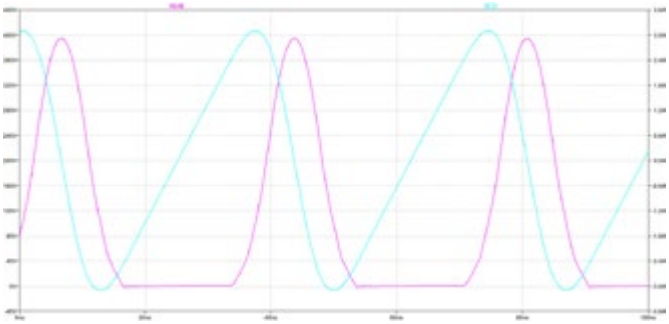

Figure 2: Simulated Drain Voltage (green) and Inductor Current (red) (Figur 1 Circuit)

C1 and L1 were chosen to have a characteristic impedance (Z_O) of about 100 ohms:

$$Z_O = (L/C)^{1/2} \qquad (1)$$

This value reduces losses in the GaN FET, L1, and C1.

Evolution of the Quasi-Class E

We started with the classic class-E equations1. Our operating point was set to 100 watts output with 100 VDC input, at the 27.12 MHz

ISM Frequency. While the topology of both the class E and our quasi-class E (Figure 3) are identical, the C1/C2/L1/L2 values in Table 1 are very different.

Component	*Sokal Class E*[(1)]	*This work*
R_LOAD	23.9 ohms	50 ohms
L1	3 uH	350 nH
C1	113 pF	56 pF
L2	570 nH	1.3 uH
C2	72 pF	29.5 pF

Table 1: Comparison of "Classic" and Proposed Components

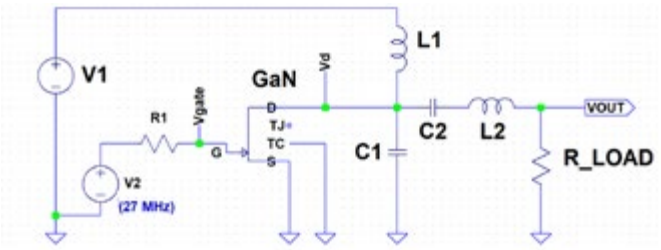

Figure 3: Generic Class E Topology

The 24 ohm load requirement derived from the Sokal equations1,2 did not match our available supply voltage, desired load impedance and required power output. 50 Ohm loads and power meters are common; 24 ohm units not so much.

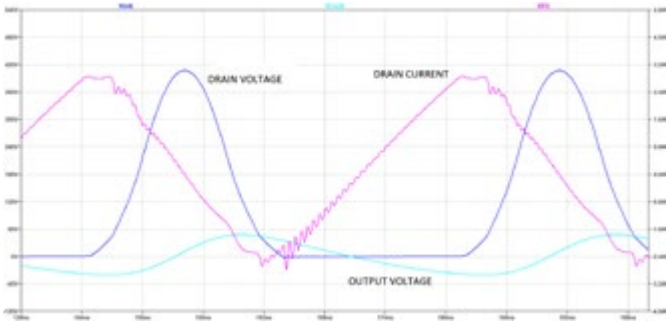

Figure 4: Minimum Power Simulation

Operation in the inductive portion of the L2-C2 series resonance curve is mandatory. If the tank circuit resonant frequency exceeds the drive frequency, the network becomes capacitive and ZVS and/or ZIS will be lost. Poor efficiency, poor commutation, and possible device destruction will result.

The inductive load causes the drain of the switching device to be driven a few volts below ground at the beginning of the "on" time. The gate is relatively positive, turning the device slightly on. This causes a small V*I loss. This loss may be reduced by turning the switch on at the moment of Vds=0. Practically speaking, square wave drive at 27 MHz is difficult. Sine wave drive from a resonant gate drive network

The Premier Global Event in Power Electronics™
Visit the APEC 2019 website for the latest information: www.apec-conf.org

IAS IEEE INDUSTRY APPLICATIONS SOCIETY Linking Research to Practice

IEEE Advancing Technology for Humanity

pels IEEE POWER ELECTRONICS SOCIETY Powering a Sustainable Future

PSMA

MARCH 17-21 | ANAHEIM, CA.

ANAHEIM CONVENTION CENTER

can provide gate drive energy recovery. In the sine wave drive case, the use of positive gate bias at or slightly above device threshold will turn on the FET earlier, reducing its I*R drop during reverse current. GaN FETs have no body diode, so charge storage effects do not occur.

Figure 5: Maximum Power Simulation

To control the output power, a series network consisting of a fixed 1.3 uH inductor (L2) and a variable capacitor (C2), shunted with a fixed capacitor (to limit the capacitance range) was added. The output power into a 50 ohm load was measured after considerable simulation and "tweaking" of C1 and L1. Maximum output power with good commutation was noted for C2 values at or slightly above 30 pf (L2 and C2 were near resonance). Increasing C2 dropped FR and moved the network away from resonance. This controlled power output over a 10:1 range as shown in the table in Table 2.

C2 (pF)	Power Output (Watts)
30 pF	104 W
34 pF	58 W
40 pF	32 W
57 pF	22 W
93 pF	10.5 W

Table 2: Power Output vs. C2

The loaded Q of this network was 4.5 with a 50 ohm load.

$$Q=X_L/R \quad (2)$$

$$F_R = 1/(2\pi (LC)^{1/2}) \quad (3)$$

(for L2= 1.3 uH, C2 = 29.5 pF, F_R is 25.7 MHz)

The need for an inductive load line and the resulting reverse FET current are major departures from conventional class E design. We noted less than 1% efficiency reduction with our topology at maximum power, compared to a similar class E circuit with constant supply voltage and output power.

In the next article of this three part series, we will investigate various means of reactive power control.

References

1. N.O. Sokal, WA1HQC, "Class E RF Power Amplifiers", QEX Magazine, Jan/Feb. 2001, ppg 9 – 20
2. N. O. Sokal et al, "High Efficiency Tuned Switching Power Amplifier", US Patent 3919656, Nov 11, 1975

About the Authors

David Pacholok has operated Creative Electronic Consultants LLC since 1981. He is active in switchmode power conversion, electronic lighting ballasts, RF power, pulse Power, and induction heating. He can be reached @ 847-809-2786 (cell), 847-428-5676 (office), and at cecinduction@gmail.com.

Paul Reich is a freelance consultant. His specialties are radio frequency design and simulation. In a previous life, he held various positions at Motorola, Inc. and the Chamberlain Group. Paul earned his BSEE in 1976.

Jim Spangler is President of Spangler Prototype Inc. Jim was a Field Applications Engineer at Motorola Semiconductor, On Semiconductor, Cirrus Logic, and Active Semiconductor. Jim was involved with several IEEE societies, and planning for the PSMA Applied Power Electronics Conference (APEC). Jim has published extensively about power electronics applications. Jim can be reached at 847-961-8588 (cell).

Optimizing Custom Magnetics Design

To meet application-specific feature specifications, many high frequency magnetics designs must now be customized. What has proven successful for customization is where experienced engineering teams can supply both the software (magnetic design and FEA) and hardware (prototyping tools) portions of the design from one power electronics laboratory location. And, being able to supply this combination of engineering talent provides time-to-market and configuration benefits in supporting a customer's initial converter prototype design.

By Cathal Sheehan, Bourns, Inc.

The article highlights the power advantages gained in using Finite Element Analysis to identify the optimum winding order before proceeding with physical prototypes. The article also points out how actual prototype measurements to simulations can vary, so having the ability to create prototypes in the same location as the simulation software is a critical requirement.

Initial Specification Case Study

The first steps in creating a magnetic component involve a preliminary specification of the power supply itself including additional information such as the topology (example: Flyback) as well the manufacturer and identifying the power management chip series. A basic electrical block diagram of the system will indicate the number of windings involved.

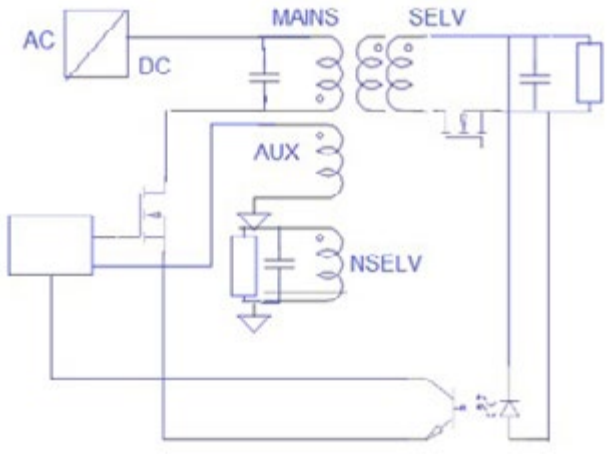

Figure 1: Block diagram of a Flyback Power Supply

Figure 1 shows an isolated AC/DC 70W Flyback power supply with reinforced isolation. The control loop consists of secondary voltage feedback as well as primary current sensing. The coordination of the MOSFET and synchronous rectifier is done using the auxiliary (AUX) winding and the controller IC for measuring the demagnetization time. In this case, the leakage inductance measurements will determine the time that the leakage inductance spike lasts and will determine the cycle time of each oscillation when the secondary is completely demagnetized. Designing the transformer to ensure optimum leakage inductance with multiple windings will be important for such a design.

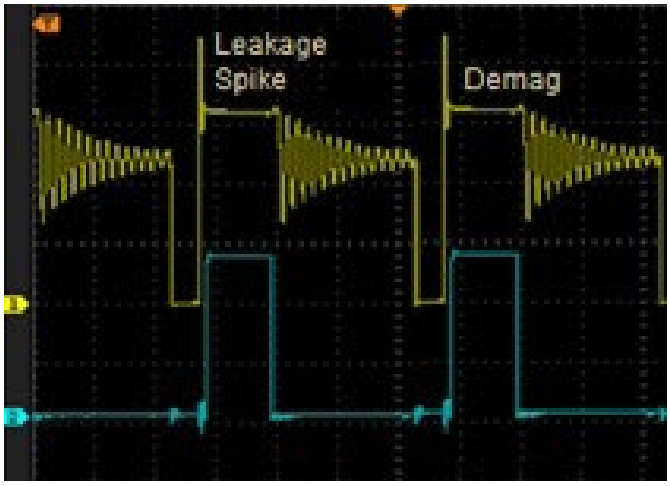

Figure 2: Auxiliary winding voltage and synchronous rectifier control voltage (blue) in Flyback power supply

If there is an application note from the power controller supplier, it can help determine the electrical parameters of the transformer including the primary inductance and peak saturation current (in the case of a Flyback). For this case study example, the primary inductance will be calculated using the energy equation for a Flyback transformer:

$$L = \frac{2(Vout + VF) * Iout}{fswIp^2}$$

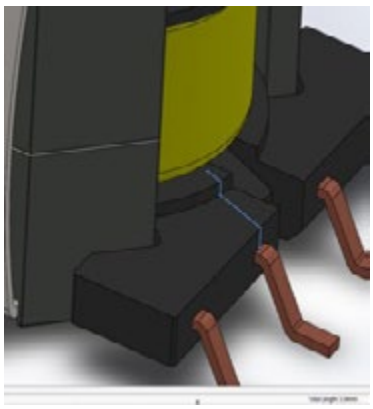

Where:
fsw = Switching Frequency
Ip = Peak Current in the Primary
VF = Synchronous Rectifier Voltage Drop

Figure 3: Example Calculation for Creepage and Clearance

The dimensions of the transformer will be determined first and foremost by the target power to be dissipated in the transformer as well as the specified operating temperatures. Also important are the customer's board and enclosure that are strictly dictated by the safety requirements as stipulated by the customer. Bourns in Europe uses Solid Works for mechanical design. Figure 3 shows one example of a Solid Works transformer design. The blue line highlighted is measuring the shortest distance between a secondary SELV pin and winding. Solid Works supports its partners in helping meet safety standards such as IEC62368-1 Edition 2.0 2014-02.

Ideal Prototype Support

If a customer requires engineering samples urgently, then having all materials in stock is a clear advantage as it helps avoid delays. Typically Bourns stocks more than 179 different shapes and sizes of MnZn Ferrite cores for new designs. These cores are "un-gapped", although custom laboratory machines can produce a flat uniform gap in less than 30 minutes. In addition, a Form-labs 3D printer is typically able to create bobbins of various types of plastic within four hours.

Optimized Simulation Software

The time-consuming trial and error of assembling and testing different variations can be simplified by first relying on tools such as ANSYS for identifying optimum structures. The Flyback transformer example in Figure 1 is designed for 12V /6A isolated output (SELV) with a non-regulated, non-isolated 12V/0.18A output (NSELV).

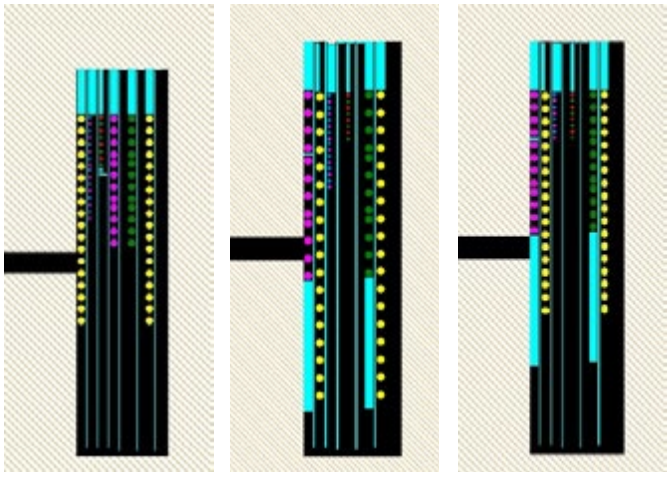

Winding	1	2	3	4	5	6
A	Winding Mains	Winding AUX	Winding NSELV	Winding SELV 1	Winding SELV 2	Winding Mains
B, B spread	Winding SELV 1	Winding MAINS	Winding AUX	Winding NSELV	Winding SELV 2	Winding Mains

Figure 4: Diagram of Winding Order for Three Different Scenarios

Some controller manufacturers will have a maximum time allowed for the leakage inductance spike on the AUX winding. Figure 2 (in yellow) shows the AUX winding voltage, which is sampled by the controller. The peak- to- peak variation (ringing) will also have a minimum value and is dependent on the leakage inductance. The coupling between the NON SELV in Figure 1 and AUX may also need to be controlled. This can be necessary in standby power situations with the Non SELV output being switched on or off. The control loop stability could be affected in these situations without optimum coupling between the AUX and NSELV windings. Therefore, placing the NON SELV close to the AUX is necessary in this situation to maximize their coupling.

Figure 4 shows three different winding structures that have been analyzed by ANSYS with the leakage inductance shown plotted in Figure 5 and Figure 6.

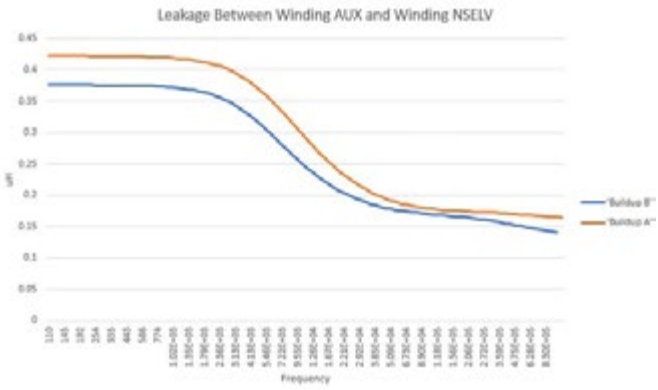

Figure 5: ANSYS Finite Element Analysis

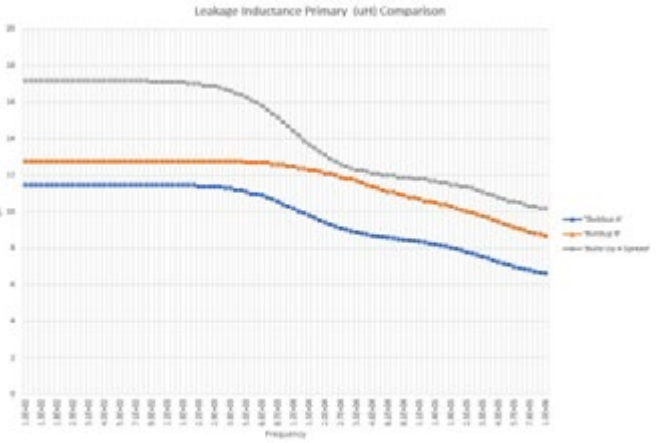

Figure 6: ANSYS Finite Element Analysis

The software will optimize the layout of the windings but allows for manual placement of the windings as well. It also allows for insulators such as tape and margin tape that can have an effect on leakage inductance. The isolation requirement between two non-isolated windings (500 Vac) is not possible if the windings are placed side by side, which would be more efficient. They have to be separated by at least one layer of tape. The spacing between turns can also be adjusted. The primary to SELV leakage in a high-power Flyback with auxiliary winding using secondary regulation is halved by splitting the primary winding. This will double the magnetic field path length and halve the magnetic field intensity. Winding Order B provided the optimum balance between the Mains to SELV and AUX to NSELV leakage. Winding Order A has the lowest Leakage inductance Mains to SELV but had a higher AUX to NSELV leakage. Spreading out the windings actually increased the leakage inductance, despite the fact that the path length increases through this approach, hence lowering the field intensity (Ampere Turns Per Meter). Increasing the distance between the turns allows uncoupled flux to pass into the space between windings. However, there is a trade-off in the space between turns and the overall length of the winding. Therefore, using margin tape to keep the turns close together was used when making initial samples. The measured results confirmed that Winding Order B was the better option. The measurements demonstrated that spreading the winding across the bobbin had the opposite effect on the leakage inductance.

Winding Buildup	Leakage Primary	Leakage AUX Winding
A	5.1uH	0.98uH
B (margin Tape)	5.5uH	0.45uH
B Spread Out	6.5uH	1.05uH

Made at 80kHz using a HP 4285 LCR

Figure 7: Physical Measurements of Prototypes made with Three Different Scenarios (80KHz HP 4285)

The differences in real and simulated measurements of leakage inductance can be partly due to the following factors:
A) Short circuit bar resistance
B) Distribution of coil along surface of bobbin
C) Tolerance in insulation material thickness

It is important to note that while simulation helps to compare different scenarios and select the appropriate winding structure, it is imperative to build a sample and test it thoroughly.

Power Laboratory Capabilities

Occasionally, customers might require support with testing transformers on application boards under certain conditions. For instance, Bourns has a license for Altium Designer for circuit and PCB design. The laboratory has a range of power sources and electronic loads together with a temperature chamber and infrared camera for testing boards. Bourns also can assist customers with EMI board testing.

Ideally, custom magnetics suppliers should also have production facilities that are certified to IATF16949 with automated manufacturing both for high volume, low power transformers as well as more complicated magnetics assemblies. This includes high-power converters (toroidal or split cores) such as power factor corrected soft switched half bridge converters. Experienced application engineers are needed to ensure prototypes are successfully transferred from initial engineering to production using industry standard AQCP (Advanced Quality Control Procedures) so the design can maintain the highest quality levels. The most efficient power electronics laboratories are set up to support customers with design, simulation and engineering samples of high frequency power magnetics. They also need to have expertise with advanced software design tools that will allow them to select the optimum magnetics design for the customer before making engineering samples. Having mechanical and electrical engineering in the same location, as well as available stock of ferrite cores and 3D printer allows for a quick, (sometimes as fast as 24-hour), turn-around on engineering samples. While simulation tools save time by identifying the optimum design, there is still no substitute for testing actual samples and verifying results.

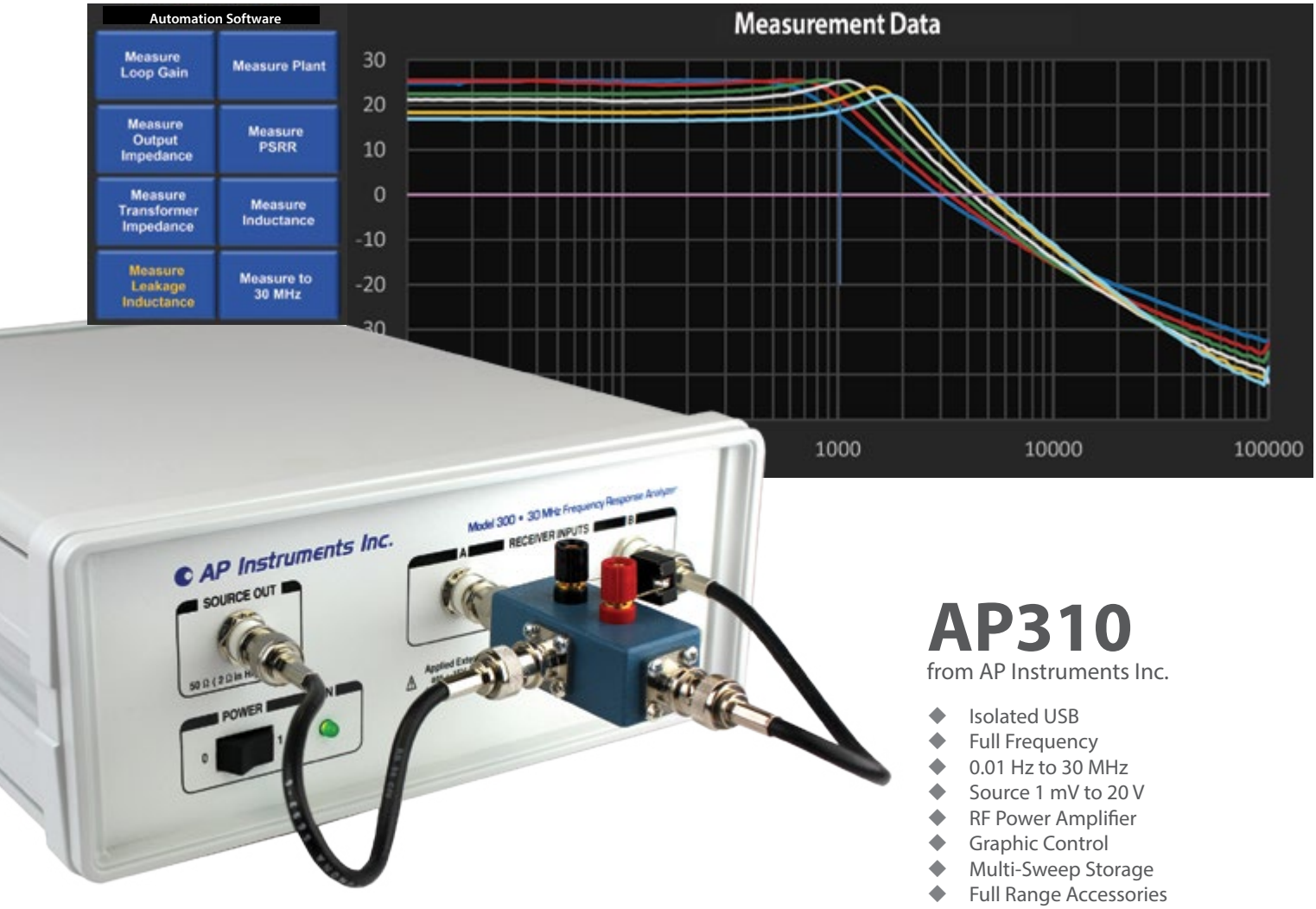

AP310

from AP Instruments Inc.

- Isolated USB
- Full Frequency
- 0.01 Hz to 30 MHz
- Source 1 mV to 20 V
- RF Power Amplifier
- Graphic Control
- Multi-Sweep Storage
- Full Range Accessories
- Maximum Productivity
- Fully-Automated Loop Design
- Support from Industry Experts
- Easy to Use
- One-Button Setup

AP310 is the industry's only full-featured frequency response analyzer designed specifically for power supplies. Enhance the experience with RidleyWorks® software for seamless integration between power supply design and measurement. *Made in California since 1995.*

RIDLEYENGINEERING.COM

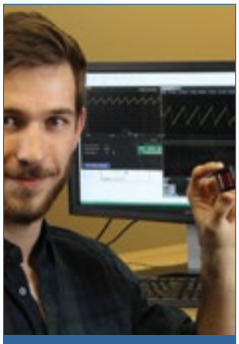
Education

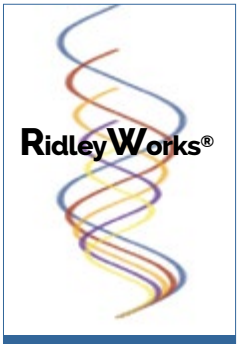

Software


Hardware


Design Ideas

RIDLEY ENGINEERING

601 E Daily Drive, Suite 112 | Camarillo CA 93010 | info@ridleyengineering.com | +1 805 504 2212 | POWER SUPPLY DESIGN CENTER GROUP on Linkedin

Get Your Power-Supply Design Right the First Time

Nobody wants to reinvent the wheel, least of all, designers of power supplies. The number of combinations of varying input/output voltages, output current and power requirements, as well as the numerous topologies available for countless applications, can be mind-boggling. Sometimes it feels like every new product needs its own custom power supply which inevitably may require several re-spins to get it to work properly. Even for experienced designers, this can be a challenge; for novice designers, it can be a nightmare! Wouldn't it be great to have, as a starting point, an actual working design that is close to what you need and that only needs a little bit of tweaking?

By Michael Jackson and Joe McClean, Maxim Integrated

Suddenly, a project that you thought would take months could be completed in a matter of weeks (or less). Even better, wouldn't it be nice to use an "off-the-shelf" design that you know will work the first time? In this article, we'll review the applications that are appropriate for different types of power-supply topologies and introduce a new power-supply methodology that accelerates both non- isolated and isolated power-supply design, with the help of a library of readily available reference designs that support applications from 2.5W to 72W.

Isolated DC-DC Industrial Applications

Industrial applications (such as process control, PLCs, SCADA systems and sensors in automation) are characterized by a 24V nominal DC voltage bus that has its history in old analog relays and remains the de-facto industry standard. However, the maximum operating voltage for industrial applications is expected to be 36V to 40V for non-critical equipment, while critical equipment, such as controllers, actuators, and safety modules, must support 60V (IEC 61131-2, 60664-1, and 61508 SIL standards). Popular output voltages are 3.3V and 5V with currents that vary from 10mA in small sensors to tens of amps in motion control, CNC, and PLC applications. Building control systems, including some industrial use cases such as smart building management, interior comfort and air quality management, field devices, and actuators utilize a rectified 24AC input voltage that further justifies the need for wide- input range DC-DC voltage converters.

The flyback topology is commonly used in industrial switch- mode power-supply, isolated step-down designs below 100W. The flyback converter (Figure 1) utilizes a gapped transformer to both transfer and store energy, thereby minimizing the number of output components. However, the high peak currents inherent in its discontinuous operation relegate its use to low-power applications. For output voltages less than 12V, a variation on the flyback using synchronous rectification (MOSFET) is used.

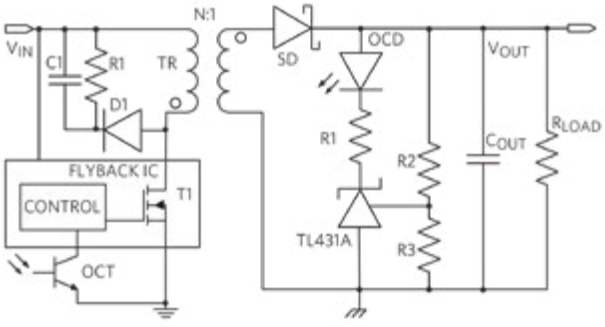

Figure 1: Flyback with Integrated Power Transistor

Recent designs of the flyback converter have seen the optocoupler circuit replaced by an IC which uses primary-winding feedback to regulate the output voltage. To speed up the design cycle for this type of power supply, several proven power- supply reference designs are available (typically with > 90% efficiency) using the MAX17690 60V, no-opto isolated flyback controller, for a variety of different input voltage ranges and output voltages and power requirements (Table 1).

Reference Design	VIN (V)	VOUT (V)	IOUT (A)
MAXREFDES1010	19 to 40	24	0.3
MAXREFDES1012	8 to 20	5.3	0.08
MAXREFDES1014	28 to 32	48	1.1
MAXREFDES1040	18 to 60	54	0.25
MAXREFDES1090	8 to 28	12	0.25
MAXREFDES1091	18 to 60	12	0.25
MAXREFDES1100	8 to 28	12	0.5
MAXREFDES1101	18 to 60	12	0.5
MAXREFDES1102	8 to 28	24	0.25

Table 1: No-Opto Flyback Reference Designs

For applications where an output voltage of 12V (or less) is required, a variation on the traditional flyback converter with synchronous rectification on the secondary side is typically used. In this version, the Schottky diode is replaced by a MOSFET (Figure 2). Table 2 lists several reference designs for this type of converter. These designs use the MAX17690 60V, no-opto isolated flyback controller and the MAX17606 secondary-side synchronous MOSFET driver for a variety of different input voltage ranges, output voltage, and power requirements.

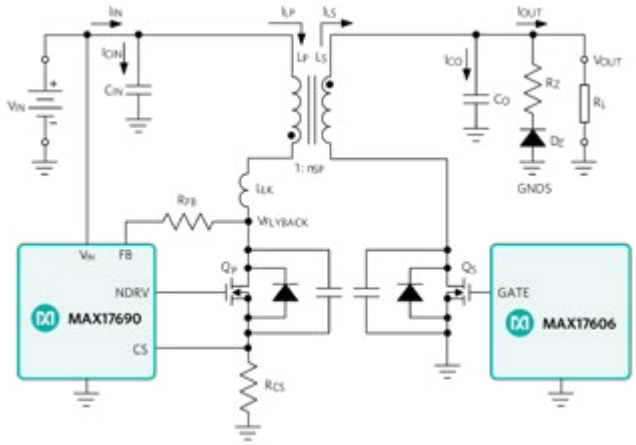

Figure 2: Simplified No-Opto Flyback Schematic with Synchronous Rectification

Reference Design	VIN (V)	VOUT (V)	IOUT (A)
MAXREFDES1002	18 to 36	12	0.5
MAXREFDES1022	10 to 50	5	2
MAXREFDES1086	8 to 28	5	0.5
MAXREFDES1087	18 to 60	5	0.5
MAXREFDES1088	8 to 28	12	0.25
MAXREFDES1089	18 to 60	12	0.25
MAXREFDES1094	8 to 28	12	0.5
MAXREFDES1095	18 to 60	12	0.5

Table 2: Synchronous No-Opto Flyback Reference Designs

Non-Isolated DC-DC Industrial Applications

For step-down DC-DC conversion at lower input voltages (<60V), where safety is not a concern, an isolated power supply is unnecessary. Where higher output current (from several milliamps for sensors to several Amps for motor controllers) is required, a synchronous buck (step-down) architecture (Figure 3) will suffice. Several variations on the multiple-output step-down DC-DC converter for a variety of input voltage ranges and output power requirements are shown in Table 3.

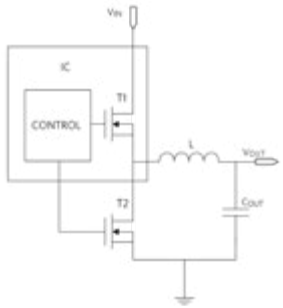

Figure 3: Simplified Synchronous Buck Architecture

Reference Design	VIN (V)	VOUT (V)	IOUT (A)
MAXREFDES1009	37 to 57	5 to 12	0.3 to 1
MAXREFDES1019	24 to 24	-20 to +20	0.05 to 2
MAXREFDES1033	11.5 to 13	3.3 to 5	3
MAXREFDES1039	36 to 51	16 to 24	2. to 4

Table 3: Synchronous Buck Reference Designs

Offline Industrial Applications

Some industrial applications require a regulated DC power supply that is generated from an AC 120V or 240V mains voltage (offline) input (Figure 4).

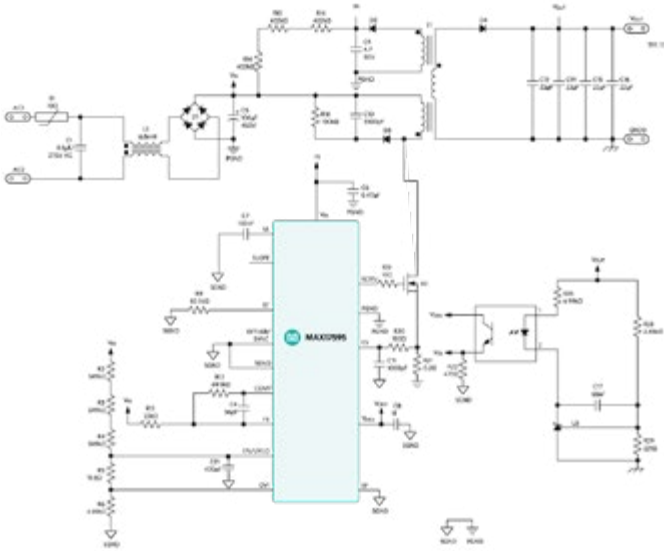

Figure 4: AC-DC Power Supply

Table 4 lists three different reference designs for these applications based on the MAX17595 peak-current-mode controller with output current drives.

Reference Design	VIN (AC V)	VOUT (V)	IOUT (A)
MAXREFDES1013	200 to 240	24	0.5
MAXREFDES1036	195 to 265	4.5	4.5
MAXREFDES1037	103 to 238	24	3

Table 4: Offline Power Supply Reference Designs

Computing Applications

Power supplies for computing applications have a requirement for low output voltages (< 5V for microprocessors and memory devices) with high output current drive. For these applications, the synchronous single output buck architecture is an appropriate solution. Some reference designs that employ this architecture are shown in Table 5.

Reference Design	VIN (V)	VOUT (V)	IOUT (A)
MAXREFDES1054	10 to 55	4	5
MAXREFDES1048	18 to 36	3	3.3
MAXREFDES1034	11.5 to 28	5	5
MAXREFDES1021	2.9 to 5.5	1.8	4
MAXREFDES1020	2.7 to 4.5	0.68	4
MAXREFDES1016	4.5 to 16	1.1	6
MAXREFDES1006	2.7 to 4.5	0.68	4

Table 5: Synchronous Buck Reference Designs

Automotive Lighting Applications

LEDs are taking the automotive industry by storm due to significant advantages over traditional technologies. To be most effective, the LED controller must accommodate a wide input voltage range and have a fast-transient response. A high, well- controlled switching frequency, outside the AM frequency band, is required to reduce

radio frequency interference and meet EMI standards. Finally, high efficiency reduces heat generation, improving the LED light system's reliability. Sophisticated headlight systems utilize a boost converter as a front–end to manage both the variabilities of the input voltage (dump or cold-crank) and the EMI emissions. The boost converter delivers a well-regulated and sufficiently high-output voltage (Figure 5). Dedicated buck converters, working from this stable input supply, can then handle the complexities of controlling the lamp's intensity and position by allowing each buck converter to control a single function, such as high beam, low beam, fog, daytime running lights, position, etc.

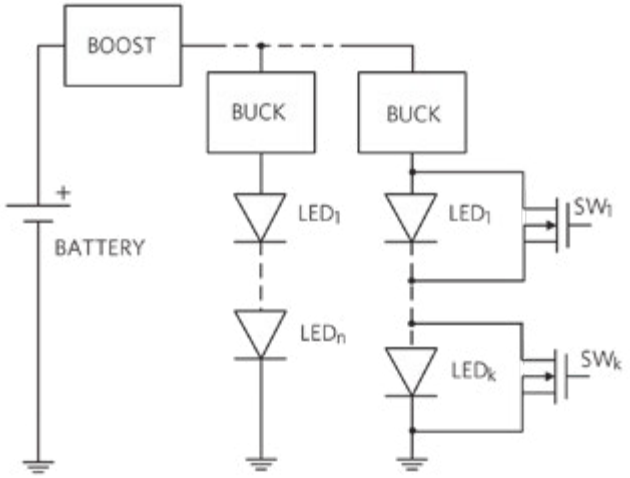

Figure 5: Advanced LED Lighting System

Table 6 lists two reference designs suitable for the automotive lighting application outlined above. The MAXREFDES1017 uses the MAX16990, which is a high-performance, current- mode PWM controller for boost/SEPIC converters with wide- input voltage ranges. The 4.5V to 36V input operating voltage range makes this ideal for front-end "pre-boost" or SEPIC power supplies and for the first boost stage in high-power LED lighting applications. Apart from automotive LED lighting, it is also suitable for use in industrial lighting and for LCD TV and desktop display LED backlights.

Reference Design	VIN (V)	VOUT (V)	IOUT (A)
MAXREFDES1003	8 to 32	5/24	0.6
MAXREFDES1017	18 to 32	19/24	0.9

Table 6: SEPIC Reference Designs

The MAXREFDES1003 uses the MAX16813 (Figure 6) which is a highly efficient, high-brightness LED (HB LED) driver that provides four integrated LED current-sink channels. An integrated current-mode switching controller drives a DC- DC converter that provides the necessary voltage to multiple strings of HB LEDs. The device accepts a wide-input voltage range and withstands direct automotive load-dump events. The wide-input range powers HB LEDs for small- to medium-sized LCD displays in automotive and general lighting applications.

Portable Applications

Smartphones and tablets are typically powered by rechargeable lithium-ion batteries where the voltage can regularly fall below 1V. The variable battery voltage needs to be converted to a stable DC voltage (which, depending on the design, can be over 10V) to drive low-current LCD displays. A "boost" topology power supply is ideal for this application. The MAXREFDES1018 power-supply reference design, shown in Table 7, uses a boost topology to produce a 13.5V output (with 6mA current drive) from an input voltage range of 1V to 3.3V. It is based on the MAX1606, which is a step-up DC-DC converter that operates from a 2.4V to 5.5V supply voltage but can boost battery voltages as low as 0.8V up to 28V.

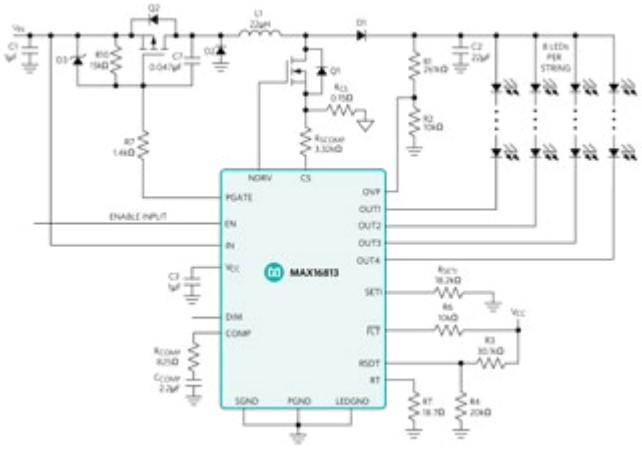

Figure 6: MAX16813 LED Driver

Reference Design	VIN (V)	VOUT (V)	IOUT (A)
MAXREFDES1018	1 to 3.3	13.5	0.006

Table 7: Boost Reference Design

Conclusion

Designing a power supply requires knowledge of the appropriate topology for the given application. Having chosen a topology, it must then be customized for an input voltage range, output voltage, and current drive as required. This can be a time- consuming procedure for the novice and experienced designer alike. In this article, we reviewed the power-supply topologies appropriate to different applications and presented a library of working power-supply reference designs with different current and voltage specifications. These designs may be immediately suitable to meet the requirements for some power-supply designs. If not, they are easily customizable using the design procedures outlined in the documentation. All designs listed include a detailed design note, verified test results, schematics, PCB artwork, and a bill of materials.

Biographies

Michael Jackson has over 20 years' professional experience as an Analog IC Design Engineer and holds the position of Senior Technical Writer at Maxim Integrated. He has a MSEE from Dublin City University.

Joe McClean, Principal Member of Technical Staff at Maxim integrated, is an experienced power electronics professional with several papers and patents in the field of power electronics and lighting technologies. He is a graduate of Trinity College Dublin and holds a bachelor's degree in physics.

www.maximintegrated.com

Messe München

Connecting Global Competence

November 13–16, 2018

Connecting everything – smart, safe & secure

Trade fair

- 17 halls
- Full range of technologies, products and solutions

Conferences & forums

- 4 conferences
- 11 forums
- New TechTalk for engineers and developers

Talent meets Industry

- electronica Experience with live demonstrations
- e-ffwd: the start-up platform powered by Elektor
- electronica Careers

SEMICON EUROPA

semi

co-located event

electronica 2018

components I systems I applications I solutions

World's leading trade fair and conference for electronics

Messe München I November 13–16, 2018 I electronica.de

POWER ELECTRONICS CONFERENCE 2018

Wide Band Gap Semiconductors

4. DECEMBER
MUNICH-AIRPORT

Wide Band Gap semiconductors have become mature during the last decade. We are facing a change of semiconductor power switches away from Silicon to SiC and GaN. It is important that systems design engineers get involved in the advanced design work using wide band gap devices for their next project. The experts from the semiconductor manufactures and the early users are important to teach the field their experience and take the barrier down using new technology.

Power-Conference.com

Contact for Speaking Opportunities:
Bodo Arlt – editor@bodospower.com

Contact for Sponsoring/Exhibiting Opportunities:
Manfred Blumoser – mblumoser@aspencore.com

Bodo's Power Systems® ASPENCORE

Reinforced Insulation Material

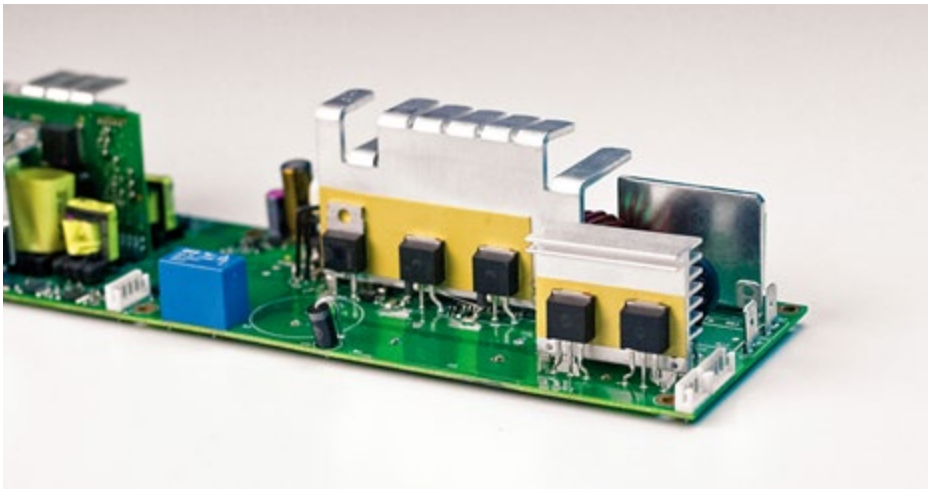

Upholding its commitment to enable customers' 2020 requirements and beyond, Henkel has developed a thicker version of its BERGQUIST® BOND-PLY® LMS-HD thermally conductive laminate material. It is a 0.018" thick thermal adhesive that complies with the Underwriter's Laboratories (UL) standard for reinforced insulation as well as IEC Class II insulation standards. This allows designers and manufacturers of power applications with stringent insulation requirements to take advantage of the benefits of BERGQUIST BOND-PLY LMS-HD, or to future-proof products that may not currently fall under this UL regulation but could be subjected to its implementation in the near future.

As compared to other materials in the portfolio, the material provides a higher standoff between the device and heat sink for reinforced insulation and maintains all of the high-performance properties of the standard thickness version. The material is a heat-curable formulation that delivers excellent thermal performance of 1.4 W/m-K and strong adhesion, eliminating the need for mechanical fasteners such as screws or clips. With a low modulus, silicone-based BERGQUIST BOND-PLY LMS-HD effectively absorbs mechanical stresses common with assembly-level coefficient of thermal expansion (CTE) mismatches, and also provides robust protection against shock and vibration.

"Any power application with critical insulation requirements, or that may need to comply with anticipated UL safety standards will benefit from the new BERGQUIST BOND-PLY material," says Justin Kolbe, Global Market Segment Manager, Power and Industrial Automation, Henkel Corporation.

www.henkel-adhesives.com/electronics

Megawatt Converter in Innovative Design

With VARIS™ PRO, GvA Leistungselektronik GmbH offers an ultra-compact converter in the megawatt range - ready for connection, flexible and suitable for the most diverse applications. Thereby, GvA adds an innovative and extremely powerful member to their well-known VARIS™ product family. The patented design uses an extremely low-inductance construction with IGBT modules of the latest generation. The liquid cooler fitted on either side and the sophisticated and space-saving arrangement of the intermediate circuit capacitors create an extremely high power density of up to 1.4MVA. The ready-to-connect converter will be delivered optionally in a customer-specific enclosure or as requested as plug-in module for control cabinet installation. The two inverter bridges flexibly fulfil the requirements of the most

diverse converter configurations, either independent of each other or together. Therefore, VARIS™ PRO is the universally applicable solution for the most diverse applications such as drives, storage systems or AC/DC converters. Moreover VARIS™ PRO eCharge is a modified variant for the growing market segment of High Power Charging (HPC) with typically 350kW.

www.gva-leistungselektronik.de

TO-Leadless Packaging Technology for High Current 400A Applications

Alpha and Omega Semiconductor Limited (AOS) introduced the TO-Leadless (TOLL) package in combination with 40V Shield-Gate Technology (SGT) to provide the highest current capability in its voltage class. The TOLL package has the highest current capacity

because of AOS' innovative technology which utilizes a clip to achieve the 400A DC at 25°C capability. It offers very low package resistance and inductance due to the clip technology in comparison to other TO-Leadless packages using standard wire-bonding technology which enables improved EMI performance.

The AOTL66401 (40V) has a 30% smaller footprint compared to a TO-263 (D2PAK) package, including having higher current carry capability that enables the designer to reduce the number of devices in parallel. This new device offers a higher power density in comparison to existing solutions, and is ideally suited for industrial BLDC motor applications and battery management to reduce the number of MOSFETs. The device has a 0.7mOhm max rating at 10Vgs with a maximum drain current of 400A at 25°C and 350A at 100°C case temperature. The pulsed current is rated at 1600A, which is limited by the maximum junction temperature of 175°C.

www.aosmd.com

Portfolio with Two True-Differential Time-Domain Reflectometers

Teledyne LeCroy announced the launch of Teledyne Test Tools (T3), a branded portfolio that adds a comprehensive range of test equipment to the Teledyne LeCroy product offering. T3 products complement and leverage Teledyne LeCroy's decades-long leadership in oscilloscope technology and are supported by the Teledyne LeCroy Sales

and Customer Care organizations. The T3 brand, which establishes a turnkey platform for test engineers, developers, and schools, takes flight with the launch of two new ultra-portable, inexpensive, reliable, and highly accurate time-domain reflectometers (TDRs). "The launch of the T3 branded test equipment portfolio complements our oscilloscope technology and leverages our decades of market knowledge and strong customer relationships to create a one-stop shop for our customers' test solutions needs," said Roberto Petrillo, Worldwide VP of Teledyne Test Tool Development. "The T3 team is getting off to an exciting start with the introduction of two cutting-edge true-differential TDRs. By offering portability, reliability and advanced functionality at an affordable cost, our 10- and 15 GHz TDRs deliver on a unique value proposition that other products in the marketplace simply don't meet." Before the availability of Teledyne LeCroy's 10- and 15-GHz TDRs, portable tools were either much costlier high-end TDRs, or single-ended instruments with limited functionality.

www.teledynelecroy.com

Bidirectional Buck-Boost Controller for 12V-12V Redundant Battery Systems

Analog Devices announces the Power by Linear™ LT8708/-1, a 98% efficient bidirectional buck-boost switching regulator controller that operates between two batteries that have the same voltage, which are ideal for redundancy in self-driving cars. The LT8708/-1 operates from an input voltage that can be above, below or equal to the output voltage, making it well suited for two each 12V, 24V or 48V batteries commonly found in electric and hybrid vehicles. It operates between two batteries and prevents system shut-down should one of the batteries fail. The device can also be used in 48V/12V and 48V/24V dual battery systems. It operates with a single inductor over a 2.8V to 80V input voltage range and can produce an output voltage from 1.3V to 80V, delivering up to several kilowatts of power depending on the choice of external components and number of phases. It simplifies bidirectional power conversion in battery/capacitor backup systems that need regulation of VOUT, VIN, and/or IOUT, IIN, both in the forward or reverse direction. This device's six independent forms of regulation allow it to be used in numerous applications. The LT8708-1 is used in parallel with the LT8708 to add power and phases. The LT8708-1 always operates as a slave to the master LT8708, can be clocked

out-of-phase and has the capability to deliver as much power as the master. One or more slaves can be connected to a single master, proportionally increasing power and current capability of the system.

www.analog.com/LT8708

175°C AEC-Q101 MOSFETs in Miniature Leadless Packages

Nexperia announced the industry's first AEC-Q101-qualified MOSFETs that are both rated for use at up to 175 °C and are available in the AOI-compatible DFN2020 package (DFN = Discrete Flat No leads). More,

the new devices measure just 2 mm x 2 mm, much smaller and lighter than SOT223 and SO8-packages yet with comparable electrical and thermal performance. Many leadless packages cannot be inspected using AOI techniques, so Nexperia pioneered the development of the DFN2020 package with side-wettable flanks (SWF), enabling Automatic optical inspection (AOI) – a critical automotive industry requirement – to be employed. Packages with SWF are now a proven, accepted solution. Comments Malte Struck, Nexperia's product manager for small signal MOSFETs: "The DFN package with side-wettable flanks is gaining significant traction with automotive manufacturers as it saves space and can be automatically inspected. Our new 175 °C parts are being used in under-the-hood applications, especially near the engine or gearbox. The unique offering of an automotive-grade MOSFET that is both qualified to 175 °C and which incorporates side-wettable flanks makes the DFN2020 additionally suitable for a wide range of medium-power automotive applications."

The new automotive-qualified parts extend Nexperia's low and medium power MOSFET portfolio. Six 40 V and 60 V devices are available with the higher temperature rating and automotive approval, each with low RDS(on) of between 20 mΩ and 40 mΩ.

www.nexperia.com

Upgrade for External Power Supply Line to Meet IEC 62368-1 Standard

CUI's Power Group announced that it has upgraded the majority of its external ac-dc power supplies to the new IEC 62368-1 standard for ICT and AV equipment. Set to supersede the outgoing IEC 60950-1 and IEC 60065 standards on December 20, 2020, IEC 62368-1 will introduce fundamentally different guidelines based on hazard-based safety engineering principles. This means that IEC 62368-1 is more significant than a simple merger of the two standards and represents an important transition for designers of ICT and AV equipment. Similar to the past standards, IEC 62368-1 will apply not only to the end system, but also to components such as external power supplies. CUI's newly compliant line ranges from 3 W to 250 W in wall plug-in, multi blade, and desktop versions, all available with a variety of dc output plug options. The models also meet the latest global efficiency standards, including US DoE Level VI and the EU's voluntary CoC Tier 2 requirements.

"CUI's mission is to provide our customers with products and tools that prepare them for the latest safety regulations and industry standards," stated Jeff Schnabel, VP of Global Marketing at CUI.

"This is why CUI has upgraded many of our power supply models to 62368-1 well ahead of the December 2020 deadline, while further developing resources such as our IEC 62368-1 whitepaper to keep customers informed," Schnabel concluded.

www.cui.com

Extension of MLCC Lines

The Knowles Precision Devices HiT range of MLCCs are designed to meet the needs of high-voltage EV applications, with an operating temperature range of -55 to +200ºC. Specifications encompass both

Stable (C0G) and ultra-stable (X7R) dielectric options in case sizes 0805 to 2220, with capacitance spread of 4.7pF to 3.3uF, and rated voltages of 16 to 630V dc. The specified max capacitor values for the 500/630V parts has recently been increased to an upper limit of 68nF, with the addition of an 0603 case size in X7R material. To better support customers in the medical devices industry, Knowles Precision Devices acquired Johanson Manufacturing, extending its portfolio of trimmers significantly to now include air, glass, sapphire, and PTFE dielectrics, that can be used from 1 MHz to over 2 GHz, and at voltages up to 20,000 VDC. In addition, a complete line of non-magnetic components for the MRI and NMR industries, including trimmer capacitors, chip capacitors, fixed and variable inductors, and hardware, is also available. Knowles PD are proud to serve a wide variety of markets and have products suitable for challenging applications including military, aerospace/avionics, medical, EMI and connector filtering, automotive, telecoms and data networks.

www.knowlescapacitors.com

Achieving Miniaturization Success – Also with Micro LEDs

As LEDs continue to shrink in size, there is a need for materials that dissipate heat quickly and solutions to ensure the effective electrical connection of micro LEDs. Heraeus has specially developed a sinter paste for LED applications, which has a thermal conductivity value twice as high as gold-tin or tin-silver alloys. The heat loss can therefore be dissipated much faster, resulting in higher luminous efficacy and ultimately protecting the LED chip from damage. Extremely fine materials are required to electrically connect the micro LEDs on the backplane, as micro

LEDs can have an edge length of less than 150 µm. Conventional solder pastes, with particle sizes of between 20 and 45 µm, cannot meet the bond line thickness and stencil opening requirements, meaning that solder alloys with a particle size of less than 11 µm are called for. Heraeus WS5112 type 7 solder paste, made with patented Welco solder powder, allows the printing of tiny solder bumps of up to 50 µm.

www.heraeus.com

200-W and 100-W USB Type-C™ and USB Power Delivery Controllers

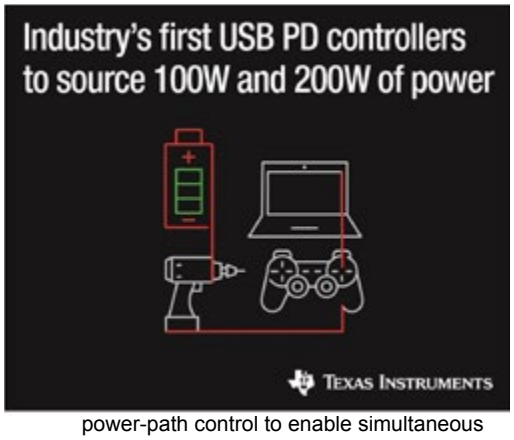

Texas Instruments (TI) introduced two USB Type-C™ and USB Power Delivery (PD) controllers, with fully integrated power paths to simplify designs, minimize solution size and speed time to market. The TPS65987D and TPS65988 offer system designers the industry's highest level of integration which can reduce design complexity and overall cost. The devices are the industry's first USB PD controllers to source 100 W and 200 W of power, respectively, to support computing applications and enable the benefits of USB Type-C in additional applications such as cordless power tools, gaming and virtual reality headsets. The TPS65987D, a single-port device designed to source 100 W of power, integrates independent 20-V, 5-A source and sink load switches. Low RDS(on) (25mΩ) and reverse current protection in the TPS65987D provide a comprehensive solution for managing a port's charging needs. The dual-port TPS65988 can source 200 W of power, and offers two integrated 5-A bidirectional load switches and external power-path control to enable simultaneous 5-A source capability. The devices are USB PD 3.0-certified, UL Recognized, and International Electrotechnical Commission (IEC) safety-certified, and come preprogrammed to support several of the most common use cases including DisplayPort™ and Thunderbolt™ applications. Additional use cases are supported through an easy-to-use configuration tool.

www.TI.com

Unspoilt Environment

Magnetically Shielded Rooms (MSR) are widely used in basic and applied research. They attenuate the influence of low-frequency interference caused, for example, by railway lines, elevators, vehicles, transformers or radio signals. VACUUMSCHMELZE (VAC) has already built up more than 150 cabins in almost 40 years and thus has unmatched experience in the conception, planning and execution of shielding cabins for the most diverse requirements. In addition to the three standard variants Basic, Advanced and Premium, high-end customer-specific designs can be realized.
The right solution for all requirements: The Basic cabin is weight- and cost-optimized and suitable for installation in upper levels. The two-layer Advanced cabin also shields at higher frequencies and the Premium cabin with an additional MU-METALL® layer is used for above-average magnetic environmental noises. The full vertical integration from melting of the alloy to the assembly of the finished cabin out of one hand has proven to be a key success factor to ensure consistently the best magnetic properties and most efficient project management.
„The latest trend in the use of optically pumped magnetometers requires uniform low residual field within the Magnetically Shielded Room. Our rooms provide the optimum precondition for this kind of application." says Lela Bauer, Product Management specialist at VAC.

www.vacuumschmelze.com

5kVRMS Reinforced Digital Isolator

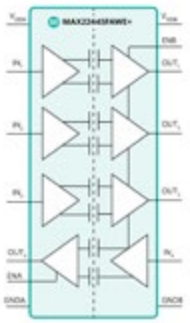

To better protect industrial systems from the dangers of high-voltage signals, equipment designers can now turn to the new robust and reliable MAX22445 5kVRMS four-channel reinforced digital isolator from Maxim Integrated Products, Inc. Delivering up to 2x greater throughput at 4x lower power consumption versus competing solutions, the MAX22445 provides reliable communication across the isolation barrier to ensure safe operation of compact industrial, medical and other equipment.

In high-voltage equipment, digital isolators provide signal isolation and level-shifting for proper operation of many circuits, while also protecting users from dangers such as electric shock. Yet, not all of these isolators are alike as many consume a large amount of power, generate significant heat and introduce large propagation delays, limiting system reliability and throughput.

Overcoming the shortcomings of other digital isolators, the MAX22445 delivers reinforced, dual insulation barrier isolation for fast digital signals. The IC, which mitigates the dangers of high-voltage power, transfers signals of up to 200Mbps with significantly less power than competitive solutions. It is available in a 16-pin wide-body SOIC package with 8mm of creepage and clearance.

www.maximintegrated.com

EiceDRIVERs Solve Ground-Shift Issues in SMPS

Every time a power MOSFET is switched on or off in a switched-mode power supply (SMPS), parasitic inductances cause ground shifts. This can lead to uncontrolled switching of gate driver ICs. In extreme cases, this results in electrical overloading of power MOSFETs and malfunctioning of the SMPS. To solve this problem, Infineon offers the 1-channel low-side gate driver ICs 1EDN7550 and 1EDN8550. Both of the gate drivers belonging to the EiceDRIVER™ family have truly differential control inputs and can effectively prevent false triggering of power MOSFETs. 1EDN7550 and 1EDN8550 are used in industrial, server and telecom SMPS as well as wireless charging applications , telecom DC-DC converters and power tools.

The EiceDRIVER 1EDN7550 and 1EDN8550 are immune to static ground offsets up to ± 70 V. Safe operation is guaranteed at dynamic ground offsets of up to ± 150V. All this is possible without having to cut ground loops. Since the gate driver ICs have truly differential inputs, only the voltage difference between the two inputs is decisive for the switching behaviour of the gate driver IC. The 1EDNx550 EiceDRIVER are ideally suited for controlling power MOSFETs with Kelvin source contact. These gate driver ICs provide more than adequate robustness against ground shifts due to parasitic source inductances of the power MOSFET. Compared with galvanically isolated gate driver ICs, these single-channel low-side gate driver ICs are more space-efficient at lower cost against to traditional solutions.

www.infineon.com/TDI

Ultra-Compact Automotive Grade Buck DC/DC Converters

ROHM has recently announced the availability of the BD9S series (BD9S400MUF-C, BD9S300MUF-C, BD9S200MUF-C, BD9S100NUX-C, BD9S000NUX-C). This series of automotive synchronous secondary buck DC/DC converters have a high reliability and low power consumption in a compact form factor with a temperature range of -40 to +125 degree.

The products are offered in a leadless package with wettable flanks. This makes them very suitable for using them in applications like radars, cameras and sensors which can be used for assisted driving. The growing demand for safety requires the adoption of accident prevention systems and the evolution of self-driving cars. This in turn requires a higher number of subsystems including sensors and camera modules, resulting in higher power consumption. At the same time, it is necessary to decrease the component size and quantities to reduce vehicle weight. In response to the challenging power supply IC requirements, ROHM delivers class-leading* performance leveraging our design and manufacturing technologies cultivated over many years along with a fully integrated production system. Our power supply ICs also contribute to improved safety, which is required in future applications. The BD9S series is comprised of a very compact, highly efficiency automotive-grade power supply ICs that include an enable function to adjust the startup time and a PGOOD output indication to improve system functional safety.

www.rohm.com

INCORE 75-100 W LED Power Supply

LinkCom Manufacturing announces its 75-100W LLC Series, the latest addition to the INCORE family of high-performance constant-current LED power supplies. The LLC Series is available in models with nominal power ratings from 75-100 W and output voltages from 12 V to 54 V – all with efficiency up to 90%. IP-67 packaging and a wide operating temperature (-30 C to >50 C) enhance the suitability of the LLC Series for both outdoor and indoor applications including high-bay and low-bay fixtures, troffers, wraparound and linear washdown lighting. The units also provide a built-in 24V, 0.2A, max. auxiliary output power source to operate environmental sensors. To assure superior, flicker-free light quality, the LLC Series features a two-stage fly-back converter with integral active power factor correction. The units also provide a full range of circuit protection (OVP, SCP, OTP) and Surge Protection (L-N 4KV, L-G/N-G 6KV) to assure reliable performance. The LLC Series units are compliant with UL8750 and PSE safety standards, FCC emission standards and meet RoHS requirements. “Our INCORE family advances LinkCom’s many years of expertise in designing LED power supplies,” said Newman Chen, LinkCom’s director of North American operations. “The 75-100W LLC Series’ power rating, robust environmental specifications and dimming control reflects our ongoing commitment to addressing customer requirements in the fast-growing LED illumination market.”

www.linkcomusa.com

Half H-Bridge uses Silicon Carbide MOSFET Technology with Integrated Gate Drive

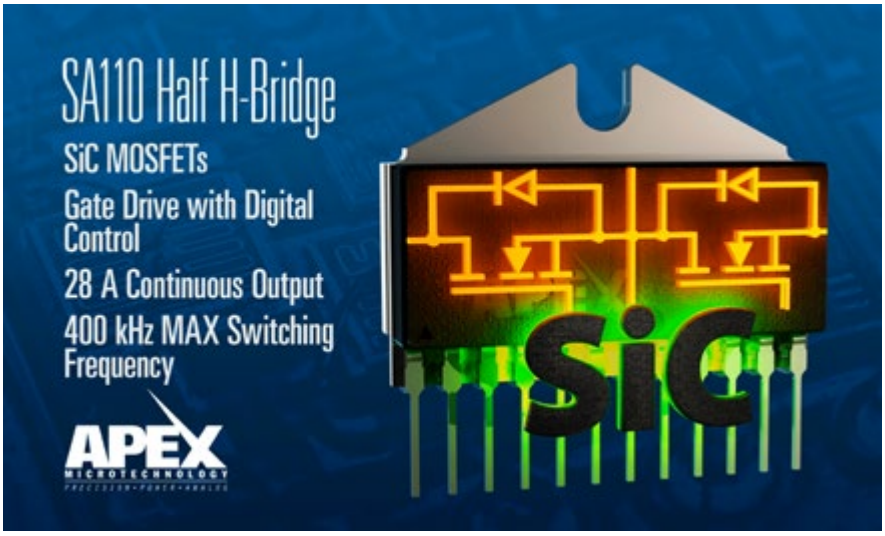

The SA110 is Apex Microtechnology's first high current, high voltage half H-bridge to combine silicon carbide (SiC) MOSFETs with a gate drive in a single module device. This hybrid switching amplifier also features digital gate driver control, a very high 400 kHz MAX switching frequency, and 28 A of continuous output current. The use of SiC technology can potentially impact a hybrid's bill of materials, but any increase in cost will most likely be offset by a significant increase in performance. This includes reduced switching losses, lower conduction losses, and a low temperature dependency of RDS(on) over a wide operating temperature range. SiC MOSFETs also provide a reduction in power loss compared to the more commonly used silicon or IGBT options. By integrating the gate drive, switching behavior is greatly improved as parasitic impacts are reduced and easier to control.

"The use of SiC MOSFETs in the SA110 represents an exciting first for Apex hybrid designers and our customers," explains Apex Strategic Marketing Director Jens Eltze. "We believe any potential uptick in the cost of the device will be more than compensated by the impressive increase in performance and reliability, as well as lower costs for cooling the components. This combination of SiC MOSFETs with integrated gate drive and control logic will shorten design cycle times and save on valuable board real estate for our customers."

www.apexanalog.com/products/sa110.html

Bidirectional Synchronous Buck-Boost Controllers

Renesas Electronics Corporation announced an innovative family of bidirectional four-switch synchronous buck-boost controllers. The ISL81601 and ISL81401 are the industry's only true bidirectional controllers that sense peak current at both ends and provide cycle-by-cycle current limit in both directions while in buck or boost mode. The controllers generate point-of-load (POL) and voltage rail conversions with peak efficiency up to 99 percent. The ISL81601 has a wide input range of 4.5V to 60V and produces a 0.8V to 60V output to support most industrial batteries: 12V, 24V, 36V and 48V. Also available is the ISL81401, a 4.5V to 40V input and 0.8V to 40V output version, and its unidirectional counterpart, the ISL81401A. The controllers are well suited for DC power backup and battery-powered medical, industrial and telecommunication systems.

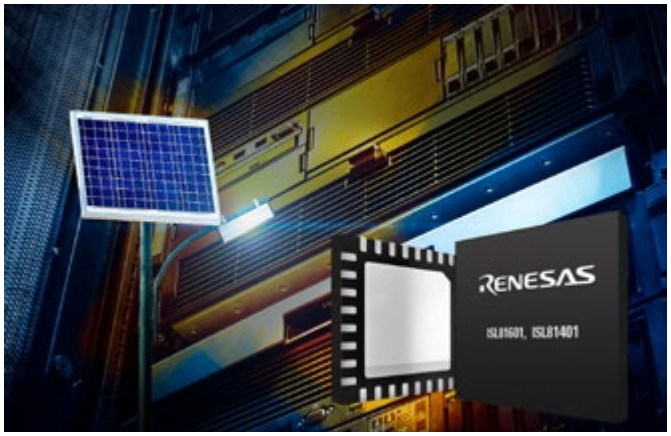

The ISL81601 and ISL81401's bidirectional peak current sensing capability eliminates complex external circuitry required for charging and discharging a battery to supply power to the loads. Their proprietary algorithm provides smooth mode transitions between buck, boost and buck-boost, while reducing low frequency ripple at Vout, ensuring minimal disturbances during line or load transients. The algorithm also ensures predictable ripple voltage under all conditions. The addition of multilayer overcurrent protection and a precision control algorithm delivers constant current down to 0.1V at Vout for reliable operation.

www.renesas.com

DOSA Converters Made in Europe

RECOM's latest innovation increases the power density of DOSA-packaged DC/DC converters to a new level. The RPM modules stand out due to their exceptional efficiency of up to 99%, enabling a low-profile package perfect for applications where space is critical. RECOM's power modules offer one of the highest power densities in a DOSA footprint on the market with a profile of only 3.75mm. They provide either 1, 2, 3, or even 6A in the same-sized package for scalability. The 6A module has at least 50% higher power density than its peers on the market, thanks to a new IC and a novel multi-layer PCB layout. It's thermally optimized to pull the heat away from the board - so without derating it delivers over 800W/in³ at up to 90°C. With a ground plane in the PCB together with the metal housing, 6-sided shielding guarantees great EMC performance. The RPM power modules have been successfully designed, tested, and manufactured – all in Europe! With input and output capacitors already included, the RPM series operates without the need for additional components. They are SMD with a land-grid-array package. To facilitate rapid testing, RECOM also developed evaluation boards, which will be released by end of October 2018 so that customers will be able to quickly and easily test these modules.

www.recom-power.com

1700V, 1 Ohm SiC MOSFET

Littelfuse, Inc. introduced its first 1700V SiC MOSFET, the LSIC-1MO170E1000, expanding its portfolio of SiC MOSFET devices. An important addition to the Littelfuse SiC MOSFET product offering, the LSIC1MO170E1000 is a powerful addition to the company's 1200V SiC MOSFETS and Schottky diodes already released. End-users will benefit from more compact, energy-efficient systems and also from a potential lower total cost of ownership. High-efficiency benefits powered by SiC MOSFET technologies offer multiple advantages to many demanding applications including electric and hybrid vehicles, datacenters, and auxiliary power supplies. When compared to similarly-rated Si IGBTs, the LSIC1MO170E1000 SiC MOSFET enables a number of system level optimization opportunities, including increased efficiency, increased power density, decreased cooling requirements, and potentially lower system level costs.

"This product can improve existing applications, and the Littelfuse application support network can help new design-in projects," said Michael Ketterer, Global Product Marketing Manager, Power Semiconductors, Semiconductor Business Unit at Littelfuse. "SiC MOSFETs offer a rewarding alternative to traditional Si-based power transistor devices. The MOSFET device structure enables lower per-cycle switching losses and improved light load efficiency when compared to similarly-rated IGBTs. Inherent material properties allow the SiC MOSFET to outclass its Si MOSFET counterparts in terms of blocking voltage, specific on resistance, and junction capacitances."

http://www.littelfuse.com/products/power-semiconductors/silicon-carbide/sic-mosfets/lsic1mo170e1000.aspx

www.littelfuse.com

Advertising Index

Thyristors

Low losses for efficient transmission.

ABB Semiconductors' new generation of thyristors enable HVDC transmission lines of up to 12 GW in a single installation, with a conversion efficiency beyond 99.6 %. Each device has the capacity to conduct in the range of 5000 A to 6250 A, has blocking capability of up to 8500 V and offers power savings up to 1 kW per device at rated current.

abb.com/semiconductors

Improved power cycling performance

PrimePACK™ with IGBT5 .XT – more efficiency in a well-established footprint, higher lifetime and reliability

The new PrimePACK™ modules feature IGBT5 – our latest chip generation with a continuous operating temperature that is 25K higher (T_{vjop} = 175°C). This allows higher power densities in 1200 V and 1700 V applications. The output power of the application can therefore be increased by 25% within the standard PrimePACK™ footprint.

PrimePACK™ has been developed with .XT joining technology to fulfill current and future lifetime requirements. This has been realized by sintering IGBT chips and diodes along with improved system soldering and replacing the aluminum bonds with copper bonds. Applications benefit from increased system availability due to a ten times longer lifetime of the PrimePACK™ module.

Key features

- Static and dynamic losses reduced by up to 20%
- Power cycling capabilities increased by a factor of 10
- Continuous operating temperature of T_{vjop} = 175°C

Benefits

- Power density increase of 25% or a 10 times longer lifetime
- Reduced cooling effort for same output power
- Reduction of overall system costs

www.infineon.com/primepack